Asynchrony between virus diversity and antibody selection limits influenza virus evolution

Dylan H. Morris[1*], Velislava N. Petrova[2], Fernando W. Rossine[1], Edyth Parker[3,4], Bryan T. Grenfell[1,5], Richard A. Neher[6], Simon A. Levin[1], and Colin A. Russell[4*]

[1]Department of Ecology & Evolutionary Biology, Princeton University, Princeton, NJ 08544, USA
[2]Department of Human Genetics, Wellcome Trust Sanger Institute, Cambridge, UK
[3]Department of Veterinary Medicine, University of Cambridge, Cambridge, UK
[4]Department of Medical Microbiology, Academic Medical Center, University of Amsterdam, Amsterdam, NL
[5]Fogarty International Center, National Institutes of Health, Bethesda, MD 20892, USA
[6]Biozentrum, University of Basel, Basel, CH
[*]Correspondence to dhmorris@princeton.edu, c.a.russell@amsterdamumc.nl.

April 27, 2020

Abstract

Seasonal influenza viruses create a persistent global disease burden by evolving to escape immunity induced by prior infections and vaccinations. New antigenic variants have a substantial selective advantage at the population level, but these variants are rarely selected within-host, even in previously immune individuals. We find that the temporal asynchrony between within-host virus exponential growth and antibody-mediated selection make within-host antigenic adaptation rare. Instead, selection for new antigenic variants acts principally at the point of initial virus inoculation, where small virus populations encounter well-matched mucosal antibodies in previously infected individuals. Selection later in infection is rare. Our results explain how virus antigenic evolution can be highly selective at the global level but nearly neutral within hosts. They also suggest new avenues for improving influenza control.

Introduction

Antibody-mediated immunity exerts evolutionary selection pressure on the antigenic phenotype of seasonal influenza viruses (Hensley et al., 2009; Archetti & Horsfall, 1950). Influenza virus infections and vaccinations induce neutralizing antibodies that can prevent re-infection with previously encountered virus antigenic variants, but such re-infections nonetheless occur (Clements, Betts, Tierney, & Murphy, 1986; Memoli et al., 2019). At the human population level, accumulation of antibody-mediated immunity creates selection pressure favoring antigenic novelty. Circulating antigenic

variants typically go rapidly extinct following the emergence of a new variant, at least for A/H3N2 viruses (Smith et al., 2004).

New antigenic variants like those that result in antigenic cluster transitions (Smith et al., 2004) and warrant updating the composition of seasonal influenza virus vaccines are likely to be produced in every infected host. Seasonal influenza viruses have high polymerase error rates (on the order of 10^{-5} mutations/nucleotide/replication (Nobusawa & Sato, 2006)), reach large within-host virus population sizes (as many as 10^{10} virions (Perelson, Rong, & Hayden, 2012)), and can be altered antigenically by single amino acid substitutions in the hemagglutinin (HA) protein (Koel et al., 2013; Linderman et al., 2014).

In the absence of antibody-mediated selection pressure, *de novo* generated antigenic variants should constitute a tiny minority of the total within-host virus population. Such minority variants are unlikely to be transmitted onward or detected with current next-generation sequencing (NGS) methods. But selection pressure imposed by the antibody-mediated immune response in previously exposed individuals could promote these variants to sufficiently high frequencies to make them easily transmissible and NGS detectable. The potential for antibody-mediated antigenic selection can be readily observed in infections of vaccinated mice (Hensley et al., 2009) and in virus passage in eggs in the presence of immune sera (Davis et al., 2018).

Surprisingly, new antigenic variants are rarely observed in human seasonal influenza virus infections, even in recently infected or vaccinated hosts (Debbink et al., 2017; Dinis et al., 2016; McCrone et al., 2018; Leonard et al., 2016; Han, Maurer-Stroh, & Russell, 2019; Valesano et al., 2019) (Fig. 1A,B). These observations contradict existing models of within-host influenza virus evolution (Luo, Reed, Mattingly, & Koelle, 2012; Volkov, Pepin, Lloyd-Smith, Banavar, & Grenfell, 2010), which predict strong within-host antibody selection and therefore frequent within-host fixation of new antigenic variants in detectable reinfections of previously immune hosts. This raises a fundamental dilemma. If within-host antibody selection is strong, why do new antigenic variants appear so rarely? If this selection is weak, how can there be protection against reinfection?

We hypothesized that influenza virus antigenic evolution is limited by the asynchrony between virus diversity and antibody-mediated selection pressure. Secretory IgA antibodies on mucosal surfaces (sIgA) in previously infected or vaccinated individuals reduce the initial probability of reinfection. But if viruses are not neutralized by these antibodies and successfully infect host cells, an antibody-mediated recall response takes multiple days to mount (Coro, Chang, & Baumgarth, 2006; Lam & Baumgarth, 2019) (see detailed review in the appendix, section 2). Virus titer – and virus shedding (Lau et al., 2010) – may peak before the production of new antibodies has even begun, leaving limited opportunity for within-host immune selection. If antibody-mediated selection pressure is strong at the point of transmission but weak during virus exponential growth, new variants could spread rapidly at the population level without being readily selected during the timecourse of a single infection.

We used a mathematical model to test our hypothesis that realistically timed antibody-mediated immune dynamics limit within-host antigenic evolution. We found three key results: (1) sIgA antibody neutralization at the point of inoculation protects

experienced hosts against reinfection and explains new antigenic variants' population level selective advantage. (2) If successful reinfection occurs, the delay between virus replication and the mounting of a recall adaptive immune response renders within-host antigenic evolution nearly neutral, even in experienced hosts. (3) It is therefore reasonable that substantial population immunity may need to accumulate before new antigenic variants are likely to observed in large numbers at the population level, whereas effective within-host selection would predict that they should be readily observable even before they proliferate.

Model overview

Our model reflects the following biological realities: 1. Seasonal influenza virus infections of otherwise healthy individuals typically last 5–7 days (Suess et al., 2012); 2. In influenza virus-naive individuals, it can take up to 7 days for anti-influenza virus antibodies to start being produced, effectively resulting in no selection (Fig. 1A); 3. In previously infected ("experienced") individuals, sIgA antibodies can block inoculating virions before they can invade host cells; (Wang et al., 2017) 4. However, if an inoculated virion manages to cause an infection in an experienced individual, it takes 2–5 days for the infected host to mount a adaptive recall response, including producing new antibodies (Coro et al., 2006; Zuccarino-Catania et al., 2014) (see Appendix Section 2 for further discussion of motivating immunology). Importantly, this contrasts with previous within-host models of virus evolution, which have assumed that antibody-mediated neutralization of virions during virus replication is strong from the point of inoculation onward and is the mechanism of protection against reinfection (Luo et al., 2012; Volkov et al., 2010). We discuss existing models and hypotheses for the rarity of population level influenza antigenic variation in section 7 of the Appendix.

We constructed a model of within-host influenza virus evolution that can be parametrized to reflect different hypothesized immune mechanisms, different host immune statuses, and different durations of infection. In the model, virions invade cells, replicate, possibly mutate, and decay. The innate immune response is modeled as depletion of invadable cells and the antibody-mediated immune response as variant specific increase in the virion decay rate. To assess the importance of transmission bottlenecks, initial virus diversity, and sIgA antibody neutralization in virus evolution, the point of transmission was modeled as a random sample of within-host virus diversity from a transmitting host, potentially thinned by neutralizing sIgA antibodies in the recipient host.

The model is continuous-time and stochastic: cell invasion, virion production, virus mutation, and virion decay are events that occur stochastically at rates governed by the current state of the system. The system is approximately well-mixed: counts of virions and cells were tracked without an explicit account of space. Infected and dead or removed cells are treated implicitly.

Parametrized as in Table 1, the model captures key features of influenza infections: rapid peaks approximately 2 days post infection and slower declines with clearance approximately a week post infection, with faster clearance in experienced hosts.

We describe our model in more detail in the Methods.

We investigated between-host and population-level consequences of our within-host dynamics using a simple transmission chain model and an SIR-like population-level model, which we describe in the Methods.

Results

With our model, we find that sufficiently strong antibody neutralization during the virus exponential growth period can potentially stop replication and block onward transmission, but this mechanism of protection results in detectable new variants in each homotypic reinfection, since the infection is terminated rapidly unless it generates a new antigenic variant that substantially escapes antibody neutralization (Fig. 2).

If there is antibody neutralization throughout virus exponential growth and it is not sufficiently strong to control the infection, this facilitates the emergence of new antigenic variants: variants can be generated *de novo* and then selected to detectable and easily transmissible frequencies (Fig. 1C,D,F, sensitivity analysis in Fig. A2). We term selection on a replicating within-host virus population "replication selection". Virus phenotypes that directly affect fitness independent of immune system interactions are likely to be subject to replication selection.

Adding a realistic delay to antibody production of two days post-infection (Lam & Baumgarth, 2019) curtails antigenic replication selection. There is no focused antibody-mediated response during the virus exponential growth phase, and so the infection is dominated by wild-type virus (Fig. 1C,D,G, sensitivity analysis in Fig. A2). Antigenic variant viruses begin to be selected to higher frequencies late in infection, once a memory response produces high concentrations of cross-reactive antibodies. But by the time this happens in typical infections, both mutant and wild-type populations have peaked and begun to decline due to innate immunity and depletion of invadable cells, so new antigenic variants remain too rare to be detectable with NGS (Fig. 1G).

We find that replication selection for antigenic novelty is viable only in prolonged infections that allow virus antigenic diversity and antibody selection pressure to coincide (Fig. 3). This reproduces the empirical observation that within-host adaptive antigenic evolution can be observed in prolonged infections of immune-compromised hosts (Xue et al., 2017) and findings that influenza within-host effective population sizes are large in prolonged infections (Lumby, Zhao, Breuer, & Illingworth, 2020).

Adding mucosal sIgA antibodies at the point of inoculation to our model produces realistic levels of protection against reinfection, and when reinfections do occur, they are overwhelmingly wild-type reinfections. New variants remain undetectably rare, reproducing observations from natural human infections (Fig. 1A–D, G–H, Fig. 4B–C)(Debbink et al., 2017; Dinis et al., 2016; McCrone et al., 2018; Leonard et al., 2016). The combination of mucosal sIgA protection and a realistically timed antibody recall response explains how there can exist immune protection against reinfection – and thus a population level selective advantage for new antigenic variants – without observable within-host antigenic selection in typical infections of experienced hosts.

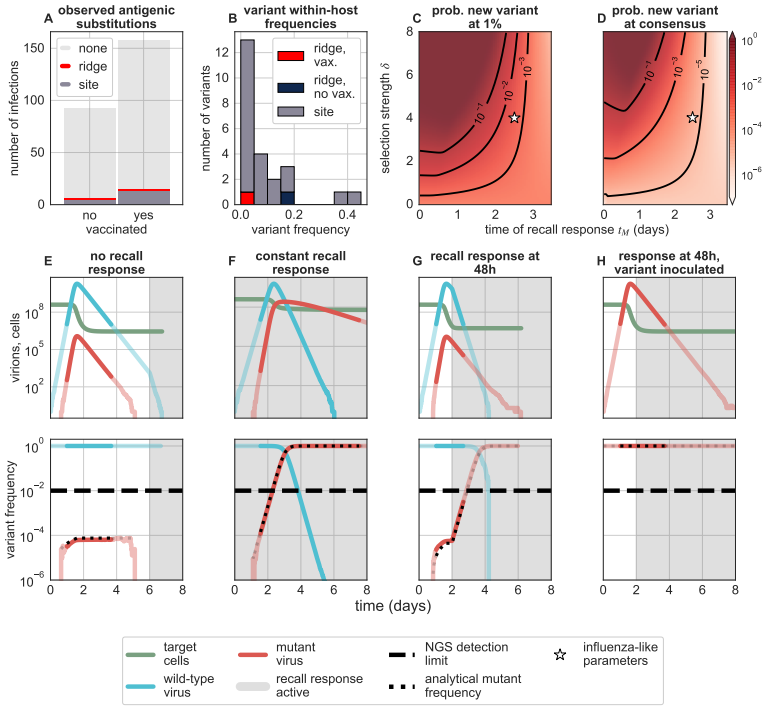

Fig. 1. Empirical and model within-host influenza virus evolutionary dynamics. (**A, B**) meta-analysis of A/H3N2 viruses from next-generation sequencing studies of naturally infected individuals (Debbink et al., 2017; McCrone et al., 2018). (**A**) Number of infections leading to substitutions in classically defined antigenic sites in HA (Wiley, Wilson, & Skehel, 1981) and in the antigenic ridge (Koel et al., 2013) regardless of within-host frequency. (**B**) Distribution of observed potential antigenicity altering substitutions from (**A**) by within-host variant frequency. (**C, D**) heatmaps showing model probability new variant selection to 50% (**C**) and NGS detection threshold of 1% (**D**) by 3 days post infection given the strength of immune selection δ, the recall response activation time t_M, and a wholly wild-type founding of size 1; from equation 35 in the Methods. Calculated with $c = 0$, but for $t_M > 1$, replication selection probabilities are approximately equal for all c, k pairs that yield a given δ (see Methods). Star denotes a plausible influenza-like parameter regime (25% escape from sterilizing-strength immunity $c = 0.75, k = 20$, recall response at 2.5 days post infection). Black lines are probability contours. (**E–H**) example model trajectories. Upper row: absolute counts of virions and target cells. Lower row: variant frequencies for wild-type (blue) and mutant (red). Dashed line shows 1% frequency, the detection limit of NGS. Dotted line shows an analytical prediction for variant frequency: $f_m(t) = \frac{e^{\delta\tau_k(t)}}{f_M^{-1} - 1 + e^{\delta\tau_k(t)}}$, where $\delta = k(1-c)$ is the fitness difference due to the adaptive immune response, $\tau_k(t) \leq t$ is the amount of time that adaptive immunity has been acting on a variant population, and f_M is the variant's frequency when positive selection begins (see Methods). Model scenarios: (**E**) naive; (**F**) experienced with $t_M = 0$; (**G**) experienced with $t_M = 2$; (**H**) experienced with $t_M = 2$ and new variant virion incoulated. All parameters in Table 1 unless otherwise stated.

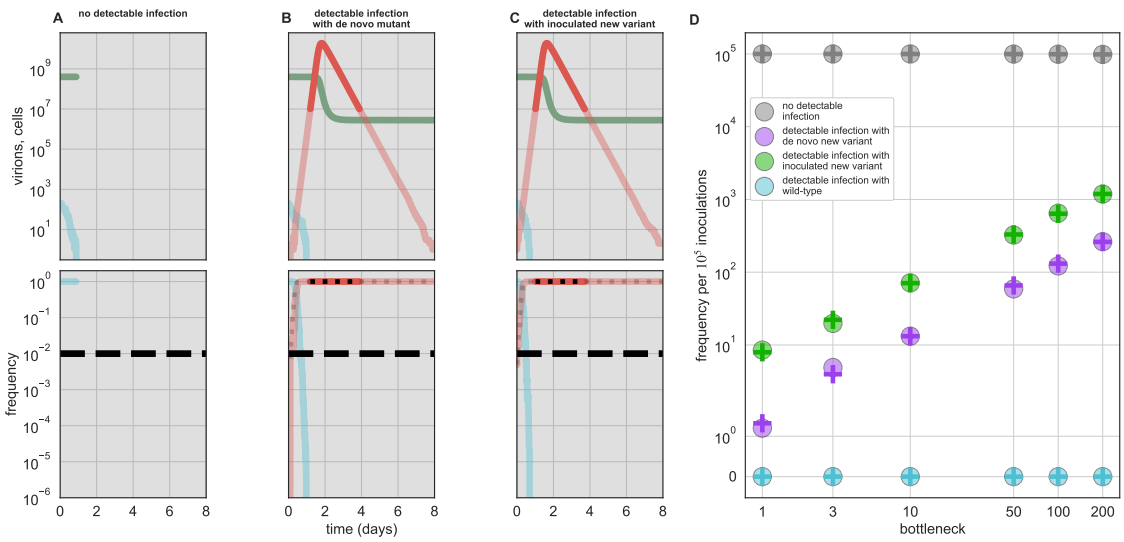

Fig. 2. Example timecourses and distribution of outcomes when adaptive immunity is active from the start of infection and sufficient to prevent detectable reinfection. $t_M = 0$, $k = 20$, yielding $\mathcal{R}^w(t = 0) < 1$ for the wild-type but $\mathcal{R}^m(t = 0) > 1$ for the mutant, where $\mathcal{R}^i(t)$ is the within-host effective reproduction number for strain i at time t (see Methods). No mucosal neutralization ($z_w = z_m = 0$); protection is only via neutralization during replication. Example timecourses from simulations with founding population (bottleneck) $b = 200$. (**A**–**C**) Top panels: absolute abundances of target cells (green), wild-type virions (blue), and mutant virions (red). Bottom panels: frequencies of virion types. Black dotted line is an analytical prediction for the mutant frequency given the emergence time. Black dashed line is the threshold for NGS detection. (**D**) Probabilities of no infection, *de novo* mutant infection, inoculated mutant infection, and wild-type infection per 10^5 inoculations of an immune host by a naive host. Circles are frequencies from simulation runs (10^6 runs for bottlenecks 1–10, 10^5 runs for bottlenecks 50–200). Plus-signs are analytical model predictions for probabilities (see Appendix section 3.8), with f_{mt} set equal to the average from donor host stochastic simulations for the given bottleneck. Parameters as Table 1 unless otherwise stated

Regardless of host immune status, an antigenic variant that has been generated *de novo* within a host must survive a series of population bottlenecks if it is to infect other individuals. To found a new infection, virions must be expelled from a currently infected host (excretion bottleneck), must enter another host (inter-host bottleneck), must escape mucus on the surface of the airway epithelium (mucus bottleneck), must avoid neutralization by sIgA antibodies on mucosal surfaces (sIgA bottleneck), and must infect a cell early enough to form a detectable fraction of the resultant infection (cell infection bottleneck) (Fig. 4A). The sum of all of these effects is the net bottleneck and typically results in infections being initiated by a single genomic variant (McCrone et al., 2018; Xue & Bloom, 2019; Ghafari, Lumby, Weissman, & Illingworth, 2020). That said, bottlenecks resulting from direct contact transmission may be substantially wider than those associated with respiratory droplet transmission (Varble et al., 2014) and more human studies are required to quantify these differences.

We find that because antigenic variants appear at very low within-host frequencies

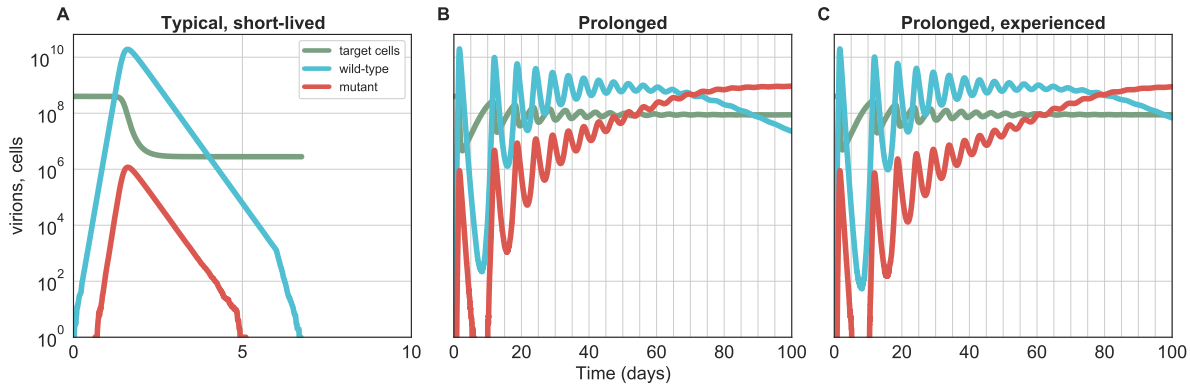

Fig. 3. Infection time courses in typical and immunocompromised individuals. (**A**) Time-course of typical, short-lived infection of a naive host where virus replication is limited by innate immunity and lack of target cells before substantial antibody production has occurred. (**B**) Time-course of infection of influenza virus naive host who is immunocompromised, modeled here as target cell replenishment and reduced adaptive immune virion kill rate. (**C**) Time-course of infection of influenza virus experienced host who is immunocompromised. Oscillations occur in prolonged infections due to replenishment of target cells. Parameters as in Table 1 except $\kappa_w = 0, p_C = 0.6$, $c = 0.5$, $k = 0.5$ in the immnunocompromised hosts. Adaptive immune response to the wild-type is activated 6 days post infection in naive hosts and 2 days post infection ($t_M = 2$) in experienced hosts. Recipient infections simulated until 100 days or clearance, whichever occurs first.

when generated *de novo* and undergo minimal or no replication selection, new variants most commonly reach detectable levels within hosts through founder effects at the point of inter-host transmission: a low-frequency antigenic variant generated in one host survives the net bottleneck to found the infection of a second host (Fig. 4D). Because the net inter-host bottleneck is tight, this is a rare event. When the recipient host is naive, new variants survive with a probability approximately equal to the donor host frequency times the bottleneck size (see Methods). New variant infections of naive hosts should occur in 1 in 10^5 to 1 in 10^4 of such infections given biologically plausible parameters (Fig. 4E–H).

If the recipient host is experienced, a new variant present in the inoculum is less likely to be neutralized than any competing wild-type virions present. The new variant is therefore disproportionately likely to survive the net bottleneck (Figs. 1, 4). We term this selection on inoculated diversity "inoculation selection". Neutralization at the point of transmission thus not only gives new variant infections their transmission advantage (population level selection) but may also increase the rate at which these new variant infections arise (inoculation selection).

The strength of inoculation selection depends on the ratio of the number of virions that compete to found an infection in the absence of well-matched sIgA antibodies (the mucus bottleneck size v) to the number of virions that actually found an infection (the final cell invasion bottleneck size b). The larger this v/b ratio is, the more inoculation selection in experienced hosts facilitates new variant emergence (Fig. 4F, Fig. A1).

When new variant immune escape is incomplete due to partial cross-reactivity with

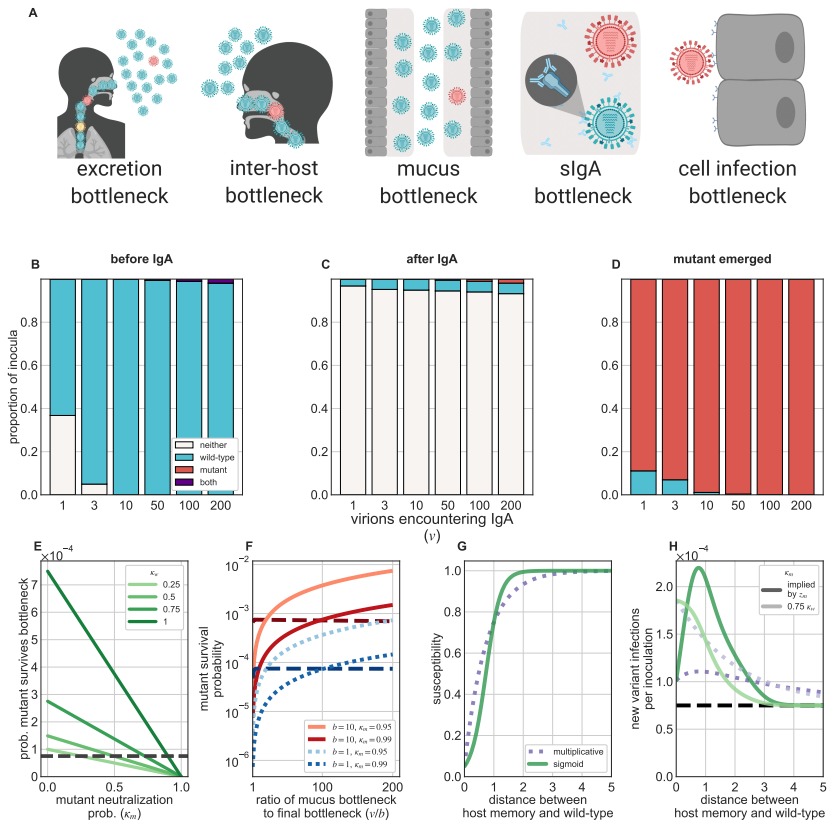

Fig. 4. Selection for antigenic variants at the point of transmission (inoculation selection). (**A**) Schematic of bottlenecks faced by both wild-type (blue) and variant (other colors) virions at the point of virus transmission. Key parameters for inoculation selection are the mucus bottleneck v – the mean number of virions that encounter sIgA – and the cell infection bottleneck size b. (**B–D**) Effect of sIgA selection at the point of inoculation with $b = 1$. (**B, C**) Analytical model distribution of virions inoculated into an immune host immediately before (**B**) and after (**C**) mucosal neutralization / the sIgA bottleneck. f_{mt} set to mean of stochastic simulations. (**D**) Distribution of founding virion populations (after the cell infection bottleneck) among individuals who developed detectable new variant infections in stochastic simulations. (**E–F**) Analytical model probability that a variant survives the final bottleneck. Dashed horizontal lines indicate probability in naive hosts. $f_{\text{mt}} = 7.5 \times 10^{-5}$ (the approximate mean in stochastic simulations for $b = 1$). (**E**) Variant probability of surviving all bottlenecks, as a function of wild-type neutralization probability κ_w and variant mucosal neutralization probability κ_m. (**F**) Mutant survival probability as a function of the ratio of v to b. (**G, H**) Effect of host susceptibility model on emergence of antigenic novelty. Per inoculation new variant emergence rates (**H**) depend on host immune status and on the relationship between virus antigenic phenotype and host susceptibility $(1 - z_w)$ (**G**). Plotted with $f_{\text{mt}} = 7.5 \times 10^{-5}$, and 25% susceptibility to (75% protection against, $z_1 = 0.75$) a variant one antigenic cluster away from host memory. Unless noted, parameters for all plots as in Table 1

previous antigenic variants, increased sIgA antibody neutralization is a double-edged sword for new variant virions. Competition to found the infection from wild-type viruses is reduced, but the new variant is itself at greater risk of being neutralized. The impact of inoculation selection therefore depends on the degree of similarity between previously encountered viruses and the new antigenic variant. An experienced recipient host could facilitate the survival of large-effect antigenic variants (like those seen at antigenic cluster transitions (Smith et al., 2004)) while retarding the survival of variants that provide less substantial immune escape (Fig. 4E, Fig. A1).

Inoculation selection is limited by the low frequency of new variants in donor hosts, the potentially small mucus bottleneck size v, and the fact that some previously infected hosts might not possess well-matched antibodies due to original antigenic sin (Davenport & Hennessy, 1956), antigenic seniority (Lessler et al., 2012), immune backboosting (Fonville et al., 2014), or other sources of individual-specific variation in antibody production (Lee et al., 2019). These factors combined make new variant onward transmission a rare event. At realistic parameter values and assuming all individuals develop well-matched antibodies to previously encountered antigenic variants, only $\sim$1 to 2 in 10^4 inoculations of an experienced host results in a new variant surviving the bottleneck (Fig. 4E,H). This rate is likely to be an overestimate due to the factors mentioned above. Moreover, it is only about 2- to 3-fold higher than the rate of bottleneck survival in naive hosts, where new variant infections should occasionally occur via neutral stochastic founder effects. In short, even in the presence of experienced hosts, antigenic selection is inefficient and most generated antigenic diversity is lost at the point of transmission. Because of these inefficiencies, new antigenic variants can be generated in every infected host without producing explosive antigenic diversification at the population level.

How readily a particular individual host or host population facilitates the emergence of new antigenic variants depends upon three important factors for which there are currently no reliable estimates: 1. how host susceptibility changes with extent of antigenic dissimilarity, 2. the ratio of virions that encounter sIgA to virions that found the infection (v/b), 3. the probability that a single variant virion inoculated alongside wild-type virions evades neutralization (Fig. 4E–H). Better estimates of these unknown quantities could shed light on how the distribution of host immunity affects the emergence of new antigenic variants. However, over a range of biologically plausible parameter values, our model contradicts the hypothesis that intermediately immune hosts who fail to block wild-type transmission are the most important source of antigenic novelty (Grenfell et al., 2004; Volkov et al., 2010); for influenza viruses, hosts whose mucosal immunity reliably blocks wild-type transmission while allowing mutant survival may be crucial (Fig. 4E,H).

To investigate the between-host consequences of within-host adaptation dominated by neutral founder effects and inoculation selection, we simulated transmission chains according to our within-host model, allowing the virus to evolve in a 1-dimensional antigenic space (Smith et al., 2004; Bedford, Rambaut, & Pascual, 2012) until a mutant becomes the majority variant. When all hosts in a model transmission chain are naive, antigenic evolution is non-directional and recapitulates the distribution of within-host mutations (Fig. 5A). When antigenic selection is constant throughout infection and even a moderate fraction of hosts are experienced, antigenic evolution is unrealistically

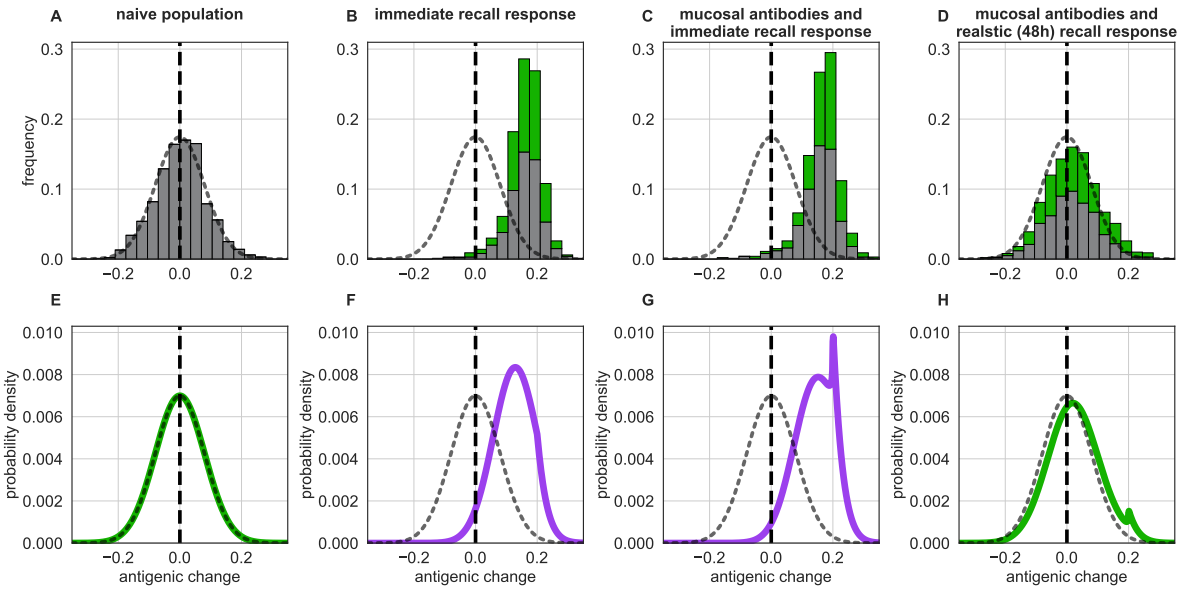

Fig. 5. Distribution of mutant effects given replication and inoculation selection. Distribution of antigenic changes along 1000 simulated transmission chains (**A**–**D**) and from an analytical model (**F**–**H**). In (**A,E**) all naive hosts, in other panels a mix of naive hosts and experienced hosts. Antigenic phenotypes are numbers in a 1-dimensional antigenic space and govern both sIgA cross immunity, σ, and replication cross immunity, c. A distance of ≥ 1 corresponds to no cross immunity between phenotypes and a distance of 0 to complete cross immunity. Gray line gives the shape of Gaussian within-host mutation kernel. Histograms show frequency distribution of observed antigenic change events and indicate whether the change took place in a naive (grey) or experienced (green) host. In (**B**–**D**) distribution of host immune histories is 20% of individuals previously exposed to phenotype -0.8, 20% to phenotype -0.5, 20% to phenotype 0 and the remaining 40% of hosts naive. In (**E**), a naive hosts inoculate naive hosts. In (**F**–**H**) a host with history -0.8 inoculate hosts with history -0.8. Initial strain has phenotype 0 in all sub-panels. Model parameters as in Table 1, except $k = 20$. Spikes in densities occur at 0.2 as this is the point of full escape in a host previously exposed to phenotype -0.8.

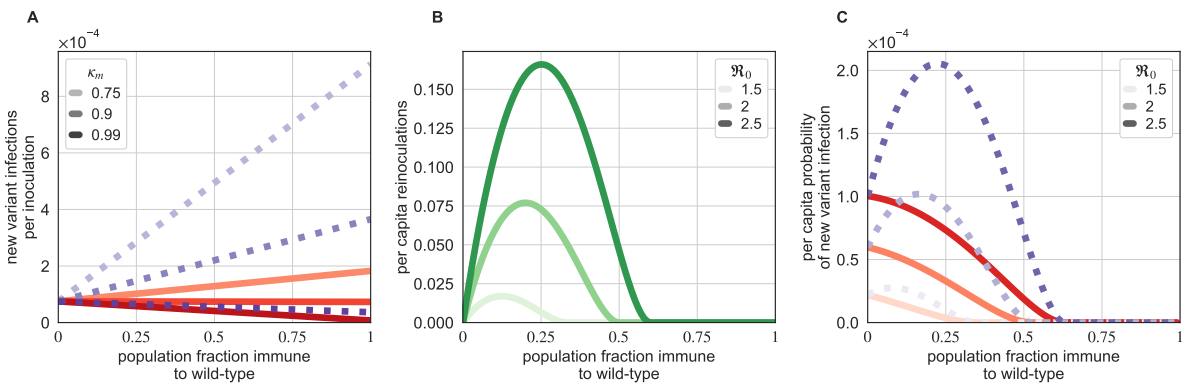

Fig. 6. Population level antigenic dynamics resulting from inoculation selection. Analytical model results (see Methods) for population-level inoculation selection, using parameters in Table 1 and $f_{\mathrm{mt}} = 7.5 \times 10^{-5}$ unless otherwise stated. (**A**) Probability per inoculation of a new variant founding an infection, as a function of fraction of hosts previously exposed to the wild-type, mucus bottleneck size v and sIgA cross immunity $\sigma = \kappa_m/\kappa_w$. Red solid lines: $v = 10$. Purple dotted lines: $v = 50$. (**B**) Expected per capita reinoculations of previously exposed hosts during an epidemic, given the fraction of previously exposed hosts in the population, if all hosts that were previously exposed to the wild-type virus are fully immune to the wild type virus, for varying population level basic reproduction number $\mathfrak{R}_0$. (**C**) Probability per individual host that a new variant founds an infection in that host during an epidemic, as a function of the fraction of hosts previously exposed to the wild type. Other hosts naive. $\sigma = 0.75$. Red solid lines: $v = 10$; purple dotted lines: $v = 50$ (as in **A**).

strong: the virus evolves directly away from existing immunity and large-effect mutants are observed frequently (Fig. 5B,C). When the model incorporates both mucosal antibodies and realistically timed recall responses, major antigenic variants become rare and the overall distribution of emerged variants better mimics empirical observations (Fig. 5D), including the phenomenon of quasi-neutral diversification within an antigenic cluster (Smith et al., 2004). A simple analytical model (see Methods) that assumes variants fix according to their replication and inoculation selective advantages also displays this behavior (Fig. 5B–H).

We used an epidemic-level model to study the consequences of individual-level inoculation selection for population-level antigenic diversification. If inoculation selection is efficient, an intermediate initial fraction of immune hosts maximizes the probability that a new variant infection is created during an epidemic (Fig. 6G). This is due to a trade-off between the frequency of naive or weakly immune "generator" hosts who can become infected and produce new antigenic variants through *de novo* mutation, and the frequency of strongly immune "selector" hosts who, if inoculated, facilitate the survival of these new variants. As selector host frequency increases, epidemics become rarer and smaller, eventually decreasing opportunities for evolution, but moderate numbers of efficient selectors can substantially increase rates of new variant emergence (Fig. 6E,G).

Discussion

Limitations

The study presented here has limitations that suggest opportunities for future investigation. We parameterized our models based on estimates from previous studies, but there are not good estimates for several important quantities. There are no high quality estimates of the rate of antibody-mediated neutralization in the presence of a homotypic adaptive immune response or of how much this rate is reduced by particular antigenic substitutions, and there may be substantial inter-individual variation (Lee et al., 2019). Within-host timeseries data from antigenically heterogeneous infections are needed to estimate these quantities. Similarly, there are no good empirical data on the size of the bottlenecks that precede or follow the sIgA bottleneck (Fig. 4A of the main text). Better estimates of these bottlenecks, and of the probabilities of neutralization for individual virions encountering mucosal IgA antibodies, would give more certainty about the strength of inoculation selection relative to neutral founder effects.

We also do not have a clear sense of exactly how neutralization probability in the mucosa (parameter κ in our model) and neutralization rate during replication (parameter k in our model) relate. We expect them to be positively related, but the exact strength and shape of this relationship is unknown. Knowing whether major antigenic changes reduces both equally or reduces one more than the other could help us better quantify the potential strength of inoculation selection and replication selection .

In short, better mechanistic understanding of mucosal naturalization could be extremely valuable for understanding and potentially predicting influenza virus evolution.

Implications

Importance of host heterogeneity

Experienced hosts are undoubtedly heterogeneous in their immunity to influenza (Lee et al., 2019), so the overall population average protection against homotypic reinfection with strain i, z_i, is in fact an average over experienced hosts. Since our model implies that the degree of neutralization difference between wild-type and mutant virions at the point of transmission strongly affects the probability of inoculation selection, it is possible that certain hosts with more focused immune responses – highly specific antibodies that neutralize wild-types well and new variants poorly – could be particularly important selector hosts. Similarly, immunocompromised hosts are excellent replication selectors (Xue et al., 2017; Lumby et al., 2020), and so their role in the generation of antigenic novelty and their impact on overall population level diversification rates deserve further study.

Small-population-like evolution

Prior modeling has suggested that despite repeated tight bottlenecks at the point of transmission, evolution of influenza viruses should resemble evolution in idealized large

populations (Sigal, Reid, & Wahl, 2018). In large populations, advantageous variants with small selective advantages should gradually fix and weakly deleterious variants should be purged. In these studies, diversity is rapidly generated and fit variants are selected to frequencies at which they are likely to pass through even a tight bottleneck. This is likely true of the phenotypes modeled in those studies, which include receptor binding avidity and virus budding time (Sigal et al., 2018). These phenotypes affect virus fitness throughout the timecourse of infection, so they can be efficiently replication-selected (where selection is manifest in the direct competition for infecting other cells rather than indirect competition by escaping antibodies). Indeed, next generation sequencing studies have found observable adaptative evolution of non-antigenic phenotypes in individual humans infected with avian H5N1 viruses (Welkers et al., 2019).

Seasonal influenza antigenic evolution does not resemble idealized large population evolution. Within an antigenic cluster, influenza viruses acquire substitutions that change the antigenic phenotype by small amounts. Given the large influenza virus populations within individual hosts, we might expect quasi-continuous directional pattern of evolution away from prior population immunity. Indeed, between clusters, evolution is strongly directional: only "forward" cluster transitions are observed. These are jumps – large antigenic changes. But incremental within-cluster evolution is *not* directional: the virus often evolves "backward" or "sideways" in antigenic space towards previously circulated variants (see Fig. 3 of (Smith et al., 2004)).

It is easy to explain this noisy jump pattern if within-host evolution is dominated by inoculation selection. Inoculation selection acts on the small sub-sample of donor-host diversity that passes through the excretion, inter-host, and mucus bottlenecks to encounter the sIgA bottleneck. Evolution via inoculation selection is therefore slower and more affected by stochasticity than evolution via replication selection (Fig. 4E–F). It resembles evolution in small populations – weakly adaptive and weakly deleterious substitutions become nearly neutral (Kimura, 1968; Ohta, 1992). If influenza virus evolution were not nearly neutral for small-effect substitutions at the within-host scale, it would be surprising to observe backward mutants and noisy evolution at higher scales (Fig. 6A–D). In fact, there may be analogous "neutralizing" population dynamics at higher scales as well, and those may also be necessary for explaining population level noisiness. But whatever happens at higher scales, within-host replication selection would create a strongly directional bias in what population-level diversity is introduced (Fig. 6A–D), and introduces many small forward mutants. Inoculation selection does not necessarily do this.

Population level neutralizing dynamics

Local influenza virus lineages rarely persist between epidemics (Russell et al., 2008; Bedford et al., 2015), and so new variants must establish chains of infections in other geographic locations in order to survive. New variant chains are most often founded when inoculations are common – that is, when existing variants are causing epidemics. Epidemics result in high levels of local competition between extant and new variant viruses for local susceptible hosts (Hartfield & Alizon, 2015) as well as metapopulation-scale competition to found epidemics in other locations. These

dynamics could create tight bottlenecks between epidemics similar to those that occur between hosts, resulting in dramatic epidemic-to-epidemic diversity losses. Further work is needed to elucidate mechanisms at the population and meta-population scales.

Population immunity sets the clock of antigenic evolution

Inoculation selection suggests a parsimonious mechanism by which accumulating population immunity could produce punctuated antigenic evolution. Population-level modeling has shown that influenza virus global epidemiological and phylogenetic patterns can be reproduced if antigenic variants emerge at the population level with increasing frequency the longer a wild-type variant circulates (Koelle, Kamradt, & Pascual, 2009). Under inoculation selection, new variant infections may emerge at an increasing rate per inoculation as the wild-type continues to circulate (Fig. 6E) because the density of strongly immune "selector" hosts increases. However, this depends on the ecology of hosts and the relative strength of inoculation selection and drift in partially and fully immune hosts.

Regardless of the strength of this effect, however, our prediction is that new variant infection foundation events should constitute a rare but non-negligible fraction of transmission events: on the order of 1 in 10^4 to 1 in 10^5. This parsimoniously explains both why new variants lineages are hard to observe prior to undergoing positive population level selection but are readily available to be selected upon (see appendix section 6) once that population level selection pressure has become sufficiently strong. The slow rate of antigenic evolution of A/H3N2 viruses in swine lends further support to this argument. A/H3N2 viruses accumulate genetic mutations at a similar pace in swine and humans, but antigenic evolution is much slower in swine (Lewis et al., 2016; De Jong et al., 2007). Slaughter for meat means that pig population turnover is high. It follows that the frequency of experienced hosts rarely becomes sufficient to facilitate observable antigenic emergence.

Implications for disease control

The dominance of inoculation selection in influenza virus antigenic evolution suggests that increased rates of influenza vaccination could slow the pace of influenza virus antigenic evolution. Well-matched intranasally administered live-attenuated influenza virus vaccines have the potential to induce high levels of sIgA production (Hoft et al., 2017), which could make it difficult even for large-effect mutants to survive the sIgA bottleneck, reducing the effective rate of population-level virus diversification. Moreover, vaccination could also reduce epidemic sizes or prevent local epidemics, thereby reducing total numbers of inoculations as herd immunity can insulate selector hosts from generator hosts (Fig. 6F,G). Future "universal" influenza vaccines that elicit antibodies targeting the more conserved stalk of the HA protein (Krammer & Palese, 2019) are also unlikely to promote the evolution of vaccine escape mutants at the human population-level. Many HA stalk targeting antibodies have limited capacity to perform initial neutralization of a virus inoculum and instead limit influenza virus infection through antibody dependent cellular cytotoxicity (ADCC), phagocytosis, or complement activation (He et al., 2015). Because HA stalk antibodies do not block

influenza receptor binding sites and require non-strain-specific virus limiting factors (innate immunity), they are likely to play limited role in both inoculation and replication selection.

The inoculation and replication selection paradigm has implications for the management of other pathogens. For example, HIV does not readily evolve resistance to contemporary pre-exposure prophylaxis (PrEP) antiviral drugs, but it can do so when these antivirals are taken by an individual who is already infected with HIV (Weis et al., 2016). Developing resistance at the moment of exposure is a difficult problem of inoculation selection for the virus, but developing resistance during an ongoing infection is an easier problem of replication selection. Selection on small un-diverse introduced populations may also be of interest in invasion biology and island biogeography.

Conclusion

The asynchrony between within-host virus diversity and antigenic selection pressure provides a simple mechanistic explanation for the phenomenon of weak within-host selection but strong population-level selection in seasonal influenza virus antigenic evolution. Measuring or even observing antibody selection in natural influenza infections is likely to be difficult because it is inefficient and consequently rare. Theoretical studies are therefore essential for understanding these phenomena and for determining which measurable quantities will facilitate influenza virus control. Our study highlights a critical need for new insights into sIgA neutralization and IgA responses to natural influenza virus infection and vaccination and shows that cross-scale dynamics can decouple selection and diversity, introducing randomness into otherwise strongly adaptive evolution.

Methods

Model notation

In all model descriptions, $X \mathrel{+}= y$ and $X \mathrel{-}= y$ denote incrementing and decrementing the state variable X by the quantity y, respectively, and $X = y$ denotes setting the variable X to the value y. $\dot{X}$ denotes the rate of event X.

Within-host model description

The within-host model is a target cell-limited model of within-host influenza virus infection with three classes of state variables:

- C: Target **C**ells available for the virus to infect. Shared across all virus variants.
- V_i: **V**irions of virus variant i

- E_i: Binary variable indicating whether the host has previously **E**xperienced infection with variant i ($E_i = 1$ for experienced individuals; $E_i = 0$ for naive individuals).

New virions are produced through infections of target cells by existing virions, at a rate $\beta C V_i$. Infection eventually renders a cell unproductive, so target cells decline at a rate $f\beta C\bar{V}$, where $\bar{V}$ is the total number of virions of all variants. The model allows mutation: a virion of variant j has some probability μ_{ji} of producing a virion of variant i when it reproduces.

Virions have a natural per-capita decay rate d_V. A fully active specific antibody-mediated immune response to variant i increases the virion per-capita decay rate for variant i by a factor k (assumed equal for all strains). The degree of activation of the immune response during an infection is given by a function $M(t)$, where t is the time since inoculation.

For this study, we consider a two-variant model with wild-type virions V_w and new variant (mutant) virions V_m, though the model generalizes to more than two variants.

$$\begin{aligned} C^+ &: \quad C \mathrel{+}= 1 \\ C^- &: \quad C \mathrel{-}= 1 \\ V_w^+ &: \quad V_w \mathrel{+}= 1 \\ V_w^- &: \quad V_w \mathrel{-}= 1 \\ V_m^+ &: \quad V_m \mathrel{+}= 1 \\ V_m^- &: \quad V_m \mathrel{-}= 1 \end{aligned} \tag{1}$$

The events occur at the following rates:

$$\begin{aligned} \dot{C}^- &= f\beta C(V_w + V_m) \\ \dot{C}^+ &= p_C C\left(1 - C/C_{\max}\right) \\ \dot{V}_w^+ &= \beta C V_w r_w (1-\mu) \\ \dot{V}_w^- &= V_w\Big(d_v + kM(t)\max\{E_w, cE_m\}\Big) \\ \dot{V}_m^+ &= \beta C\Big(V_m r_m + V_w r_w \mu\Big) \\ \dot{V}_m^- &= V_m\Big(d_v + kM(t)\max\{E_m, cE_w\}\Big) \end{aligned} \tag{2}$$

where $M(t)$ is a minimal model of a time-varying adaptive immune response given by:

$$M(t) = \begin{cases} 1, & t > t_M \\ 0, & \text{otherwise} \end{cases} \tag{3}$$

For simplicity, the equations are symmetric between wild-type and variant viruses, except that we neglect back mutation, which is expected to be rare during a single infection, particularly before mutants achieve large populations. The parameter c controls the degree of cross immunity between the two strains in the presence of an active antibody response, the parameters r_w and r_m allow the two strains optionally to

have distinct within-host replication fitnesses; for all results shown, we assumed no replication fitness difference ($r_w = r_m = r$), unless otherwise stated. A *de novo* adaptive immune response raised to a not-previously-encountered variant i can be modeled by setting $E_i = 1$ at a time $t_N^i \geq t_M$ post-infection.

We characterize a virus strain i by its within-host basic reproduction number $\mathcal{R}_0^i$, the mean number of new virions produced before decay by a single virion at the start of infection in a naive host:

$$\mathcal{R}_0^i := \frac{\beta C_{\max} r_i}{d_V} \tag{4}$$

When parametrizing our model, we fixed the within-host basic reproduction number $\mathcal{R}_0^i$, the initial target cell population $C_{\max}$, the virus reproduction rate r_i, and the shared virion decay rate d_V. We then calculated the implied β according to (4).

Another useful quantity is the within-host effective reproduction number $\mathcal{R}^i(t)$ of strain i at time t: the mean number of new virions produced before decay by a single virion of strain i at a given time t post-infection.

$$\mathcal{R}^i(t) := \frac{\beta C(t) r_i}{d_V + kM(t)\max\{E_m, cE_w\}} \tag{5}$$

Note that $\mathcal{R}_0^i$ is $\mathcal{R}^i(0)$ in a naive host, and that if $\mathcal{R}^i < 1$, the virus population will usually decline.

The distribution of virions that encounter sIgA antibody neutralization depends on the mean mucosal bottleneck size v (i.e. the mean number of virions that would pass through the mucosa in the absence of antibodies) and on the frequency of new variant $f_{\text{mt}} = f_m(t_{\text{inoc}})$ in the donor host at the time of inoculation t_{inoc}. n_w wild-type virions and n_m new variant virions encounter sIgA. The total number of virions $n_{\text{tot}} = n_w + n_m$ is Poisson distributed with mean v and each virion is independently a mutant with probability f_{mt} and otherwise a wild-type. The principle of Poisson thinning then implies:

$$\begin{aligned} n_m &\sim \text{Poisson}\Big(v f_{\text{mt}}\Big) \\ n_w &\sim \text{Poisson}\Big(v(1 - f_{\text{mt}})\Big) \end{aligned} \tag{6}$$

Note that since f_{mt} is typically small the results should also hold for a binomial model of n_w and n_m with a fixed total number of virions encountering sIgA antibodies: $v_{\text{tot}} = v$.

We then model the sIgA bottleneck – neutralization of virions by mucosal sIgA antibodies. Each virion of strain i is independently neutralized with a probability κ_i. This probability depends upon the strength of protection against homotypic reinfection κ and the sIgA cross immunity between strains σ, ($0 \leq \sigma \leq 1$):

$$\begin{aligned} \kappa_w &= \kappa \max\{E_w, \sigma E_m\} \\ \kappa_m &= \kappa \max\{E_m, \sigma E_w\} \end{aligned} \tag{7}$$

Since each virion of strain i in the exposure inoculum is independently neutralized with probability κ_i, then given n_w and n_m, the populations that compete the pass through the cell infection bottleneck x_w and x_m are binomially distributed:

$$\begin{aligned} x_w &\sim \text{Binomial}(n_w, \kappa_w) \\ x_m &\sim \text{Binomial}(n_m, \kappa_m) \end{aligned} \tag{8}$$

By Poisson thinning, this is equivalent to:

$$\begin{aligned} x_w &\sim \text{Poisson}\Big(v(1 - f_{\text{mt}})(1 - \kappa_w)\Big) \\ x_m &\sim \text{Poisson}\Big(v f_{\text{mt}}(1 - \kappa_m)\Big) \end{aligned} \tag{9}$$

At this point, the remaining virions are sampled without replacement to determine what passes through the cell infection bottleneck, b, with all virions passing through if $x_w + x_m \leq b$, so the final founding population is hypergeometrically distributed given x_w and x_m.

If $\kappa_w = \kappa_m = 0$, f_{mt} is small, and v is large, this is approximated by a binomially distributed founding population of size b, in which each virion is independently a new variant with (low) probability f_{mt} and is otherwise a wild-type (or by a Poisson distribution with a small mean of $f_{\text{mt}} b \ll 1$ mutants):

$$p_{\text{drift}} \approx 1 - (1 - f_{\text{mt}})^b \approx f_{\text{mt}} b \tag{10}$$

When there is mucosal antibody neutralization, the variant's survival probability can be reduced below this (inoculation pruning) or promoted above it (inoculation promotion), depending upon parameters. There can be inoculation pruning even when the variant is more fit (neutralized with lower probability, positive inoculation selection) than the wild-type (see Fig. 4E).

Within-host model parameters

Default parameter values for the minimal model and sources for them are given in Table 1.

Table 1: Model parameters, default values, and sources/justifications

Parameter	Meaning	Units	Value	Source or justification
t_M	time post infection onset of adaptive immune response in experienced hosts	days	2	literature (see review in Section 2)
t_N^w	time post infection of a novel immune response to the wild-type	days	6	literature (see review in Section 2)
p_C	per capita growth rate of target cells at low density	$\frac{1}{\text{days}}$	0	ignored on the timescale of a single infection
$C_{\max}$	maximum number of target cells	cells	4×10^8	standard in the modeling literature (Baccam, Beauchemin, Macken, Hayden, & Perelson, 2006; Luo, Reed, Mattingly, & Koelle, 2012; Hadjichrysanthou et al., 2016)
$\mathcal{R}_0$	within-host basic reproduction number for the virus	unitless	5	empirical fits of target cell models (Hadjichrysanthou et al., 2016)
r_w	average number of virions produced by a cell infected with wild-type virus	virions	100	literature (Frensing et al., 2016)
r_m	average number of virions produced by a cell infected with new variant virus	virions	100	no within-host deleteriousness for new variants
z_w	probability of no infection given homotypic re-inoculation for a host previously exposed to the wild-type	unitless	0.95	challenge studies (Clements, Betts, Tierney, & Murphy, 1986; Memoli et al., 2019)
β	rate of infectious contact between virions and target cells per cell per virion	$\frac{1}{\text{virions cells days}}$	calculated	from $\mathcal{R}_0$
f	number of target cells lost per infectious contact	cells	1	one cell lost per cell infection
k	additional per virion neutralization rate in the presence of an adaptive immune response	$\frac{1}{\text{days}}$	6	varied to test hypotheses
κ_w	probability an individual inoculated wild-type virion inoculated into an experienced host is neutralized in the mucosa	unitless	set from z_w	calculated from equation 19
κ_m	probability an individual inoculated wild-type virion inoculated into an experienced host is neutralized in the mucosa	unitless	$\sigma\kappa_w$	reduced relative to κ_m by immune escape
c	percentage cross immunity during viral replication between wild-type and new variant	unitless	0	full escape variant
σ	percentage cross immunity at sIgA bottleneck between wild-type and new variant	unitless	0	full escape variant
b	size of final / cell infection bottleneck	virions	1	NGS studies (McCrone et al., 2018; Xue & Bloom, 2019)
v	number of virions encountering sIgA	virions	$10 \times b$	
θ	transmission threshold	virions	10^7	chosen to give realistic transmission window (Tsang et al., 2015) and based on prior modeling studies (Russell et al., 2012)

Within host model analysis

Probability of bottleneck survival

If there are x_w wild-type virions and x_m variant virions, at least one variant passes through the cell infection bottleneck with probability:

$$p_{\text{cib}}(x_w, x_m, b) = 1 - \frac{\binom{x_w}{b}}{\binom{x_w+x_m}{b}} \tag{11}$$

Summing $p_{\text{cib}}(x_w, x_m)$ over the possible values of x_w and x_m weighted by their joint probabilities yields the variant's overall probability of successful onward transmission $p_{\text{surv}}(f_{\text{mt}}, v, b, \kappa, c)$:

$$p_{\text{surv}} = \sum_{x_m, x_w} P(x_m, x_w) p_{\text{cib}}(x_w, x_m, b) \tag{12}$$

$P(x_w, x_m)$ is the product of the probability mass functions for x_w and x_m:

$$P(x_m, x_w) = \frac{\bar{w}^{x_w}}{x_w!} \frac{\bar{m}^{x_m}}{x_m!} e^{-(x_w+x_m)} \tag{13}$$

where $\bar{w} = v(1 - f_{\text{mt}})(1 - \kappa_w)$ and $\bar{m} = v f_{\text{mt}}(1 - \kappa_m)$

At low donor host variant frequencies $f_{\text{mt}} \ll 1$ p_{surv} can be approximated using the fact that almost all probability is given to $x_m = 0$ and $x_m = 1$ (0 or 1 new variant after the sIgA bottleneck).

At least one new variant survives the sIgA bottleneck with probability:

$$p_{\text{inoc}}(\kappa_m, v, f_{\text{mt}}) = 1 - e^{-v f_{\text{mt}}(1-\kappa_m)} \tag{14}$$

If f_{mt} is small, there will almost always be only one such virion ($x_m = 1$). That new variant's probability of surviving the cell infection bottleneck depends upon how many wild-type virions are present after neutralization, x_w:

$$p_{\text{cib}}(x_w, 1, b) = 1 - \frac{\binom{x_w}{b}}{\binom{x_w+1}{b}} = 1 - \frac{x_w - b + 1}{x_w + 1} = \frac{b}{x_w + 1} \tag{15}$$

Summing over the possible x_w, we obtain a closed form for the unconditional probability $p_{\text{cib}}(\kappa_w, v, b)$ (see section 9.5 for a derivation):

$$p_{\text{cib}}(\kappa_w, v, b) = (1 - e^{-\bar{w}}) \frac{b}{\bar{w}} + e^{-\bar{w}} \sum_{j=0}^{b-1} \frac{\bar{w}^j}{j!} \left(1 - \frac{b}{j+1}\right) \tag{16}$$

where $\bar{w} = v(1 - f_{\text{mt}})(1 - \kappa_w)$ is the mean number of wild-type virions present after sIgA neutralization. If $b = 1$, this reduces the just the first term, and it is approximately equal to just the first term when $\bar{w}$ is large, since $e^{-\bar{w}}$ becomes small.

It follows that there is an approximate closed form for the probability that a variant survives the final bottleneck:

$$p_{\text{surv}}(\kappa_m, \kappa_w, v, b, f_{\text{mt}}) \approx p_{\text{inoc}}(\kappa_m, v, f_{\text{mt}}) * p_{\text{cib}}(\kappa_w, v, b) \tag{17}$$

We used this expression to calculate the analytical variant survival probabilities shown in the main text, and to gain conceptual insight into the strength of inoculation selection relative to neutral processes (see section 4.5).

Neutralization probability and probability of no infection

A given per-virion sIgA neutralization probability κ_i implies a probability z_i that a transmission event involving only virions of strain i fails to result in an infected cell.

Some transmissions fail even without sIgA neutralization; this occurs with probability $\exp(-v)$. Otherwise, with probability $1 - \exp(-v)$, n_i virions must be neutralized by sIgA to prevent an infection. We define z_i as the probability of no infection given inoculated virions in need of neutralization (i.e. given $n_i > 0$).

The probability that there are no remaining virions of strain i after mucosal neutralization is $\exp\big(-v(1-\kappa_i)\big)$. So we have:

$$z_i = \frac{\exp\big(-v(1-\kappa_i)\big) - \exp(-v)}{1 - \exp(-v)} \tag{18}$$

This can be solved algebraically for κ_i in terms of z_i, but it is more illuminating first to find the overall probability of no infection given inoculation p_{no} and then solve:

$$\begin{aligned} p_{\text{no}} &= \exp\big(-v(1-\kappa_i)\big) \\ \kappa_i &= 1 + \frac{\ln(p_{\text{no}})}{v} \end{aligned} \tag{19}$$

An infection occurs with probability $(1 - \exp(-v))(1 - z_i)$ (the probability of at least one virion needing to be neutralized times the conditional probability that it is not) so:

$$p_{\text{no}} = 1 - (1 - \exp(-v))(1 - z_i) \tag{20}$$

This yields the same expression for κ_i in terms of z_i as a direct algebraic solution of 18.

For moderate to large v, $1 - \exp(-v)$ approaches 1 so p_{no} approaches z_i and κ_i approaches $1 + \frac{\ln(z_i)}{v}$. This reflects the fact that for even moderately large v, it is almost always the case that $n_i > 0$: a least one virion must be neutralized to prevent infection. In those cases, z_i can be interpreted as the (approximate) probability of no infection given a transmission event (i.e. as p_{no}).

Note also that seeded infections can also go stochastically extinct; this occurs with approximate probability $\frac{1}{\mathcal{R}_0}$. Since $\mathcal{R}_0$ is large (5 to 10) at the start of infection in the absence of an adaptive immune response, stochastic extinction probabilities should be

low ($\frac{1}{5}$ to $\frac{1}{10}$), and equal in immune and naive hosts. We have therefore parametrized our model in terms of z_i, the probability that no cell is ever invaded, as that probability determines to leading order the frequency with which immunity protects against detectable reinfection given challenge.

Susceptibility models

Translating host immune histories into wild-type and mutant neutralization probabilities for the analysis in Fig. 4G,H requires a model of how susceptibility decays with antigenic distance, which we measure in terms of the typical distance between two adjacent "antigenic clusters" (Smith et al., 2004). Fig. 6 shows results for two candidate models: a multiplicative model used in a prior modeling and empirical studies of influenza evolution (Boni, Gog, Andreasen, & Feldman, 2006; Asaduzzaman, Ma, & van den Driessche, 2018), and a sigmoid model as parametrized from data on empirical HI titer and protection against infection (Coudeville et al., 2010).

In the multiplicative model, the probability $z(i,x)$ of no infection with strain i given that the nearest strain to i in the immune history is strain x is given by:

$$z(i,x) = z_0 \left(\frac{z_1}{z_0}\right)^{d(i,x)} \tag{21}$$

where z_0 is the probability of no infection given homotypic reinfection, $d(i,x)$ is the antigenic distance in antigenic clusters between i and x, and z_1 is the probability of no infection given $d(i,x) = 1$.

In the sigmoid model:

$$z(i,x) = 1 - \frac{1}{1 + e^{b\left(\ln\left(T(i,x)\right) - a\right)}} \tag{22}$$

where $a = 2.844$ and $b = 1.299$ (α and β estimated in (Coudeville et al., 2010)) and $T(i,x)$ is the individual's HI titer against strain i (Coudeville et al., 2010). To convert this into a model in terms of z_0 and z_1 we calculate the typical homotypic titer T_0 implied by z_0 and the k-fold-drop D in titer per unit of antigenic distance implied by z_1, since units in antigenic space correspond to a k-fold reductions in HI titer for some value k (Smith et al., 2004). We calculate T_0 by plugging z_0 and T_0 into equation 22 and solving. We calculate D by plugging z_1 and $T_1 = T_0 D^{-1}$ into equation 22 and solving. We can then calculate $T(i,x)$ as:

$$T(i,x) = T_0 D^{-d(i,x)} \tag{23}$$

Probability of replication selection

The approximate probability of replication selection to frequency x by time t used here relies on the fact that the within-host frequency of variant f_m obeys a replicator

equation of the form:

$$\frac{\mathrm{d}f_m}{\mathrm{d}t} = f_m(1 - f_m)\delta(t) \tag{24}$$

where $\delta(t)$ is the fitness difference between variant and wild-type at time t (see appendix section 3 for a derivation).

If the variant is neutral in the absence of adaptive immunity, then $\delta(t) = k(1 - c)$ if $t > t_M$ and $\delta(t) = 0$ otherwise. So if the new variant has emerged by t_M, then at a time $t > t_M$:

$$f_m(t) = \frac{e^{\delta(t-t_M)}}{e^{\delta(t-t_M)} + f_M^{-1} - 1} \tag{25}$$

where $\delta = k(1 - c)$ and $f_M = f_m(t_M)$

When additional mutations after the first cannot be neglected, we add a correction term to $\frac{\mathrm{d}f_m}{\mathrm{d}t}$ for $t_e < t < \min\{t_M, t_{\text{peak}}\}$ (see appendix section 3.4):

$$\frac{\mathrm{d}f_m}{\mathrm{d}t} = f_m(1 - f_m)\delta(t) + \mu\mathcal{R}_0 d_V \tag{26}$$

If a new variant is to achieve a frequency of at least x by time t, we must have:

$$f_M^{-1} < e^{\delta(t-t_M)}\frac{1-x}{x} + 1 \tag{27}$$

f_M depends upon the time t_e that the mutant emerges. When $t_e < t_M$, we make the following approximation for f_M (see section 3 for derivation):

$$\begin{aligned} f_M = f_m(t_M) = f_0 + \left(1 - \frac{1}{\mu g_0(t_M - t_e) + \frac{1}{1-f_0}}\right) &\approx f_0 + \mu g_0(t_M - t_e) \\ f_0 &:= \frac{1}{be^{(g_0-d_V)t_e}} \\ g_0 &:= \mathcal{R}_0 d_V \end{aligned} \tag{28}$$

The first term in the expression, f_0, is the frequency of the mutant when it emerges. This is simply one over the expected wild-type population size at t_e. The second term accounts for contributions to the mutant frequency from further mutations after the first to occur; it is relatively unimportant if the first emergence time t_e is early but can be meaningful if t_e is relatively late.

Both terms depend on g_0, the approximate per capita production rate of wild-type virions early in infection. In the absence of adaptive immunity, new virions are produced at a per capita rate $g(t) = \mathcal{R}_0 d_V \frac{C(t)}{C_{\max}}$. We make the approximation that $C(t) \approx C_{\max}$ early in infection, and therefore $g(t) \approx g(0) = \mathcal{R}_0 d_V = g_0$.

The dependence of f_M on t_e implies a time t^* before which the new variant must emerge if it is to reach a target frequency x by a time t. Ignoring ongoing mutation and assuming $t_e < t_M$:

$$t^*(x,t) = \frac{\ln\left(\left(e^{\delta(t-t_M)\frac{1-x}{x}}\right)+1\right) - \ln b}{g_0 - d_V} \tag{29}$$

If $t_e > t_M$, we can only calculate an approximate value for t^*. We choose an underestimate of t^* (i.e. $t^*_{\text{approx}} < t^*$ to avoid overestimating the probability of replication selection at small t_M.

$$t^*_{\text{approx}}(x,t) = \frac{\ln\left(\frac{1-x}{x}\right) - \ln(b) + \delta t - k t_M}{g_0 - d_V - k + \delta} \tag{30}$$

See appendix section 3 for full derivations of equations 29 and 30.

Assuming new variant emergence occurs according to a continuous-time, variable-rate Poisson process the cumulative distribution function of the variant emergence time t_e, is given by:

$$\lambda_m(t) = \mu g_w(t) V_w(t)(p_{\text{sse}}) \tag{31}$$

where $g_w(t) = r_w \beta C(t)$ is the per capita rate at which the wild-type virions are produced, μ is the mutation rate, and p_{sse} is the probability that the generated new variant survives stochastic extinction, which is given by

$$p_{\text{sse}} = \frac{r_m \beta C(t)}{r_m \beta C(t) + d_v + kM(t)\max\{E_m, cE_w\}} \tag{32}$$

It follows that:

$$P(t_e < x) = 1 - e^{-\Lambda_m(x)} \tag{33}$$

where

$$\Lambda_m(x) = \int_0^x \lambda_m(x)dx \tag{34}$$

Given this distribution function, it is straightforward to calculate the probability of replication selection to a given frequency a by time t:

$$p_{\text{repl}}(a,t) = P(t_e < t^*(a,t)) = 1 - e^{-\Lambda(t^*(a,t))} \tag{35}$$

This analytical model agrees well with simulations (Figs. 7,8), and is used to calculate the heatmaps shown in Fig. 1, with the approximations that early in infection $g_w(t) \approx g_w(0) = g_0$ and

$$V_w(t) \approx \begin{cases} b\exp\Big((g_0 - d_V)t\Big) & t < t_M \\ V_w(t_M)\exp\Big((g_0 - d_V - k)(t_M - t)\Big) & t \geq t_M \end{cases} \tag{36}$$

These approximations give us a closed form for $\Lambda_m(x)$. When $t^* > t_M$, the integral $\int_0^{t^*} \lambda_m(x)dx$ can be evaluated piecewise, first from 0 to t_M, and then from t_M to t^*. This can also be used to find evaluate the probability density function (PDF) of emergence times, as needed.

Finally, note that for $t_e < t_M$, the expression for p_{repl} in practice depends only on $\delta = (1-c)k$, not on c and k separately. In the absence of an antibody response, the mutant is generated with near certainty by 1 day post-infection ($P(t_e < 1) \approx 1$, Fig. 7B). So when $t_M \geq 1$, values for p_{repl} calculated with $c = 0, \delta = k$ – as in (Fig. 1C,D) – will in fact hold for any c and k that produce that fitness difference δ.

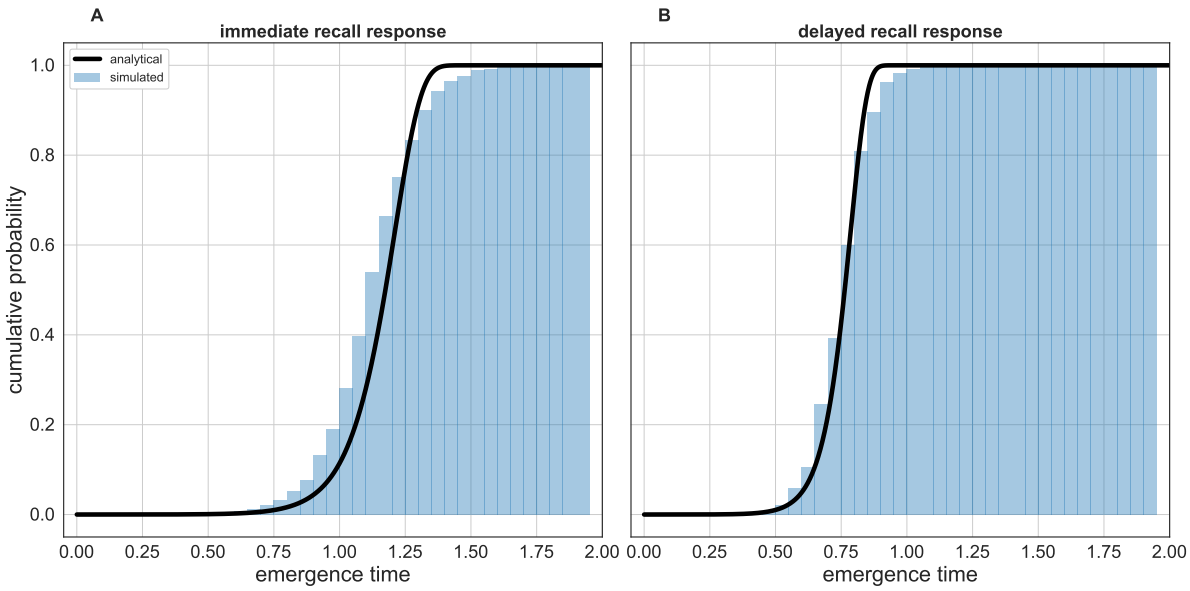

Fig. 7. Comparison of analytically calculated mutant emergence time cumulative distribution function (CDF) with simulations. Black line shows analytically calculated CDF. Blue cumulative histogram shows distribution of mutant emergence times for 250 000 simulations from the stochastic within-host model with (**A**) an immediate recall response ($t_M = 0$) and (**B**) a realistic recall response at 48 hours post-infection ($t_M = 2$). Other model parameters as parameters in Table 1.

Model abstractions and limitations

This is a simple target cell-limited model, but the decrease in infectible cells as the infection proceeds has a more qualitative interpretation: any and all antigenicity-agnostic limiting factors that come into play as the virion and infected cell populations grow. This could include the action of innate immunity (see immunological review in SI), which acts in part by killing infected cells and by rendering healthy cells difficult to invade via inflammation. The key mechanistic role played by the target cells is to introduce a non-antigenic limiting factor on infections. This prevents an infection from successively evolving out from under successive adaptive responses, as occurs in HIV and in influenza patients with compromised immune systems (Xue et al., 2017).

Similarly, the adaptive immune response we introduce at 48 hours is qualitative – it is modeled simply as an increase in the virion decay rate for matching virions. This

response could represent IgA, but other antigenicity-specific mode of virus control could also be subsumed under the increased virion decay rate, for instance IgG antibodies, antibody dependent cellular cytotoxicity (ADCC), et cetera. The key point we establish is that none of these mechanisms can efficiently replication select because they all emerge once non-antigenic limiting factors have come into play. They speed clearance, but do not substantially alter viral evolution. A corollary to this point is that there are many mechanisms – and interventions – that could reduce the severity of influenza infections without selecting for antigenic evolution, including universal vaccines, as we discuss in the main text.

Within-host simulations (Figs. 1, 4)

To evaluate the relative likelihood of new variant emergence in experienced hosts through replication selection and inoculation selection and to check the validity of the analytical results, we simulated 10^6 transmissions from a naive host to a previously immune host. The transmitting host was simulated for 10 days, which given the selected model parameters is sufficient time for almost all infections to be cleared. Time of transmission was randomly drawn from the time period during which the infected host had a transmissible virus population and an inoculum of fixed size was drawn from the within-host virus population at that time. Variant counts in the inoculum were Poisson distributed with probability equal to the variant frequency within the transmitting host at the time of transmission. We simulated the recipient host until the clearance of infection and found the mean and maximum frequencies of transmissible variant: that is, the variant frequencies when total virus population was above an assumed transmission threshold of 10^7 virions (Russell et al., 2012). For Fig. 4D, we defined an infection with an emerged new variant as an infection with a maximum new variant frequency during the transmission window of greater than 50%.

Transmission chain model (Fig. 5)

To study evolution along transmission chains with mixed host immune statuses, we modeled the virus phenotype as existing in a 1-dimensional antigenic space. Host susceptibility s_x to a given phenotype x was $s_x = \min\{1, \min\{|x - y_i|\}\}$ for all phenotypes y_i in the host's immune history.

Within-host cross immunity c between two phenotypes y_i and y_j was equal to $\max\{0, 1 - |y_i - y_j|\}$. When mucosal antibodies were present, protection against infection z_x was equal to the strength of homotypic protection $z_{\max}$ scaled by susceptibility: $z_x = (1 - s_x)z_{\max}$. κ_x was calculated from z_x by $\exp\big(-v(1 - \kappa_x)\big) = z_x$. We used $z_{\max} = 0.95$. Note that this puts us in the regime in which intermediately immune hosts are the best inoculation selectors (Fig. 4H). We set $k = 20$ so that there would be protection against reinfection in the condition with an immediate recall response condition but without mucosal antibodies.

We then simulated a chain of infections as follows. For each inoculated host, we tracked two virus variants: an initial majority antigenic variant and an initial minority antigenic variant. If there were no minority antigenic variants in the inoculum, a new focal

minority variant (representing the first antigenic variant to emerge *de novo*) was chosen from a Gaussian distribution with mean equal to the majority variant and a given variance, which determined the width of the mutation kernel (for results shown in Fig. 6, we used a standard deviation of 0.08). We simulated within-host dynamics in the host according to our within-host stochastic model.

We then chose a random timepoint from the host's infection during which the viral population was above the 10^7 virion transmission threshold. We chose a random immune history for our recipient host according to a pre-specified distribution of host immune histories. We then simulated an inoculation and, if applicable, subsequent infection, according to the within-host model described above. If the recipient host developed a transmissible infection, it became a new donor host. If not, a new random timepoint from the old donor host and new recipient host were chosen, and the process was repeated. We iterated this until the first phenotypic change event (i.e. a generated or transmitted minority phenotype became the new majority phenotype) and examined the observed distribution of phenotypic changes compared to the mutation kernel.

We founded each chain with an individual infected with all virions of phenotype 0, representing the current wild-type. For the results shown in Fig. 6, we set the population distribution of immune histories as follows: 20% -0.8, 20% -0.5, 20% 0.0, and the remaining 40% of hosts naive. This qualitatively models the directional pressure that is thought to canalize virus evolution (Bedford et al., 2012) once a cluster has begun to circulate.

Analytical mutation kernel shift model (Fig. 5)

To assess the causes of the observed behavior in our transmission chain model, we also studied analytically how replication and inoculation selection determine the distribution of observed fixed mutants given the mutation kernel when a host with one immune history inoculates another host with a different immune history.

We fixed a transmission time $t = 2$ days, roughly corresponding to peak within-host virus titers. We calculated the probability density function of the values of the emergence time t_e according to equation 33. For each possible phenotype, we calculated f_{mt} at the point of transmission for each possible emergence time t_e, according to equation 26, determining k and c according to the wild-type phenotype, mutant phenotype, and host immune history. We then calculated the probability of mutant survival at the point of transmission according to equation 17, integrating over the possible emergence times and determining κ_w and κ_m according to the wild-type phenotype, mutant phenotype, and host immune history. Finally, we multiplied each phenotype's survival probability by the same Gaussian mutation kernel used in the chain simulations (with mean 0 and s.d. 0.08), and normalized to determined the predicted distribution of surviving mutants given the mutation kernel and the differential survival probabilities for different phenotypes.

Population-level model (Fig. 6)

To evaluate the probability of variants being selected and proliferating during a local influenza virus epidemic, we first noted that the per-inoculation rate of new variant chains for a population with n_s susceptibility classes (which can range from full susceptibility to full immunity) is:

$$\sum_{i=1}^{n_s} s_i(0) p_{\text{surv}}(\kappa_m(i), \kappa_w(i), v, b, f_{\text{mt}}) \tag{37}$$

where $\kappa_w(i)$ and $\kappa_m(i)$ are the mucosal antibody neutralization probabilities for wild-type and variant associated with susceptibility class i, and $s_i(0) = \frac{S_i(0)}{N}$ is the initial fraction of individuals in susceptibility class i.

We then considered a well-mixed population with and frequency-dependent transmission, where infected individuals from all susceptibility classes are equally infectious if infected. There is an existing result for the final total average total number infected R_∞ in such a population if an epidemic occurs (Magal, Seydi, & Webb, 2018). The average total number of times any individual is inoculated during that epidemic is $\mathfrak{R}_0 R_\infty$, where $\mathfrak{R}_0$ is the population-level basic reproduction number (Miller, 2012). We can then calculate the probability that a variant transmission chain is started in an arbitrary focal individual:

$$\mathfrak{R}_0 R_\infty \sum_{i=1}^{n_s} s_i(0) p_{\text{surv}}(\kappa_m(i), \kappa_w(i), v, b, f_{\text{mt}}) \tag{38}$$

Sensitivity analysis (Fig. A2)

We assessed the sensitivity of our results to parameter choices by re-running our simulation models with randomly generated parameter sets chosen via Latin Hypercube Sampling from across a range of biologically plausible values. Figure A2 gives a summary of the results.

We simulated 50 000 infections of experienced hosts according to each of 10 random parameter sets. We selected parameter sets using Latin Hypercube sampling to maximize coverage of the range of interest without needing to study all possible permutations. We did this for the following bottleneck sizes: 1, 3, 10, 50.

We analyzed two cases: one in which the immune response is unrealistically early and one in which it is realistically timed. In the unrealistically early antibody response model, t_M varied between $t_M = 0$ and $t_M = 1$. In the realistically timed antibody response model, t_M varied between $t_M = 2$ and $t_M = 4.5$. Other parameter ranges were shared between the two models (Table 2).

Discussion of sensitivity analysis results can be found in Section 8 below.

Table 2: Sensitivity analysis parameter ranges shared between models

Parameter	Minimum value	Maximum value
t_N	6	9
$C_{\max}$	10^8	10^9
$\mathcal{R}_0$	5	15
r	10	500
z_w	0.70	0.99
z_m/z_w	0.5	0.9
μ	0.33×10^{-6}	0.33×10^{-4}
d_V	2	8
k	3	16
c	0.5	1
θ	10^6	10^8
v/b	1	50

Meta-analysis (Fig. 1)

We downloaded processed variant frequencies and subject metadata from the two NGS studies of immunocompetent human subjects naturally infected with A/H3N2 with known vaccination status (Debbink et al., 2017; McCrone et al., 2018) from the study Github repositories and journal websites. We independently verified that reported antigenic site and antigenic ridge amino acid substitutions were correctly indicated, determined the number of subjects with no NGS-detectable antigenic amino acid substitutions, and produced figures from the aggregated data.

Computational methods

For within-host model stochastic simulations, we used the Poisson Random Corrections (PRC) tau-leaping algorithm (Hu & Li, 2009). We used an adaptive step size; we chose step sizes according to the algorithm of Hu and Li (Hu & Li, 2009) to ensure that estimated next-step mean values were non-negative, with a maximum step size of 0.01 days. Variables were set to zero if events performed during a timestep would have reduced the variable to a negative value. For the sterilizing immunity simulations in Figure 2, we used a smaller maximum step size of 0.001 days in recipient hosts to better handle mutation dynamics involving very small numbers of replicating virions.

We obtained numerical solutions of equations, including systems of differential equations and final size equations, in Python using solvers provided with SciPy (Jones, Oliphant, Peterson, et al., 2001).

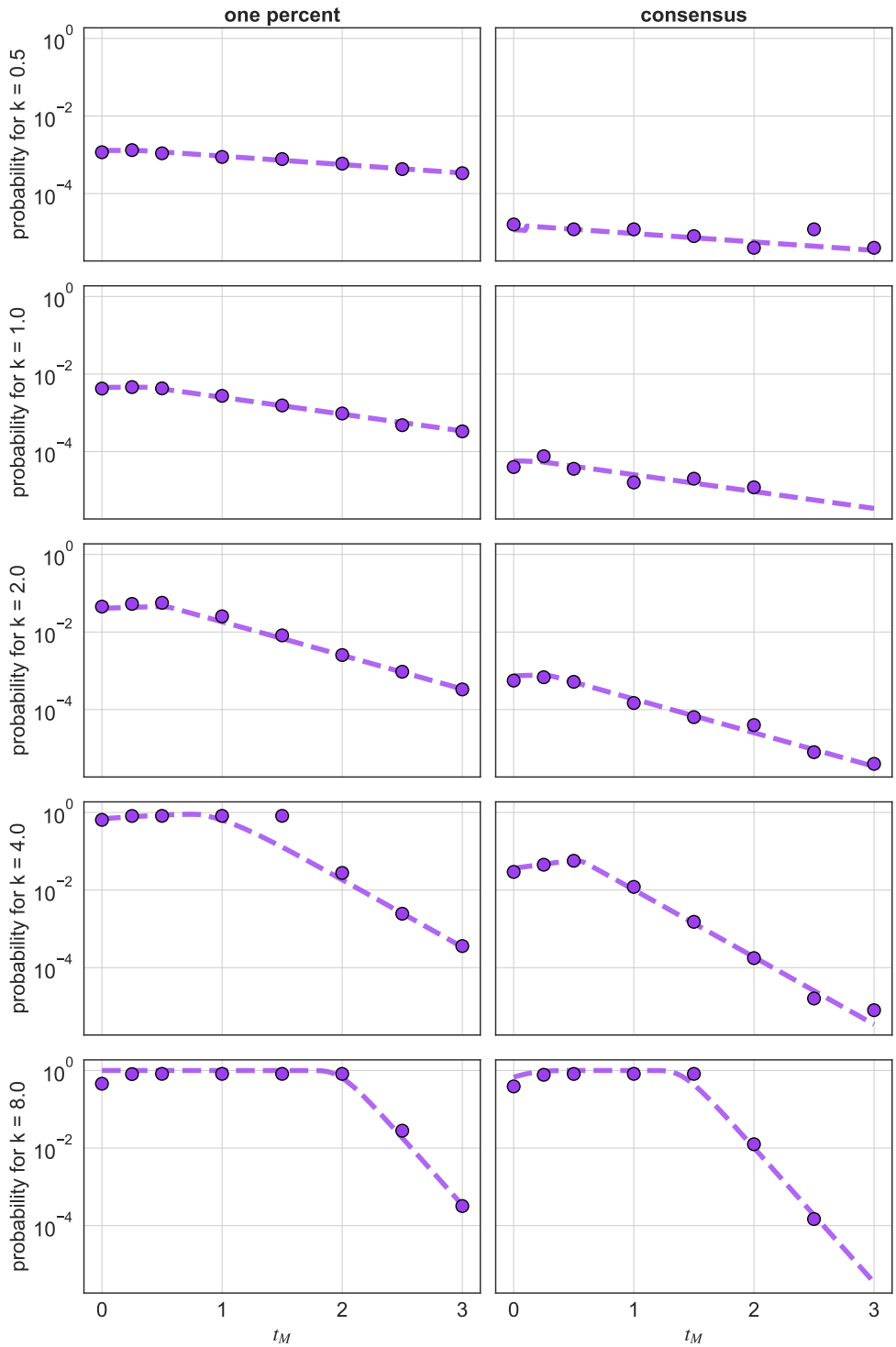

Fig. 8. Comparison of analytically calculated probability of replication selection with stochastic simulations. Probability of replication selection to one percent (left column) or consensus (right column) by $t = 3$ days post-infection as a function of k and t_M for 250 000 simulations from the stochastic within-host model. $c = 0$ (so the fitness difference $\delta = k$). Other model parameters as parameters in Table 1. Dashed lines show analytical prediction and dots show simulation outcomes.

References

Archetti, I. & Horsfall, F. L. (1950). Persistent antigenic variation of influenza A viruses after incomplete neutralization in ovo with heterologous immune serum. *Journal of Experimental Medicine*, *92*(5), 441–462.

Asaduzzaman, S. M., Ma, J., & van den Driessche, P. (2018). Estimation of cross-immunity between drifted strains of influenza A/H3N2. *Bulletin of Mathematical Biology*, *80*(3), 657–669.

Baccam, P., Beauchemin, C., Macken, C. A., Hayden, F. G., & Perelson, A. S. (2006). Kinetics of influenza A virus infection in humans. *Journal of Virology*, *80*(15), 7590–7599.

Ball, F., Britton, T., & Neal, P. (2016). On expected durations of birth–death processes, with applications to branching processes and sis epidemics. *Journal of Applied Probability*, *53*(1), 203–215.

Bazinet, A. L., Zwickl, D. J., & Cummings, M. P. (2014). A gateway for phylogenetic analysis powered by grid computing featuring GARLI 2.0. *Systematic Biology*, *63*(5), 812–8. doi:10.1093/sysbio/syu031

Bedford, T., Rambaut, A., & Pascual, M. (2012). Canalization of the evolutionary trajectory of the human influenza virus. *BMC Biology*, *10*(1), 38.

Bedford, T., Riley, S., Barr, I. G., Broor, S., Chadha, M., Cox, N. J., … Kelso, A., et al. (2015). Global circulation patterns of seasonal influenza viruses vary with antigenic drift. *Nature*, *523*(7559), 217.

Bonhoeffer, S., Lipsitch, M., & Levin, B. R. (1997). Evaluating treatment protocols to prevent antibiotic resistance. *Proceedings of the National Academy of Sciences*, *94*(22), 12106–12111.

Boni, M. F., Gog, J. R., Andreasen, V., & Feldman, M. W. (2006). Epidemic dynamics and antigenic evolution in a single season of influenza A. *Proceedings of the Royal Society B: Biological Sciences*, *273*(1592), 1307–1316.

Burke, D. F. & Smith, D. J. (2014). A recommended numbering scheme for influenza A HA subtypes. *PLoS one*, *9*(11), e112302. doi:10.1371/journal.pone.0112302

Cao, P. & McCaw, J. M. (2017). The mechanisms for within-host influenza virus control affect model-based assessment and prediction of antiviral treatment. *Viruses*, *9*(8), 197.

Caton, A. J., Brownlee, G. G., Yewdell, J. W., & Gerhard, W. (1982). The antigenic structure of the influenza virus A/PR/8/34 hemagglutinin (H1 subtype). *Cell*, *31*(2), 417–427.

Clements, M., Betts, R., Tierney, E., & Murphy, B. (1986). Serum and nasal wash antibodies associated with resistance to experimental challenge with influenza A wild-type virus. *Journal of Clinical Microbiology*, *24*(1), 157–160.

Coro, E. S., Chang, W. W., & Baumgarth, N. (2006). Type I IFN receptor signals directly stimulate local B cells early following influenza virus infection. *Journal of Immunology*, *176*(7), 4343–4351.

Coudeville, L., Bailleux, F., Riche, B., Megas, F., Andre, P., & Ecochard, R. (2010). Relationship between haemagglutination-inhibiting antibody titres and clinical protection against influenza: Development and application of a bayesian random-effects model. *BMC Medical Research Methodology*, *10*(1), 18.

Davenport, F. M. & Hennessy, A. V. (1956). A serologic recapitulation of past experiences with influenza A; antibody response to monovalent vaccine. *Journal of Experimental Medicine*, *104*(1), 85–97.

Davis, A. K., McCormick, K., Gumina, M. E., Petrie, J. G., Martin, E. T., Xue, K. S., ... Hensley, S. E. (2018). Sera from individuals with narrowly focused influenza virus antibodies rapidly select viral escape mutations in ovo. *Journal of Virology*, *92*(19), e00859–18.

De Jong, J., Smith, D. J., Lapedes, A., Donatelli, I., Campitelli, L., Barigazzi, G., ... Osterhaus, A., et al. (2007). Antigenic and genetic evolution of swine influenza A (H3N2) viruses in europe. *Journal of Virology*, *81*(8), 4315–4322.

Debbink, K., McCrone, J. T., Petrie, J. G., Truscon, R., Johnson, E., Mantlo, E. K., ... Lauring, A. S. (2017). Vaccination has minimal impact on the intrahost diversity of H3N2 influenza viruses. *PLoS Pathogens*, *13*(1), e1006194. doi:10.1371/journal.ppat.1006194

Dinis, J. M., Florek, N. W., Fatola, O. O., Moncla, L. H., Mutschler, J. P., Charlier, O. K., ... Friedrich, T. C. (2016). Deep sequencing reveals potential antigenic variants at low frequencies in influenza A virus-infected humans. *Journal of Virology*, *90*(7), 3355–3365.

Ferguson, N. M., Galvani, A. P., & Bush, R. M. (2003). Ecological and immunological determinants of influenza evolution. *Nature*, *422*(6930), 428.

Fonville, J. M., Wilks, S., James, S. L., Fox, A., Ventresca, M., Aban, M., ... Pham, Q., et al. (2014). Antibody landscapes after influenza virus infection or vaccination. *Science*, *346*(6212), 996–1000.

Frensing, T., Kupke, S. Y., Bachmann, M., Fritzsche, S., Gallo-Ramirez, L. E., & Reichl, U. (2016). Influenza virus intracellular replication dynamics, release kinetics, and particle morphology during propagation in mdck cells. *Applied Microbiology and Biotechnology*, *100*(16), 7181–7192.

Ghafari, M., Lumby, C. K., Weissman, D., & Illingworth, C. J. R. (2020). Inferring transmission bottleneck size from viral sequence data using a novel haplotype reconstruction method. *bioRxiv*.

Gog, J. R. (2008). The impact of evolutionary constraints on influenza dynamics. *Vaccine*, *26*, C15–C24.

Grenfell, B. T., Pybus, O. G., Gog, J. R., Wood, J. L., Daly, J. M., Mumford, J. A., & Holmes, E. C. (2004). Unifying the epidemiological and evolutionary dynamics of pathogens. *Science*, *303*(5656), 327–332.

Hadjichrysanthou, C., Cauët, E., Lawrence, E., Vegvari, C., de Wolf, F., & Anderson, R. M. (2016). Understanding the within-host dynamics of influenza A virus: From theory to clinical implications. *Journal of The Royal Society Interface*, *13*(119), 20160289.

Han, A. X., Maurer-Stroh, S., & Russell, C. A. (2019). Individual immune selection pressure has limited impact on seasonal influenza virus evolution. *Nature Ecology & Evolution*, *3*(2), 302.

Hartfield, M. & Alizon, S. (2014). Epidemiological feedbacks affect evolutionary emergence of pathogens. *The American Naturalist*, *183*(4), E105–E117.

Hartfield, M. & Alizon, S. (2015). Within-host stochastic emergence dynamics of immune-escape mutants. *PLoS Computational Biology*, *11*(3), e1004149.

He, W., Mullarkey, C. E., Duty, J. A., Moran, T. M., Palese, P., & Miller, M. S. (2015). Broadly neutralizing anti-influenza virus antibodies: Enhancement of neutralizing

potency in polyclonal mixtures and iga backbones. *Journal of Virology*, *89*(7), 3610–3618.

Hensley, S. E., Das, S. R., Bailey, A. L., Schmidt, L. M., Hickman, H. D., Jayaraman, A., ... Bennink, J. R., et al. (2009). Hemagglutinin receptor binding avidity drives influenza A virus antigenic drift. *Science*, *326*(5953), 734–736.

Hoft, D. F., Lottenbach, K. R., Blazevic, A., Turan, A., Blevins, T. P., Pacatte, T. P., ... Belshe, R. B. (2017). Comparisons of the humoral and cellular immune responses induced by live attenuated influenza vaccine and inactivated influenza vaccine in adults. *Clin. Vaccine Immunol.* *24*(1), e00414–16.

Hu, Y. & Li, T. (2009). Highly accurate tau-leaping methods with random corrections. *Journal of Chemical Physics*, *130*(12), 03B618.

Iwasa, Y., Michor, F., & Nowak, M. A. (2004). Evolutionary dynamics of invasion and escape. *Journal of Theoretical Biology*, *226*(2), 205–214.

Jones, E., Oliphant, T., Peterson, P., et al. (2001). SciPy: Open source scientific tools for Python. Retrieved from http://www.scipy.org/

Katoh, K., Misawa, K., Kuma, K., & Miyata, T. (2002). MAFFT: a novel method for rapid multiple sequence alignment based on fast Fourier transform. *Nucleic Acids Research*, *30*(14), 3059–3066. doi:10.1093/nar/gkf436

Kennedy, D. A. & Read, A. F. (2017). Why does drug resistance readily evolve but vaccine resistance does not? *Proceedings of the Royal Society B: Biological Sciences*, *284*(1851), 20162562.

Kimura, M. (1968). Evolutionary rate at the molecular level. *Nature*, *217*(5129), 624–626.

Koel, B. F., Burke, D. F., Bestebroer, T. M., van der Vliet, S., Zondag, G. C., Vervaet, G., ... Russell, C. A., et al. (2013). Substitutions near the receptor binding site determine major antigenic change during influenza virus evolution. *Science*, *342*(6161), 976–979. doi:10.1126%2Fscience.1244730

Koelle, K., Cobey, S., Grenfell, B. T., & Pascual, M. (2006). Epochal evolution shapes the phylodynamics of interpandemic influenza A (H3N2) in humans. *Science*, *314*(5807), 1898–1903. doi:10.1126/science.1132745

Koelle, K., Kamradt, M., & Pascual, M. (2009). Understanding the dynamics of rapidly evolving pathogens through modeling the tempo of antigenic change: Influenza as a case study. *Epidemics*, *1*(2), 129–137.

Koelle, K. & Rasmussen, D. A. (2015). The effects of a deleterious mutation load on patterns of influenza A/H3N2's antigenic evolution in humans. *eLife*, *4*, e07361.

Krammer, F. (2019). The human antibody response to influenza A virus infection and vaccination. *Nature Reviews Immunology*, 1.

Krammer, F. & Palese, P. (2019). Universal influenza virus vaccines that target the conserved hemagglutinin stalk and conserved sites in the head domain. *Journal of Infectious Diseases*, *219*(Supplement_1), S62–S67.

Kucharski, A. J., Lessler, J., Read, J. M., Zhu, H., Jiang, C. Q., Guan, Y., ... Riley, S. (2015). Estimating the life course of influenza A (H3N2) antibody responses from cross-sectional data. *PLoS Biology*, *13*(3), e1002082.

Kucharski, A. & Gog, J. R. (2011). Influenza emergence in the face of evolutionary constraints. *Proc. R. Soc. Lond. B: Biol. Sci.*

Lam, J. H. & Baumgarth, N. (2019). The multifaceted B cell response to influenza virus. *Journal of Immunology*, *202*(2), 351–359.

Lau, L. L., Cowling, B. J., Fang, V. J., Chan, K.-H., Lau, E. H., Lipsitch, M., ... Peiris, J. M., et al. (2010). Viral shedding and clinical illness in naturally acquired influenza virus infections. *Journal of Infectious Diseases*, *201*(10), 1509–1516.

Lee, J. M., Eguia, R., Zost, S. J., Choudhary, S., Wilson, P. C., Bedford, T., ... Bloom, J. D. (2019). Mapping person-to-person variation in viral mutations that escape polyclonal serum targeting influenza hemagglutinin. *bioRxiv*, 670497.

Leonard, A. S., McClain, M. T., Smith, G. J., Wentworth, D. E., Halpin, R. A., Lin, X., ... Gilbert, A. S., et al. (2016). Deep sequencing of influenza A virus from a human challenge study reveals a selective bottleneck and only limited intrahost genetic diversification. *Journal of Virology*, *90*(24), 11247–11258.

Lessler, J., Riley, S., Read, J. M., Wang, S., Zhu, H., Smith, G. J., ... Cummings, D. A. (2012). Evidence for antigenic seniority in influenza A (H3N2) antibody responses in southern china. *PLoS Pathogens*, *8*(7), e1002802.

Lewis, N. S., Russell, C. A., Langat, P., Anderson, T. K., Berger, K., Bielejec, F., ... Fouchier, R. A., et al. (2016). The global antigenic diversity of swine influenza A viruses. *eLife*, *5*, e12217.

Linderman, S. L., Chambers, B. S., Zost, S. J., Parkhouse, K., Li, Y., Herrmann, C., ... Zheng, N.-Y., et al. (2014). Potential antigenic explanation for atypical H1N1 infections among middle-aged adults during the 2013–2014 influenza season. *Proceedings of the National Academy of Sciences*, *111*(44), 15798–15803.

Lumby, C. K., Zhao, L., Breuer, J., & Illingworth, C. J. R. (2020). A large effective population size for within-host influenza virus infection. *bioRxiv*. doi:10.1101/2020.04.17.046250

Luo, S., Reed, M., Mattingly, J. C., & Koelle, K. (2012). The impact of host immune status on the within-host and population dynamics of antigenic immune escape. *Journal of The Royal Society Interface*, *9*(75), 2603–2613.

Magal, P., Seydi, O., & Webb, G. (2018). Final size of a multi-group SIR epidemic model: Irreducible and non-irreducible modes of transmission. *Mathematical Biosciences*, *301*, 59–67.

Matrosovich, M. N., Matrosovich, T. Y., Gray, T., Roberts, N. A., & Klenk, H.-D. (2004). Neuraminidase is important for the initiation of influenza virus infection in human airway epithelium. *Journal of Virology*, *78*(22), 12665–12667.

McCrone, J. T., Woods, R. J., Martin, E. T., Malosh, R. E., Monto, A. S., & Lauring, A. S. (2018). Stochastic processes constrain the within and between host evolution of influenza virus. *eLife*, *7*, e35962.

Memoli, M. J., Han, A., Walters, K.-A., Czajkowski, L., Reed, S., Athota, R., ... Morens, D. M., et al. (2019). Influenza A reinfection in sequential human challenge: Implications for protective immunity and "universal" vaccine development. *Clinical Infectious Diseases*, ciz281.

Miller, J. C. (2012). A note on the derivation of epidemic final sizes. *Bulletin of Mathematical Biology*, 1–17.

Moncla, L. H., Zhong, G., Nelson, C. W., Dinis, J. M., Mutschler, J., Hughes, A. L., ... Friedrich, T. C. (2016). Selective bottlenecks shape evolutionary pathways taken during mammalian adaptation of a 1918-like avian influenza virus. *Cell Host & Microbe*, *19*(2), 169–180.

Neuzil, K. M., Jackson, L. A., Nelson, J., Klimov, A., Cox, N., Bridges, C. B., ... Shay, D. (2006). Immunogenicity and reactogenicity of 1 versus 2 doses of

trivalent inactivated influenza vaccine in vaccine-naive 5–8-year-old children. *Journal of Infectious Diseases*, *194*(8), 1032–1039.

Nobusawa, E. & Sato, K. (2006). Comparison of the mutation rates of human influenza A and B viruses. *Journal of Virology*, *80*(7), 3675–3678.

Ohta, T. (1992). The nearly neutral theory of molecular evolution. *Annual Review of Ecology and Systematics*, *23*(1), 263–286.

Perelson, A. S., Rong, L., & Hayden, F. G. (2012). Combination antiviral therapy for influenza: Predictions from modeling of human infections. *Journal of Infectious Diseases*, *205*(11), 1642–1645.

Perron, G. G., Inglis, R. F., Pennings, P. S., & Cobey, S. (2015). Fighting microbial drug resistance: A primer on the role of evolutionary biology in public health. *Evolutionary Applications*, *8*(3), 211–222.

Recker, M., Pybus, O. G., Nee, S., & Gupta, S. (2007). The generation of influenza outbreaks by a network of host immune responses against a limited set of antigenic types. *Proceedings of the National Academy of Sciences*, *104*(18), 7711–7716.

Russell, C. A., Fonville, J. M., Brown, A. E., Burke, D. F., Smith, D. L., James, S. L., ... Schrauwen, E. J., et al. (2012). The potential for respiratory droplet–transmissible A/H5N1 influenza virus to evolve in a mammalian host. *Science*, *336*(6088), 1541–1547.

Russell, C. A., Jones, T. C., Barr, I. G., Cox, N. J., Garten, R. J., Gregory, V., ... Hurt, A. C., et al. (2008). The global circulation of seasonal influenza A (H3N2) viruses. *Science*, *320*(5874), 340–346.

Sigal, D., Reid, J. N., & Wahl, L. M. (2018). Transmission cycles generate diversity in pathogenic viruses. *bioRxiv*, 339861.

Smith, D. J., Lapedes, A. S., de Jong, J. C., Bestebroer, T. M., Rimmelzwaan, G. F., Osterhaus, A. D., & Fouchier, R. A. (2004). Mapping the antigenic and genetic evolution of influenza virus. *Science*, *305*(5682), 371–376.

Stamatakis, A. (2014). RAxML version 8: A tool for phylogenetic analysis and post-analysis of large phylogenies. *Bioinformatics*, *30*(9), 1312–3. doi:10.1093/bioinformatics/btu033

Suess, T., Remschmidt, C., Schink, S. B., Schweiger, B., Heider, A., Milde, J., ... Braun, C., et al. (2012). Comparison of shedding characteristics of seasonal influenza virus (sub) types and influenza A (H1N1) pdm09; Germany, 2007–2011. *PloS one*, *7*(12), e51653.

Tsang, T. K., Cowling, B. J., Fang, V. J., Chan, K.-H., Ip, D. K., Leung, G. M., ... Cauchemez, S. (2015). Influenza A virus shedding and infectivity in households. *Journal of Infectious Diseases*, *212*(9), 1420–1428.

Valesano, A. L., Fitzsimmons, W. J., McCrone, J. T., Petrie, J. G., Monto, A. S., Martin, E. T., & Lauring, A. S. (2019). Influenza b viruses exhibit lower within-host diversity than influenza a viruses in human hosts. *BioRxiv*, 791038.

Varble, A., Albrecht, R. A., Backes, S., Crumiller, M., Bouvier, N. M., Sachs, D., García-Sastre, A., et al. (2014). Influenza A virus transmission bottlenecks are defined by infection route and recipient host. *Cell Host & Microbe*, *16*(5), 691–700.

Volkov, I., Pepin, K. M., Lloyd-Smith, J. O., Banavar, J. R., & Grenfell, B. T. (2010). Synthesizing within-host and population-level selective pressures on viral populations: The impact of adaptive immunity on viral immune escape. *Journal of The Royal Society Interface*, *7*(50), 1311–1318.

Wang, Y.-Y., Harit, D., Subramani, D. B., Arora, H., Kumar, P. A., & Lai, S. K. (2017). Influenza-binding antibodies immobilise influenza viruses in fresh human airway mucus. *European Respiratory Journal*, *49*(1), 1601709.

Weis, J. F., Baeten, J. M., McCoy, C. O., Warth, C., Donnell, D., Thomas, K. K., ... Matsen IV, F. A., et al. (2016). Prep-selected drug resistance decays rapidly after drug cessation. *AIDS*, *30*(1), 31.

Welkers, M. R., Pawestri, H. A., Fonville, J. M., Sampurno, O. D., Pater, M., Holwerda, M., ... Setiawaty, V., et al. (2019). Genetic diversity and host adaptation of avian h5n1 influenza viruses during human infection. *Emerging Microbes & Infections*, *8*(1), 262–271.

Wikramaratna, P. S., Sandeman, M., Recker, M., & Gupta, S. (2013). The antigenic evolution of influenza: Drift or thrift? *Philosophical Transactions of the Royal Society B: Biological Sciences*, *368*(1614), 20120200.

Wiley, D., Wilson, I., & Skehel, J. (1981). Structural identification of the antibody-binding sites of Hong Kong influenza haemagglutinin and their involvement in antigenic variation. *Nature*, *289*(5796), 373.

Wilker, P. R., Dinis, J. M., Starrett, G., Imai, M., Hatta, M., Nelson, C. W., ... Kawaoka, Y., et al. (2013). Selection on haemagglutinin imposes a bottleneck during mammalian transmission of reassortant h5n1 influenza viruses. *Nature Communications*, *4*, 2636.

Wrammert, J., Smith, K., Miller, J., Langley, W. A., Kokko, K., Larsen, C., ... Helms, C., et al. (2008). Rapid cloning of high-affinity human monoclonal antibodies against influenza virus. *Nature*, *453*(7195), 667.

Xue, K. S. & Bloom, J. D. (2019). Reconciling disparate estimates of viral genetic diversity during human influenza infections. *Nature Genetics*, 1.

Xue, K. S., Stevens-Ayers, T., Campbell, A. P., Englund, J. A., Pergam, S. A., Boeckh, M., & Bloom, J. D. (2017). Parallel evolution of influenza across multiple spatiotemporal scales. *eLife*, *6*, e26875. doi:10.7554/eLife.26875

Yu, G., Smith, D. K., Zhu, H., Guan, Y., & Lam, T. T.-Y. (2017). ggtree: An r package for visualization and annotation of phylogenetic trees with their covariates and other associated data. *Methods in Ecology and Evolution*, *8*(1), 28–36. doi:10.1111/2041-210X.12628

Zinder, D., Bedford, T., Gupta, S., & Pascual, M. (2013). The roles of competition and mutation in shaping antigenic and genetic diversity in influenza. *PLoS Pathogens*, *9*(1), e1003104.

Zuccarino-Catania, G. V., Sadanand, S., Weisel, F. J., Tomayko, M. M., Meng, H., Kleinstein, S. H., ... Shlomchik, M. J. (2014). CD80 and PD-L2 define functionally distinct memory B cell subsets that are independent of antibody isotype. *Nature Immunology*, *15*(7), 631.

Acknowledgments

We thank Daniel B. Cooney, Andrea L. Graham, Joseph Gibson, Katelyn M. Gostic, Alvin X. Han, Chadi M. Saad-Roy, and Edward C. Schrom for helpful discussions.

We thank the GISAID Initiative and the influenza surveillance and research groups who openly shared the genetic sequence data used in this work (a table with accession numbers and associated labs is available online in the project materials and data repositories on Github and OSF, see below for links).

Author contributions

CAR, DHM, and VNP conceived and designed the research. DHM designed and analyzed the mathematical models with support from FWR, RAN, and SAL. DHM analyzed the within-host data. EP conducted phylogenetic analyses. DHM produced the figures. All authors contributed substantially to the interpretation of results and the writing and revising of the manuscript.

Competing interests

The authors declare no competing interests.

Data and materials availability

All code, data, and other materials needed to reproduce the analysis in this paper are provided online on the project Github repository:
https://github.com/dylanhmorris/asynchrony-influenza

They are also available on OSF:
https://doi.org/10.17605/OSF.IO/jdsbp/

Output data generated by stochastic simulations, within-host NGS meta-analysis, and phylogenetic analyses are archived on OSF:
https://doi.org/10.17605/OSF.IO/jdsbp/

Appendix

Asynchrony between virus diversity and antibody selection limits influenza virus evolution

Dylan H. Morris[1*], Velislava N. Petrova[2], Fernando W. Rossine[1], Edyth Parker[3,4], Bryan T. Grenfell[1,5], Richard A. Neher[6], Simon A. Levin[1], and Colin A. Russell[4*]

[1]Department of Ecology & Evolutionary Biology, Princeton University, Princeton, NJ 08544, USA
[2]Department of Human Genetics, Wellcome Trust Sanger Institute, Cambridge, UK
[3]Department of Veterinary Medicine, University of Cambridge, Cambridge, UK
[4]Department of Medical Microbiology, Academic Medical Center, University of Amsterdam, Amsterdam, NL
[5]Fogarty International Center, National Institutes of Health, Bethesda, MD 20892, USA
[6]Biozentrum, University of Basel, Basel, CH
[*]Correspondence to dhmorris@princeton.edu, c.a.russell@amsterdamumc.nl.

April 27, 2020

Contents

1 Summary **4**

2 Immunological underpinnings of the inoculation selection model **4**
2.1 Strong selection at the point of inoculation 4
2.2 Weak selection during exponential virus growth 5
2.3 Selection during exit of an infected host 6
2.4 Nature and timing of previous exposure and effects on inoculation selection 6

3 Detailed within-host model analysis **7**
3.1 Expression for the within-host mutant frequency 7
3.2 CDF of mutant emergence times 9
3.3 Accuracy of the replication selection analytical result 9
3.4 Derivation of mutant frequency over time given ongoing *de novo* mutation and no selection 9
3.5 Consequences of ongoing *de novo* mutation 11
3.6 Approximations underestimate replication selection 11
3.7 Replication selection is helped when individual infected cells are more productive 12
3.8 Replication selection in the presence of sterilizing immunity 12

4 Point of transmission analysis **14**
4.1 Distinction between selection and drift at the point of transmission . . . 14
4.2 The inoculation selection paradigm 14

4.3 Expression for and properties of the new variant survival probability . . . 15
4.3.1 Properties of these probabilities . . . 15
4.4 Mutant survival probability increases as transmitted mutant frequency increases . . . 16
4.5 The relative importance of selection and drift at the point of inoculation 16
4.6 Effect of sIgA cross immunity on probability of inoculation selection . . . 17

5 Parameter uncertainties and sensitivity analysis 19
5.1 Strength of selection . . . 19
5.1.1 Antibody-mediated virion neutralization rate . . . 20
5.1.2 Small values of k are a sub-hypothesis . . . 20
5.2 Relationship between mucosal and replication neutralization rates . . . 21
5.3 Bottleneck sizes . . . 21
5.4 Sensitivity analysis . . . 22

6 Polyphyletic emergence of antigenicity altering substitutions 27
6.1 Background . . . 27
6.2 Phylogenetic Methods . . . 27
6.3 A/H1N1 . . . 28
6.4 A/H3N2 2008-2011 . . . 30
6.5 A/H3N2 2012–2014 . . . 32

7 Prior studies and alternative hypotheses 34
7.1 Models with protection through neutralization during replication . . . 34
7.2 The importance of inoculated diversity . . . 35
7.3 Limits to immune escape through non-strain specific limiting factors . . . 36
7.4 Fitness costs for antigenic mutants . . . 37
7.5 Previous discussion of selective bottlenecks in the literature . . . 38
7.6 Comparison with the antimicrobial resistance literature . . . 38
7.7 Alternative explanations for rare within-host antigenic variants . . . 38
7.7.1 Protection through neutralization during replication, i.e. an immediate recall response . . . 39
7.7.2 Heterogeneous neutralization rates during early viral replication . 39
7.7.3 A key role for intermediately immune hosts . . . 40
7.7.4 Within-host deleteriousness . . . 40

8 Further implications 41
8.1 Consequences for modeling influenza virus dynamics . . . 41
8.2 Egg and mouse passage experiments . . . 42
8.3 Magnitude of antigenic change and population level patterns . . . 43
8.4 Preview substitutions and mutation limitation . . . 43
8.5 Selection on bottlenecked diversity at higher scales . . . 44

9 Mathematical derivations in full 45
9.1 Full derivation of the within-host replicator equation . . . 45
9.2 Replicator equation with symmetric mutation . . . 46
9.3 Replicator equation with one-way mutation . . . 46
9.4 Derivation of t-star . . . 46

9.5 Derivation of the closed form for probability of passing through cell infection bottleneck . . . 49
9.6 The probability of surviving the cell infection bottleneck is one only if there is no competition . . . 50
9.7 The probability that a new variant survives the cell infection bottleneck is decreasing in the mean number of competing wild-type virions . . . 50
9.8 The probability that a new variant survives the cell infection bottleneck is increasing in the bottleneck size . . . 51
9.9 Selection is less important relative to drift at large bottlenecks . . . 52
9.10 In the absence of selection, the probability that a new variant survives the cell infection bottleneck is approximately linear for large v and small new variant frequency . . . 53

1 Summary

This appendix contains additional information for the paper "Asynchrony between virus diversity and antibody selection limits influenza virus evolution ".

We provide a detailed review of virological and immunological evidence supporting our model of the interaction between influenza viruses and the (human) host immune system (Section 2). We give a more detailed mathematical analysis of our within-host model, deriving the approximate and exact analytical results that are used in the main text and provide intuition to explain model behavior and limitations (Section 3). We do the same for our model of the point of transmission, and assess which hosts are most likely to act as inoculation selectors and which mutants are most likely to be inoculated selected (Section 4).

We next discuss parameter uncertainties and report the results of a sensitivity analysis for our within-host models (Section 5). We report an additional empirical analysis showing that new variants often emerge polyphyletically: they appear simultaneously on multiple branches of the influenza virus phylogeny. We discuss how this is more easily explained in light of our model than in light of existing models (Section 6).

We then review these prior studies and models of within-host influenza antigenic evolution and general pathogen immune escape in depth. We argue that they are insufficient to explain within-host influenza antigenic evolution and that inoculation selection is the most likely competing hypothesis (Section 7). We elaborate on the conclusions that can be drawn from our study and its implications for influenza control and for future basic research (Section 8). We conclude by providing complete step-by-step mathematical derivations of lemmas and approximations from elsewhere in the text (Section 9).

2 Immunological underpinnings of the inoculation selection model

In this section, we review relevant immunology to establish the biological realities that we built our model to capture. We also discuss some unmodeled biological complexities, and why they are unlikely to change our qualitative conclusions.

2.1 Strong selection at the point of inoculation

The establishment of successful influenza virus infection requires access to respiratory epithelial cells covered by a mucosal layer, which acts as a protective barrier for virus entry. Sialic acid residues present in the mucus act as decoys for virions and the enzymatic activity of influenza neuraminidase is essential for penetration of the mucosal layer (Matrosovich, Matrosovich, Gray, Roberts, & Klenk, 2004). The mucosal layer does not act only as a mechanical barrier. Secretory IgA (sIgA) mucosal antibodies specific to influenza virus proteins can apply virus-specific neutralization by

immobilizing virions and slowing down the process of virus infection (Wang et al., 2017). Depending on their specificity, sIgA can either play a role in reduction of total virus population size or in providing specific competitive advantage to mutant viruses. Antibodies against influenza neuraminidase (NA) will slow down the virus passage through the mucosal barrier irrespective of the HA antigenic phenotype of the newly infecting virus. By contrast, anti-HA antibodies are essential for inoculation selection because they recognise previously encountered viruses providing a competitive advantage to antigenically distinct variants. The variants with strongest competitive advantage are those with large antigenic affects as they have the lowest probability to be neutralized by cross-reactive anti-HA sIgAs.

2.2 Weak selection during exponential virus growth

Virions that successfully cross the mucosal barrier can infect epithelial cells in the respiratory tract. Upon initiation of replication in host cells, newly generated virions can be subjected to replication selection via virus-specific antibodies. Replication selection can take place only if influenza-specific antibodies are present in mucosa-associated lymphoid tissue (MALT) at the time of virus replication.

Influenza-specific antibodies in the MALT are secreted by local plasmablast populations, generated following activation of B naive cells or B memory cells. The exposure history of the host determines the timing and the immunological trajectory for the generation of influenza-specific antibodies. In individuals without previous exposure to influenza virus, newly generated virions are recognised by naive B cells which undergo rounds of affinity maturation and somatic hypermutation to produce highly-specific antibodies to the virus. This process typically occurs in germinal centres, requires T-cell help, and takes around 7 days for production of highly-specific antibodies (Wrammert et al., 2008).

In individuals with previous exposure history to influenza, where the newly generated influenza virions are antigenically matched or have some degree of cross-reactivity to previous strains, the generation of influenza-specific antibodies mainly results from B memory recall response. The activation of pre-existing memory pools enables the immune system to respond quicker to previously encountered antigens without the need to recruit naive B cell populations. The generation of antigen-specific antibodies from recalled B memory pools does not typically start until 3–5 days post infection (Coro et al., 2006; Lam & Baumgarth, 2019).

The B naive and B memory cells generating serological responses to influenza are referred to as B-2 cells. The activation of this cell types is dependent on the recognition of virus protein via the B-cell receptor and sufficient affinity of binding to trigger stimulatory signal. Depending on their specificity to the recognised virus antigen, the antibodies produced by these cell types have the potential to apply replication selection to newly generated mutant and wild-type virions during the course of infection. Antibodies against influenza viruses can also be generated from the so called B-1 cells, which do not require specific recognition of virus antigen and are activated by innate mechanisms (Lam & Baumgarth, 2019).

B-1 cells produce natural IgM antibodies with low affinity which constitute the earliest

humoral response generated in the first 48–72h of infection (Lam & Baumgarth, 2019). As the activation of B-1 cells is independent of the specific recognition of influenza virus virions, the natural IgM antibodies act as a non-specific limiting factor for virus population sizes and cannot apply replication selection to specific virus antigenic variants.

The peak of influenza virus replication occurs in the first 24–48 hours post infection (Hadjichrysanthou et al., 2016). Despite the presence of several immunological routes for generation of influenza-specific antibodies, the timing of the serological immune response is always later than the time of peak of virus titer (at least in typical infections of otherwise healthy individuals), thus limiting the opportunity for replication selection during the course of infection.

2.3 Selection during exit of an infected host

The design of the inoculation selection model focuses on selection applied by the mucosal layer upon the entry of influenza virus in naïve or previously exposed hosts. We do not take into account the potential bottleneck applied during exit of viruses from the respiratory tract of an infected host. Selection of newly generated virions at the point of exit of an infected host is technically possible as the virions released from infected epithelial cells need to cross the mucosal barrier again to reach the lumen of the respiratory tract. Such selection upon virus exit would have the same directional effect as inoculation selection – it would provide a competitive advantage for mutant viruses with large antigenic effects. However, the magnitude of this selection would be dependent on the presence of enough antigen-free sIgA antibodies which are not already virus-bound at the point of inoculation. Incorporating such mucosal selection upon virus exit requires better knowledge of the quantities of sIgA antibodies in given volume of mucus and what proportion of the available sIgA antibodies are engaged with antigen upon inoculation. Such data is not currently available and would require well-designed cellular culture models which take into account the role of mucosal layer in the process of virus infection and release of newly generated viruses.

2.4 Nature and timing of previous exposure and effects on inoculation selection

According to our model, the strongest inoculation selection can take place in infection of previously exposed individuals and the highest probability of antigenic diversification occurs in populations with an intermediate proportion of immune hosts. In deriving this result, we have assumed homogeneous and static quantities of sIgA antibodies among previously exposed individuals. This is an oversimplification. There is substantial variation in level of sIgA antibodies across individuals depending on the nature of their previous exposures (through vaccination or natural infection). For example, intranasal inoculation with influenza virus via live attenuated influenza virus vaccines leads to generation of better mucosal immunity (Hoft et al., 2017) than intramuscular administration of trivalent inactivated vaccines and thus previously exposed individuals are likely to vary in the degree of inoculation selection applied during homotypic infections depending on the route of administration of previous vaccinations.

The model also does not account for waning of sIgA antibody titers in the months and years following each exposure. The waning of sIgA titers is likely to be substantial in absence of re-exposure but the waning process should only decrease the efficiency of inoculation selection and make the accumulation of population level selection pressure – and thus the emergence of new variants – rarer.

The dynamics of mucosal immunity with age are also likely to have impact on the selector phenotype of previously exposed hosts. In older individuals, multiple previous exposures will eventually lead to preferential activation of recall responses for antibody production to new variants as a result of original antigenic sin (Davenport & Hennessy, 1956), immune backboosting (Fonville et al., 2014), or antigenic seniority (Lessler et al., 2012).

Even if the recall responses result in backboosting and higher levels of sIgA, these antibodies are unlikely to be well-matched to the new variant or succeeding variants, as continuous re-exposure favours responses to conserved epitopes (Krammer & Palese, 2019; Krammer, 2019) rather than receptor-binding site epitopes suspected to be most important for immune escape.

As a result of the limited ability to generate novel immune responses and the phenomenon of antigenic seniority, an elderly individual who has been exposed multiple times in the past is likely to exert very weak inoculation selection to newly infecting viruses. By contrast, a child recently exposed to influenza virus is more likely to act as a strong selector, due to the availability of mucosal sIgA antibodies and the more limited impact of original antigenic sin. However, due to the acute nature of influenza virus infection, very young children are likely to require more than one infection before they begin to develop highly specific antibody responses to influenza virus infection able to exert inoculation selection (Neuzil et al., 2006).

Most current efforts for characterizing humoral immunity to influenza virus infections are focused on antibody responses in the serum. However, there is limited understanding of the relationship between antibodies in the serum measured via HI and the levels of mucosal antibodies, able to exert inoculation selection. Better characterisation of the dynamics of mucosal immunity with age and across individuals is needed to understand the implications of inoculation selection to influenza virus evolution depending on the host population structure.

3 Detailed within-host model analysis

Here we analyze the within-host model in depth, and find expressions for within-host mutant frequencies over time, the probability distribution of mutant emergence times, and an approximate probability of replication selection to a given frequency by a given time.

3.1 Expression for the within-host mutant frequency

In our minimal model, new variant and wild-type virions competition obey a simple replicator equation.

The within-host frequency of new variant virus is $f_m(t) = \frac{V_m(t)}{V_m(t)+V_w(t)} = \frac{V_m(t)}{V_{\text{tot}}(t)}$. Its rate of change is $\frac{\mathrm{d}f_m}{\mathrm{d}t}$. We observe that $\frac{\mathrm{d}V_i}{\mathrm{d}t}$ is of the form $\frac{\mathrm{d}V_i}{\mathrm{d}t} = V_i\Big[g_i(t) - d_i(t)\Big]$ for both new variant and wild-type, where, neglecting mutation, $g_i(t) = r_i\beta C(t)$ and $d_i(t)$ is a (possibly time-varying) neutralization or decay rate. Differentiating $f_m(t)$ with respect to time demonstrates that the frequency of new variant over time is governed by the following replicator equation (see section 9 for an explicit derivation):

$$\frac{\mathrm{d}f_m}{\mathrm{d}t} = f_m(1 - f_m)\Big(\big[g_m(t) - g_w(t)\big] - \big[d_m(t) - d_w(t)\big]\Big) \tag{A1}$$

If the new variant is neutral in the absence of antibody-mediated selection, $r_w = r_m = r$, and therefore $g_m(t) = g_w(t)$. It follows that despite changing target cell populations and virion population sizes, the strains compete in a manner independent of V_{tot}, provided each $d_i(t)$ is independent of V_{tot}. We have competition only through the respective death rates of wild-type and new variant virions. These may be affected by antibody-mediated neutralization of virions.

If the fitness difference $\delta(t) = \Big[g_w(t) - g_m(t)\Big] - \Big[d_m(t) - d_w(t)\Big]$ is a constant δ, this differential equation has a closed-form solution:

$$f_m(t) = \frac{e^{\delta t}}{e^{\delta t} + f_0^{-1} - 1} \tag{A2}$$

where $f_0 = f_m(0)$

If $\delta = 0$, $f_m(t)$ is constant and equal to f_0, as expected. If $\delta(t)$ is piecewise-constant, we can apply the constant-δ solution iteratively to find the mutant frequency.

It is therefore straightforward to apply this expression to the within-host model with binary immunity by evaluating different immunity regimes piece-wise.

We consider the case of a host who is experienced to the wild-type ($E_w = 1$) but naive to the mutant ($E_m = 0$).

If first appears at a time $t_e \geq 0$ post-infection at an initial frequency $f_m(t_e)$, then if $t_e < t_M$:

$$f_m(t) = \begin{cases} 0 & t < t_e \\ f_m(t_e) & t_e \leq t < t_M \\ \frac{e^{\delta(t-t_M)}}{e^{\delta(t-t_M)} + f_m(t_e)^{-1} - 1} & t_M \leq t \end{cases} \tag{A3}$$

if $t_e > t_M$:

$$f_m(t) = \begin{cases} 0 & t < t_e \\ \frac{e^{\delta(t-t_e)}}{e^{\delta(t-t_e)} + f_m(t_e)^{-1} - 1} & t_e \leq t \end{cases} \tag{A4}$$

where $\delta = k(1 - c)$ is the fitness difference between the variants due to the recall adaptive response.

3.2 CDF of mutant emergence times

Deriving a probability of replication selection to a given level requires an expression for the probability distribution of t_e, the time of first successful emergence. As shown in the Methods, we calculate an approximate closed form for the cumulative distribution function (CDF) of t_e given a time-varying rate of emergence $\lambda_m(t)$

$$P(t_e < x) = 1 - e^{-\Lambda_m(x)} \tag{A5}$$

where

$$\Lambda_m(x) = \int_0^x \lambda_m(x)dx \tag{A6}$$

Comparing our approximation to simulations from the full stochastic within-host model reveals that it is a good representation of the full model (Fig. 7). The slightly earlier simulated emergence times in the immediate recall response case (Fig. 7A) would only make replication selection even more likely than our analytical approximation suggests.

3.3 Accuracy of the replication selection analytical result

Comparisons between simulated infections of experienced hosts seeded with a single wild-type virion and our analytical expression for replication selection used to generate the heatmaps in the main text reveals good agreement, with replication selection probabilities more likely to be underestimated than overestimated (Fig. 8)

3.4 Derivation of mutant frequency over time given ongoing *de novo* mutation and no selection

Thus far we have neglected mutation apart from a single event of first emergence. In fact, with symmetric mutation between the two types of interest, we have:

$$\begin{aligned} \frac{\mathrm{d}V_w}{\mathrm{d}t} &= V_w\Big[(1-\mu)g_w(t) - d_w(t)\Big] + \mu g_m(t)V_m \\ \frac{\mathrm{d}V_m}{\mathrm{d}t} &= V_m\Big[(1-\mu)g_m(t) - d_m(t)\Big] + \mu g_w(t)V_w \end{aligned} \tag{A7}$$

The rate of fitness-irrelevant mutation is assumed to be equal for the two types, and to preserve antigenic type (w or m). The rate of lethal or deleterious mutants is assumed equal for the two types and is captured in g.

It can be shown (see section 9) that the equation for $\frac{\mathrm{d}f_m}{\mathrm{d}t}$ in this case is:

$$\frac{\mathrm{d}f_m}{\mathrm{d}t} = f_m(1-f_m)(\alpha_m - \alpha_w) + \mu\Big(g_w(t) - 2g_w(t)f_m + g_w(t)f_m^2 - g_m(t)f_m^2\Big) \tag{A8}$$

When $g_w(t) = g_m(t) = g(t)$:

$$\frac{\mathrm{d}f_m}{\mathrm{d}t} = f_m(1 - f_m)\Big(d_m(t) - d_w(t)\Big) + \mu g(t)(1 - 2f_m) \tag{A9}$$

When $f_m \ll 0.5$, the net effect of symmetric mutation on f_m is to increase it at rate $\approx \mu$ (note that the symmetric mutation term becomes zero at $f_m = 1/2$). In other words, it is roughly equivalent to a case with no back mutation at all:

$$\begin{aligned} \frac{\mathrm{d}V_w}{\mathrm{d}t} &= V_w\Big[(1-\mu)g_w(t) - d_w(t)\Big] \\ \frac{\mathrm{d}V_m}{\mathrm{d}t} &= V_m\Big[g_m(t) - d_m(t)\Big] + \mu g_w(t)V_w \end{aligned} \tag{A10}$$

in that case, we have:

$$\frac{\mathrm{d}f_m}{\mathrm{d}t} = f_m(1-f_m)\Big(\big[g_m(t)-(1-\mu)g_w(t)\big]-\big[d_m(t)-d_w(t)\big]\Big)+\mu g_w(t)(1-2f_m+f_m^2) \tag{A11}$$

In either case, we mainly study a situation in which $g_w(t) = g_m(t) = g(t)$ at all times (though note that $g(t)$ varies in time), $d_w(t) = d_m(t) = d(t) = d_V$ prior to the onset of the adaptive immune response, and $d_w(t) = d_V + k$, $d_m(t) = d_V + ck$ after the onset of the adaptive immune response.

If f_m is large relative to μ, the mutant growth term $V_m g(t)$ is large relative to the *de novo* mutation term $\mu g(t)V_w$. We can see this from the fact that $V_m = f_m V_{\text{tot}} \geq f_m V_w$, with equality if and only if $f_m = 0$. It follows that if $f_m > \mu > 0$, then:

$$g(t)V_m > g(t)f_m V_w > g(t)\mu V_w$$

In this case ($f_m \gg \mu$), additional *de novo* mutation can be neglected when calculating $f_m(t)$. Ignoring ongoing mutation is particularly valuable when selection is occurring, as it allows us to use the closed form for $f_m(t)$ given in equation A2. In the presence of selection, there is a closed form for the equation with ongoing mutation if mutation is symmetric and only if $g_w(t)$ is constant, so it provides less analytical tractability for minimal, if any, additional realism. For these reasons, we typically ignore ongoing mutation in analyzing the dynamics of $f_m(t)$

But if the first mutant emergence is sufficiently late and there is no positive selection, we do not necessarily have $f_m \gg \mu$, so ongoing mutation cannot be ignored in the dynamics of f_m. In that case, we can consider either the $\mu g(t)(1 - 2f_m + f_m^2)$ term in equation A11 or the $\mu g(t)(1 - 2f_m)$ term in equation A9. The other term in $\frac{\mathrm{d}f_m}{\mathrm{d}t}$ is zero in the absence of selection, and we can approximate $g(t) \approx g_0 = g(0) = \mathcal{R}_0 d_V$ early in infection, since for small t, $C(t) \approx C_{\max}$ and therefore $g(t) = r\beta C(t) \approx g_0$.

So we have:

$$f_m(t) \approx (f_0 - \frac{1}{2})e^{-\mu g_0 t} + \frac{1}{2} \tag{A12}$$

for the symmetric mutation case case and

$$f_m(t) \approx \frac{\mu g_0 t + \frac{1}{1-f_0} - 1}{\mu g_0 t + \frac{1}{1-f_0}} = 1 - \frac{1}{\mu g_0 t + \frac{1}{1-f_0}} \tag{A13}$$

for the one-way mutation case.

And since μ is small and therefore f_m must be small for ongoing mutation to matter either of these differential equations will be approximated in cases of interest by:

$$\frac{\mathrm{d}f_m}{\mathrm{d}t} = \mu g_0 \tag{A14}$$

and therefore:

$$f_m(t) \approx f_0 + \mu g_0 t \tag{A15}$$

We can also see this by inspecting the other two expressions for $f_m(t)$ and seeing that they are quasi-linear for small μ and small t. This further confirms that it is not crucial to decide whether symmetric or one-way mutation is more realistic, as they will be functionally the same from the point of view of practical mutant frequencies in the absence of positive selection.

Note that once $g(t)$ begins to decline, contributions to f_m from ongoing mutation will also decline, so good approximate maximal value for $f_m(t)$ in the absence of selection can be calculated as $f_m(t_{\text{peak}})$. For a mutation rate of 0.33×10^{-5}, typical mutant frequencies at infection peak in the absence of selection should range from 10^{-5} to 2×10^{-4}, depending on $\mathcal{R}_0$ and t_{peak}.

3.5 Consequences of ongoing *de novo* mutation

The effect of ongoing mutation is to further enhance possibilities for both replication and inoculation selection. It acts to truncate the left tail of the distribution of $f_m(t_M)$ and of the transmission time mutant frequency f_{mt}. Whenever t_M is sufficiently late that we have reached $V_w \ll \frac{1}{\mu}$, $f_m(t_M)$ will have a minimum value on the order of the inverse mutation rate, provided t_M so that mutant production is occurring quasi-deterministically.

The consequence is that probabilities of replication selection and inoculation selection should both be somewhat higher than those estimated simply based on the emergence time of the first *de novo* mutant.

3.6 Approximations underestimate replication selection

The approximations made above were used to produce main text figure 1C,D, which shows how probability of escape varies for a fixed δ and t_M. A more realistic portrait tends to make the prospects for replication selection in the presence of fixed immunity

better rather than worse: t_e can be less early than our approximations demand, and ongoing mutation truncates the left tail of $f_m(t_M)$, increasing the probability of replication selection. This further strengthens the case for the importance of an adaptive response at 48 hours or later in explaining the absence of replication selection.

3.7 Replication selection is helped when individual infected cells are more productive

For a fixed $\mathcal{R}_0$, replication selection becomes more likely if the virions produced per infected cell r becomes large – that is, if every infected cell produces more individual virions.

For a given d_v, and f, a virus can achieve a large $\mathcal{R}_0$ either by having a high cell productivity r or by having a high cell invasion rate β.

The expected number of virus replications per lost target cell is given by $\frac{\dot{\bar{V}}^+}{\dot{\bar{C}}^-} = \frac{r\beta C\bar{V}}{f\beta C\bar{V}} = \frac{r}{f}$. The infection peaks and begins to decline when $\frac{\mathrm{d}V}{\mathrm{d}t} = 0$, which occurs when $g(t) = d(t)$, or $\frac{C_{\max}}{C} = \mathfrak{R}_0$, provided $d(t)$ is fixed. It follows that $C_{\text{peak}} = \frac{C_{\max}}{\mathcal{R}_0}$. So the virus peaks once $C_{\max}\left(1 - \frac{1}{\mathcal{R}_0}\right)$ target cells have been consumed (assuming negligible target cell replenishment during the timecourse of infection), and $\frac{r}{f}C_{\max}\left(1 - \frac{1}{\mathcal{R}_0}\right)$ viral replication events have occurred (this is a slight overestimate due to target cell depletion).

Fixing d_V and $\mathcal{R}_0$, as $r \to \infty$, $\beta \to 0$ and the number of viral replication events before peak viral load goes to ∞. Since each generated mutant survives stochastic extinction roughly proportional to $1/\mathcal{R}_0$, these earlier mutants also are lost stochastically less frequently. In other words, a mutant that survives stochastic extinction is generated with certainty well before the infection peaks and can spend arbitrarily long under selection. Conversely, as $r \to 0$, $\beta \to \infty$, the number of replication events that occur before the infection peaks goes to 0, and replication selection becomes impossible.

A virus of a given $\mathcal{R}_0$ that takes a shotgun approach of producing many not-especially-infectious virions is more likely to result in the proliferation of a mutant of interest under replication selection than one that produces a small number of highly infectious virions.

In other words, the relatively large infected cell productivity of influenza viruses – perhaps as large as hundreds or thousands of viable virions per cell (Frensing et al., 2016) – makes potential replication selection more efficient. This in turn makes the absence of observed replication selection harder to explain unless another mechanism can be invoked, such as inoculation selection with replication selection only occurring 2–3 days post-infection.

3.8 Replication selection in the presence of sterilizing immunity

One special case bears mentioning, because it corresponds to multiple existing models (Luo et al., 2012; Volkov et al., 2010; Kennedy & Read, 2017) and may be relevant for

other systems. If there is an immediate recall response ($t_M = 0$), a founding population of size b, and k is large enough such that $\mathcal{R}^w(t = 0) < 1$ (the virus population is initially declining, in expectation), then the infection will go extinct after generating q new virions for some finite q.

Each virions has a probability μ of being an escape mutant with $\mathcal{R}^m(0) > 1$ and each mutant independently survives stochastic extinction with probability $p_{\text{sse}} = (1 - 1/\mathcal{R}^m(0))$ (per the theory of supercritical branching processes). The conditional probability of replication selection given q is therefore:

$$p_{\text{repl}}(q) = 1 - \Big(1 - \mu p_{\text{sse}})\Big)^q \tag{A16}$$

if μp_{sse} is small, this is approximately equal to:

$$p_{\text{repl}}(q) \approx 1 - e^{-q\mu p_{\text{sse}}} \approx q\mu p_{\text{sse}} \tag{A17}$$

The approximations use the Poisson approximation to the binomial and the approximation $e^x \approx 1 + x$ when $|x| \ll 1$.

The unconditional probability of replication selection p_{repl} is the expectation in q of $p_{\text{repl}}(q)$: $E_q(p_{\text{repl}})$. But since p_{repl} is approximately linear in q, the linearity of expectation implies:

$$p_{\text{repl}} \approx E_q(q\mu p_{\text{sse}}) = \bar{q}\mu p_{\text{sse}}$$

where $\bar{q}$ is the expected value of q.

Given $\mathcal{R}^w(0) < 1$, branching process theory predicts that the virus will produce on average $\bar{q} = \frac{b}{1-\mathcal{R}^w(0)} - b$ new copies before the infection is cleared (expected total length of b independent subcritical branching processes, each with expected length $\frac{1}{1-\mathcal{R}^w(0)}$, minus the initial virions present (Ball, Britton, & Neal, 2016)). This can be simplified to $\bar{q} = \frac{b\mathcal{R}^w(0)}{1-\mathcal{R}^w(0)}$.

So we have

$$p_{\text{repl}} \approx \bar{q}\mu p_{\text{sse}} = \frac{\mathcal{R}^w(0)}{1 - \mathcal{R}^w(0)} b\mu p_{\text{sse}} \tag{A18}$$

Note that Iwasa, Michor, and Nowak (2004) have previously derived this approximate result for the probability that a subcritical replicator mutates to a supercritical one prior to going extinct in the context of analyzing tumor cell mutations. They use a more rigorous generating function approach.

4 Point of transmission analysis

4.1 Distinction between selection and drift at the point of transmission

In our model, mucosal antibodies acting at the point of transmission provide a mechanism for population level selection pressure – some protection of experienced hosts against infection with the wild-type virus, and worse protection against infection with a new variant. In particular, it provides a mechanism that produces selection pressure for new antigenic variants while still predicting that reinfections consisting of wild-type viruses (without observable new variant viruses) should be observed. Prior models (see section 7) predict that in fully immune hosts, the only observable reinfections should show antigenic variant viruses at consensus.

It is clear that mucosal antibodies play a key role in influenza evolution: they produce the selection pressure that allows new variants to spread more reliably and thus rapidly from host to host than old variants. But they may play a second role as well: promoting of new variants in frequency from the low frequencies at which they are typically generated to high frequencies at which they can be observed and reliably transmitted onward. This inoculation selection takes on the role of previously held by replication selection in explaining why inoculations of experienced hosts might produce new variant infections at a higher rate (per inoculation) than inoculations of naive hosts.

4.2 The inoculation selection paradigm

In the absence of strong replication selection, mutants can reach high within-host frequencies through founder effects. Given that influenza bottlenecks are thought to be on the order of a single virion (McCrone et al., 2018), any replication-competent mutant that founds an infection should occur at NGS-detectable levels, and likely at consensus.

This founder effect could be a purely neutral sampling process. It is likely quite close to neutral in a truly naive host who does not possess well-matched IgA antibodies to the infecting variant: all inoculated virions, regardless of antigenic phenotype, have an equal chance of becoming part of the new infection's founding population. If there are v virions that compete to found the infection and $b = 1$, then each virion founds the infection with probability $1/v$

But if different virions have different chances of being neutralized by IgA antibodies, this foundation process may be selective. Among the virions that encounter IgA antibodies, those that are less likely to be neutralized have a higher than average chance of undergoing stochastic "promotion" to consensus while those that are more likely to be neutralized have a lower than average chance.

As mentioned in the Methods, in a fully naive host with large v and small transmitting host new variant frequency, the sampling process approximates a low-probability binomial or a low frequency Poisson:

$$p_{\text{drift}} \approx 1 - e^{-f_{\text{mt}} b} \tag{A19}$$

When $f_{\text{mt}} \ll 1$, this is approximately equal to bf_{mt}

When there is mucosal antibody neutralization, the variant's survival probability can be reduced below this (inoculation pruning) or promoted above it (inoculation promotion), depending upon parameters. There can be inoculation pruning even when the variant is more fit than the wild-type (neutralized with lower probability, i.e. undergoes positive inoculation selection). If there is subsequent bottlenecking after IgA antibody neutralization, mutant survival may be higher in inoculations of experienced hosts relative to inoculations of naive hosts (inoculation promotion).

Whether inoculation selection improves mutant survival relative to p_{drift} depends on the ratio of v/b, and on the mutant's probability of avoiding neutralization $1 - \kappa_m$ (main text Fig. 4F, Fig. A1, and sec. 4.5 below).

4.3 Expression for and properties of the new variant survival probability

As shown in the Methods, the probability that a new variant survives the cell infection bottleneck of size b is well approximated for small f_{mt} by:

$$p_{\text{surv}}(\kappa_m, \kappa_w, v, b, f_{\text{mt}}) \approx p_{\text{inoc}}(\kappa_m, v, f_{\text{mt}}) * p_{\text{cib}}(\kappa_w, v, b) \tag{A20}$$

where p_{inoc} is the probability that at least one mutant survives the sIgA bottleneck:

$$p_{\text{inoc}}(\kappa_m, v, f_{\text{mt}}) = 1 - e^{-vf_{\text{mt}}(1-\kappa_m)} \tag{A21}$$

and $p_{\text{cib}}(\kappa_w, v, b)$ is the probability that a mutant that survives the sIgA bottleneck is not lost at the final bottleneck (as given in equation 16 above):

$$p_{\text{cib}}(\kappa_w, v, b) = (1 - e^{-\bar{w}})\frac{b}{\bar{w}} + e^{-\bar{w}} \sum_{j=0}^{b-1} \frac{\bar{w}^j}{j!}\left(1 - \frac{b}{j+1}\right)$$

where $\bar{w} = v(1 - f_{\text{mt}})(1 - \kappa_w)$. If $b = 1$, this reduces the exactly the first term.

Note that when $f_{\text{mt}} \ll 1, p_{\text{inoc}} \approx vf_{\text{mt}}(1 - \kappa_m)$

4.3.1 Properties of these probabilities

These probabilities have several intuitive and useful properties:

- $p_{\text{cib}} < 1$ if $\kappa_w < 1$ and $f_{\text{mt}} < 1$, and $p_{\text{cib}} = 1$ if $\kappa_w = 1$ or $f_{\text{mt}} = 1$. That is, surviving the cell infection bottleneck is certain only if there is no competition. See section 9.6 for derivation.
- The correction term in p_{cib}, $e^{-\bar{w}} \sum_{j=0}^{b-1} \frac{\bar{w}^j}{j!}\left(1 - \frac{b}{j+1}\right)$, is always negative. Each term except the last in the summation is negative, since $b > j + 1$ for $j < b - 1$. The last term is zero (the last term is included for notational reasons, so that the

formula is correct with $b = 1$). This implies that the first term is always $\geq p_{\text{cib}}$, with equality if and only f $b = 1$.

- If $\kappa_m = \sigma\kappa_w$, then p_{inoc} is decreasing in κ_w for $0 < \sigma \leq 1$. This is as expected: the more likely the new variant is to be neutralized, the smaller p_{inoc} becomes. It suffices to show that $\frac{\mathrm{d}p_{\text{inoc}}}{\mathrm{d}\kappa_w} < 0$ for $0 < \sigma \leq 1$. We find:

$$\frac{\mathrm{d}p_{\text{inoc}}}{\mathrm{d}\kappa_w} = -e^{-vf_{\text{mt}}(1-\sigma\kappa_w)}(vf_{\text{mt}}\sigma) \tag{A22}$$

  Since $f_{\text{mt}}, v > 0$, this is negative whenever $\sigma > 0$, and 0 if σ is 0.

  It is sometimes useful to write this as:

$$\frac{\mathrm{d}p_{\text{inoc}}}{\mathrm{d}\kappa_w} = vf_{\text{mt}}\sigma(p_{\text{inoc}} - 1) \tag{A23}$$

- p_{cib} is decreasing in $\bar{w}$ (see section 9.7 for derivation). This is intuitive: the less competition in the form of (expected numbers of) un-neutralized wild-type virions, the more likely a surviving mutant is to pass through the cell infection bottleneck.

- p_{cib} is increasing in κ_w and f_{mt} and decreasing in v. Since v, $1 - \kappa_w$, and $1 - f_{\text{mt}}$ are all ≥ 0, it is clear that $\bar{w}$ is decreasing in κ_w and f_{mt} and increasing in v. It follows that p_{cib} is increasing in κ_w and f_{mt} and decreasing in v. In all cases, this reflects the parameters' effect on the mean amount of competition for the mutant from wild-type virions for the cell infection bottleneck.

- p_{inoc} is increasing in f_{mt}, since a larger f_{mt} implies an $vf_{\text{mt}}(1 - \kappa_m)$ term that is larger in absolute value, so $e^{-vf_{\text{mt}}(1-\kappa_m)}$ becomes smaller and $p_{\text{inoc}} = 1 - e^{-vf_{\text{mt}}(1-\kappa_m)}$ becomes larger.

4.4 Mutant survival probability increases as transmitted mutant frequency increases

For given values of the other parameters, larger f_{mt} implies larger p_{surv}. Since both p_{inoc} and p_{cib} are increasing in f_{mt} and are both always positive, it follows that $p_{\text{surv}} = p_{\text{inoc}}p_{\text{cib}}$ is also increasing in f_{mt}. This makes intuitive sense: all else equal, higher frequency mutants always have a better chance of surviving at the point of transmission, regardless of the effects of the sIgA bottleneck.

4.5 The relative importance of selection and drift at the point of inoculation

Consider $p_{\text{surv}}/\ p_{\text{drift}}$. This ratio quantifies the degree to which sIgA neutralization at the point of transmission facilitates (or hinders) mutant survival of the final bottleneck relative to a purely neutral founder effect.

For realistically small b and f_{mt}, we can use the approximations $p_{\text{drift}} \approx b f_{\text{mt}}$ and $p_{\text{inoc}} \approx v f_{\text{mt}}(1-\kappa_m)$

Then we have

$$p_{\text{surv}}/p_{\text{drift}} = \frac{p_{\text{inoc}} p_{\text{cib}}}{p_{\text{drift}}} \approx \frac{v}{b}(1-\kappa_m) p_{\text{cib}}(\kappa_w, v, b) \tag{A24}$$

Several intuitive results follow:

- If we hold κ_w constant, increasing κ_m makes inoculation selection less effective relative to drift, because the inoculated new variant is at greater risk of neutralization.
- Conversely, if we hold κ_m constant, increasing κ_w makes inoculation selection more effective relative to drift (this follows from the fact that p_{cib} is increasing in κ_w, see section 4.3.1 above).
- Since p_{cib} is increasing in f_{mt} (section 4.3.1), $p_{\text{surv}}/p_{\text{drift}}$ is increasing in f_{mt}. That is, inoculation selection is more efficient relative to drift when promoting higher frequency mutants, all else equal.
- $p_{\text{surv}}/p_{\text{drift}}$ is decreasing in b (see section 9.9 for a derivation). In other words, when the cell infection bottleneck is wider, inoculation selection is less important relative to drift. The large bottleneck gives the mutant a reasonably good chance of surviving even in the absence of any neutralization of competing wild-type virions.

For a bottleneck of size $b = 1$, we can also see that inoculation selection becomes more efficient relative to drift as v increases, since:

$$\begin{aligned} p_{\text{surv}}/p_{\text{drift}} &\approx \frac{v}{b}(1-\kappa_m) p_{\text{cib}} \\ &= v(1-\kappa_m)\frac{1-\exp\big(-v(1-f_{\text{mt}})(1-\kappa_w)\big)}{v(1-f_{\text{mt}})(1-\kappa_w)} \\ &= \frac{1}{1-f_{\text{mt}}}\frac{1-\kappa_w}{1-\kappa_m}[1-\exp\big(-v(1-f_{\text{mt}})(1-\kappa_w)\big)] \end{aligned}$$

This is increasing in v.

4.6 Effect of sIgA cross immunity σ on probability of inoculation selection

We are interested in which hosts best promote the emergence of antigenic novelty, given a level of cross-immunity σ, or a degree of escape $1-\sigma$. We will show that whereas replication selection suggests that intermediately immune hosts should be key sources of antigenic novelty (Grenfell et al., 2004), in an inoculation selection regime, it is possible for fully immune hosts to be the strongest promoters of new variants, depending upon parameters. We do this by analyzing an expression for p_{surv}, the probability that a mutant survives transmission to found an infection in a new host, and showing how it

changes with wild-type neutralization κ_w and sIgA cross immunity $\sigma = \kappa_m/\kappa_w$. We find that transmission survival probability can be maximized in strongly immune or fully naive hosts, depending on parameters.

We optimize $p_{\text{surv}}(\kappa_w)$ given some value of σ by differentiating.

$$\begin{aligned}\frac{\mathrm{d}p_{\text{surv}}}{\mathrm{d}\kappa_w} &= \frac{\mathrm{d}p_{\text{cib}}}{\mathrm{d}\kappa_w}p_{\text{inoc}} + p_{\text{cib}}\frac{\mathrm{d}p_{\text{inoc}}}{\mathrm{d}\kappa_w} \\ &= \frac{\mathrm{d}p_{\text{cib}}}{\mathrm{d}\kappa_w}p_{\text{inoc}} + p_{\text{cib}}(f_{\text{mt}}\sigma)(p_{\text{inoc}} - 1)\end{aligned} \tag{A25}$$

Consider the endpoint at $\kappa_w = 1$. $p_{\text{cib}} = 1$, $p_{\text{inoc}} \approx f_{\text{mt}}v(1-\kappa_m) = f_{\text{mt}}v(1-\sigma)$, and $\bar{w} = v(1-f_{\text{mt}})(1-\kappa_w) = 0$.

So $\frac{\mathrm{d}p_{\text{cib}}}{\mathrm{d}\kappa_w} = -v(1-f_{\text{mt}})e^{-\bar{w}}\Big[S'(\bar{w}) - S(\bar{w})\Big]$ can be evaluated, and it evaluates to 0 except if $b = 1$ (when it is undefined).

Case 1: $b > 1$. For $b > 1$, it follows from the above that

$$\frac{\mathrm{d}p_{\text{surv}}}{\mathrm{d}\kappa_w} = 0 - p_{\text{cib}}\frac{\mathrm{d}p_{\text{inoc}}}{\mathrm{d}\kappa_w} \tag{A26}$$

Since $\frac{\mathrm{d}p_{\text{inoc}}}{\mathrm{d}\kappa_w} \geq 0$, $\frac{\mathrm{d}p_{\text{surv}}}{\mathrm{d}\kappa_w} < 0$ unless $\frac{\mathrm{d}p_{\text{inoc}}}{\mathrm{d}\kappa_w} = 0$, which occurs in cases of interest when $\sigma = 0$ (complete escape mutant).

In other words, if immune escape is incomplete for $b > 1$, there is always some less strongly immune host (though possibly very slightly less, see Fig. A1) that improves new variant survival relative to a host who neutralizes wild-type virions with 100% certainty. Note, however, that hosts with $\kappa_w = 1$ are very unlikely to exist in nature. Our study is motivated precisely by the fact that even an experienced encountering homotypic reinfection neutralizes virions with probability $\kappa_w < 1$, and therefore can be productively reinfected (Clements et al., 1986; McCrone et al., 2018). It follows that in practice the most strongly immune hosts (with κ_w large but less than 1) could still be the best selectors.

Case 2: $b = 1$. When the bottleneck is 1, $\lim_{\bar{w}\to 0}\frac{\mathrm{d}p_{\text{cib}}}{\mathrm{d}\bar{w}} = -\frac{1}{2}$. So in this case, the derivative at $\kappa_w = 1$ may be positive or negative, depending on whether:

$$\frac{\mathrm{d}p_{\text{cib}}}{\mathrm{d}\kappa_w}p_{\text{inoc}} + p_{\text{cib}}(vf_{\text{mt}}\sigma)(p_{\text{inoc}} - 1) > 0 \tag{A27}$$

substituting $\frac{\mathrm{d}p_{\text{cib}}}{\mathrm{d}\bar{w}}\frac{\mathrm{d}\bar{w}}{\mathrm{d}\kappa_w} = -\frac{1}{2}(-v(1-f_{\text{mt}}))$ and $p_{\text{cib}} = 1$, we have:

$$\frac{1}{2}(1-f_{\text{mt}})p_{\text{inoc}} + f_{\text{mt}}\sigma p_{\text{inoc}} > f_{\text{mt}}\sigma$$

$$\frac{1}{2f_{\text{mt}}}(1-f_{\text{mt}})p_{\text{inoc}} + \sigma p_{\text{inoc}} > \sigma$$

$$\frac{1}{2f_{\text{mt}}}(1-f_{\text{mt}})p_{\text{inoc}} > \sigma(1-p_{\text{inoc}})$$

$$\frac{1-f_{\text{mt}}}{2f_{\text{mt}}}\frac{p_{\text{inoc}}}{1-p_{\text{inoc}}} > \sigma$$

When p_{inoc} is small, we have approximately $p_{\text{inoc}} \approx f_{\text{mt}}v(1-\sigma)$ and $1-p_{\text{inoc}} \approx 1$, so:

$$\frac{1-f_{\text{mt}}}{2}v(1-\sigma) > c$$

$$v\frac{1-f_{\text{mt}}}{2} > \frac{\sigma}{1-\sigma} \tag{A28}$$

In other words, with extremely small cell infection bottlenecks like those observed for influenza viruses, fully immune hosts are the best selectors provided that the number of virions v encountering IgA antibodies is sufficiently large given the degree of escape achieved. Less immune escape (larger sIgA cross immunity σ) necessitates a larger v to make fully immune hosts the best selectors. Since $f_{\text{mt}} \ll 1$, a rule of thumb is that $v > \frac{2\sigma}{1-\sigma}$.

The intuition is that larger v means more competition for the cell infection bottleneck among virions that reach IgA, and thus a greater opportunity for the mutant's selective advantage to be realized, but that this only works provided that this advantage is large enough so that the mutant is not at self at too large a risk of being neutralized.

5 Parameter uncertainties and sensitivity analysis

Here we discuss parameter uncertainty in our models and how they affect our conclusions. We also conduct a simulation-based sensitivity analysis of the central within-host model.

5.1 Strength of selection

A crucial parameter in our model is δ: the magnitude of the fitness difference between new variant and wild-type during viral replication in an infected individual. One possible objection to our analysis here is that the antibody mediated virion neutralization rate k is low enough or functional cross immunity between mutants and wild-types c is strong enough to make the fitness difference $\delta = k(1-c)$ small. In that case, replication selection to consensus will be rare even if t_M is very small, and the adaptive response is mounted immediately (main text Fig. 1C,D). Despite uncertainty about both k and c, k is likely to be high, perhaps extremely so. And in the presence of high k, even moderate c produces substantial fitness differences. Moreover, assuming small k early in infection grants our basic hypothesis: antibodies mediated selection is weak early in infection, neutralization during viral replication is not the mechanism of protection against reinfection, and there is asynchrony between antigenic diversity and meaningful antigenic selection.

5.1.1 Antibody-mediated virion neutralization rate (k) may be very high

Parameter estimates for antibody-mediated virion neutralization in the presence of substantial well-matched antibody correspond to values of k that are extremely high. For instance, by fitting a single-strain within-host model to data, Cao and McCaw (Cao & McCaw, 2017) estimate antibody neutralization rates between 0.4 and 0.8 per virion-day per pg/mL of antibody, and antibody concentrations of over 100 pg/mL by day 6 in an infection of a naive host. This corresponds to a k of 40 to 80 in our more phenomenological model.

For $t_M = 0$ (constant immunity) if k is sufficiently large that the wild-type virus has an initial $\mathcal{R}(0) < 1$ (which occurs if $k > d_v(\mathcal{R}_0 - 1)$), then all visible reinfections will be mutant infections. At $\mathcal{R}_0 < 10$ with $d_V = 4$, this corresponds to a k of 40, the lower end of the Cao and McCaw estimates.

A k of this magnitude has several implications that support our hypotheses of asynchrony between diversity and selection. Such a k would suffice to drive $\mathcal{R}(0)$ below 1. A sufficiently early activation of a recall antibody response would then imply that all observable infections of experienced hosts would be mutant infections (Fig. 2). In intermediately immune hosts, there could be a substantial fitness difference $\delta = (c_w - c_m)k$ between mutant and wild-type viruses (where $c_m < c_w$ are the cross immunities to the host's memory strain for the wild-type and the mutant, respectively).

With large k and $t_M = 0$, intermediately immune hosts who cannot block transmission could easily have $\mathcal{R}(0) \approx 1$ for the wild-type; this would make them excellent at generating and selecting for mutant before an infection is cleared.

A final reason why a high k supports the hypotheses of this paper is that antigenic evolution is extremely rapid if a sufficiently strong recall antibody responses becomes active after viral replication begins but before the infection peaks. New antigenic variants should be generated with near-certainty by virus exponential growth well before the infection's peak – roughly when the number replications that have occurred is at or above the order of magnitude of the inverse mutation rate (Fig. 7). Suppose a strong ($\mathcal{R}(t_e) < 1$) recall response is mounted at that point t_e. The mutant then has target cell resources on which to grow (since $C(t_e) \gg C_{\text{peak}}$) and experiences negligible replication competition from the wild-type (since the wild-type population is not growing but in fact is shrinking). If not lost stochastically, it should therefore emerge to detectable and transmissible levels. We do not observe this. This suggests that if k is large, not only must the antibody response not be immediate ($t_M > 0$), but it must also be late enough enough to make this effect unlikely: it must happen either just before or after the peak of infection. Evidence suggests that this is indeed the case. Infections peak by 36–48 hours post-infection, and antibody responses only begin 48–72 hours post infection.

5.1.2 Small values of k are a sub-hypothesis of the general model of asynchrony between diversity and selection

Small k early in infection does produce weak replication selection, but it means that neutralization during viral replication cannot explain protection against reinfection. In such a scenario, it is still necessary to invoke mucosal sIgA antibodies or another

mechanism of protection at the point of transmission, and so inoculation selection again comes into play.

Indeed, it is unlikely that k is truly zero before the adaptive response is mounted. Occasionally, a virion may encounter residual IgA antibodies, for instance (see section 2. But the effective value of k is likely to be small – too small to curtail the growing infection or produce substantial replication selection. We set it to 0 before t_M for simplicity of model analysis, but our simple binary model approximates the likely scenario in which k is small but non-zero before t_M and then increasingly large afterwards (see 5.1.1).

5.2 Relationship between k and κ

As noted in the Discussion, the relationship between the mucosal antibody neutralization rate κ and the antibody neutralization rate during replication k is unknown, though we have every reason to expect it to be positive.

κ values are particularly difficult to calculate. In our model, we have generally assumed that all virions of type i inoculated into an experienced host are independently neutralized with probability κ_i, and therefore $z_i = e^{-v(1-\kappa_i)}$ for an inoculum consisting only of type i. But this assumption may be violated in practice. Consider a focal virion. Given that another virion has been neutralized, there are fewer antibodies remaining to neutralize our focal virion. This is particularly important for mixed inocula. Wild-type virions, which have higher affinity for the inoculated host's IgA antibodies, may indirectly protect the new variant by competing with it for antibody binding. The new variant virion may have a higher individual chance of being neutralized by those same antibodies as part of a monomorphic inoculum composed of other new variants. These hypotheized interactions could strengthen inoculation selection relative to the independent neutralization we have modeled here.

5.3 Bottleneck sizes

A key component of the argument that replication selection improves mutant survival relative to neutral drift (see Fig. 4F, Fig. A1, and section 4) is that a non-antigenic bottlenecking follows IgA antibody neutralization, so the ratio $v/b \gg 1$

There is reason to suspect that a non-antigenic bottleneck occurs after the sIgA bottleneck because bottlenecks measured in vaccinated and non-vaccinated hosts are of comparable size (indistinguishable from one), suggesting that founding virion population sizes are cut down to small numbers even in the absence of IgA antibodies, though this would also be consistent with the case of $v = 1$ (i.e. IgA antibodies must neutralize on average a single virion to prevent infection, and this virion, if not neutralized or otherwise lost, uniquely founds the infection).

Furthermore, an empirical study of adaptation of an avian influenza virus to a naive mammalian host (ferrets) found that as the virus adapted, measured transmission bottlenecks became tighter (Moncla et al., 2016). The fact that bottlenecks tightened rather than loosening with host adaptation supports our conjecture that when an

influenza virus is well-adapted to its host and replicates rapidly, the first virion or first few virions to invade a cell will be the ancestor of the vast majority of progeny viruses.

5.4 Sensitivity analysis

As described in the Methods, we further assessed sensitivity of the within-host model to variation in key parameters by studying random parameter sets chosen from biologically plausible parameter ranges.

We analyzed two cases: one in which the immune response is unrealistically early ($0 \leq t_M \leq 1$, Fig. A3), and one in which it is realistically-timed ($2 \leq t_M \leq 4.5$) Fig. A4, see also Fig. A2 and other model parameters in table 2.

We found that with early immunity, regardless of particular parameter values, new variants are frequently seen when experienced hosts are detectably reinfected, and the overall probability of new variant infections is unrealistically high. These observable new variants are most often generated *de novo* and replication selected (Fig. A3, see also Fig. A2).

When immunity is realistically-timed, the pattern of much rarer replication selection is robust to variation in parameters. New variant infections compose a realistically small fraction of all detectable reinfections (Fig. A4, Fig. A2). Moreover, inoculation selection is sometimes more common than replication selection as a source of new antigenic variants (Fig. A4, see also Fig. A2).

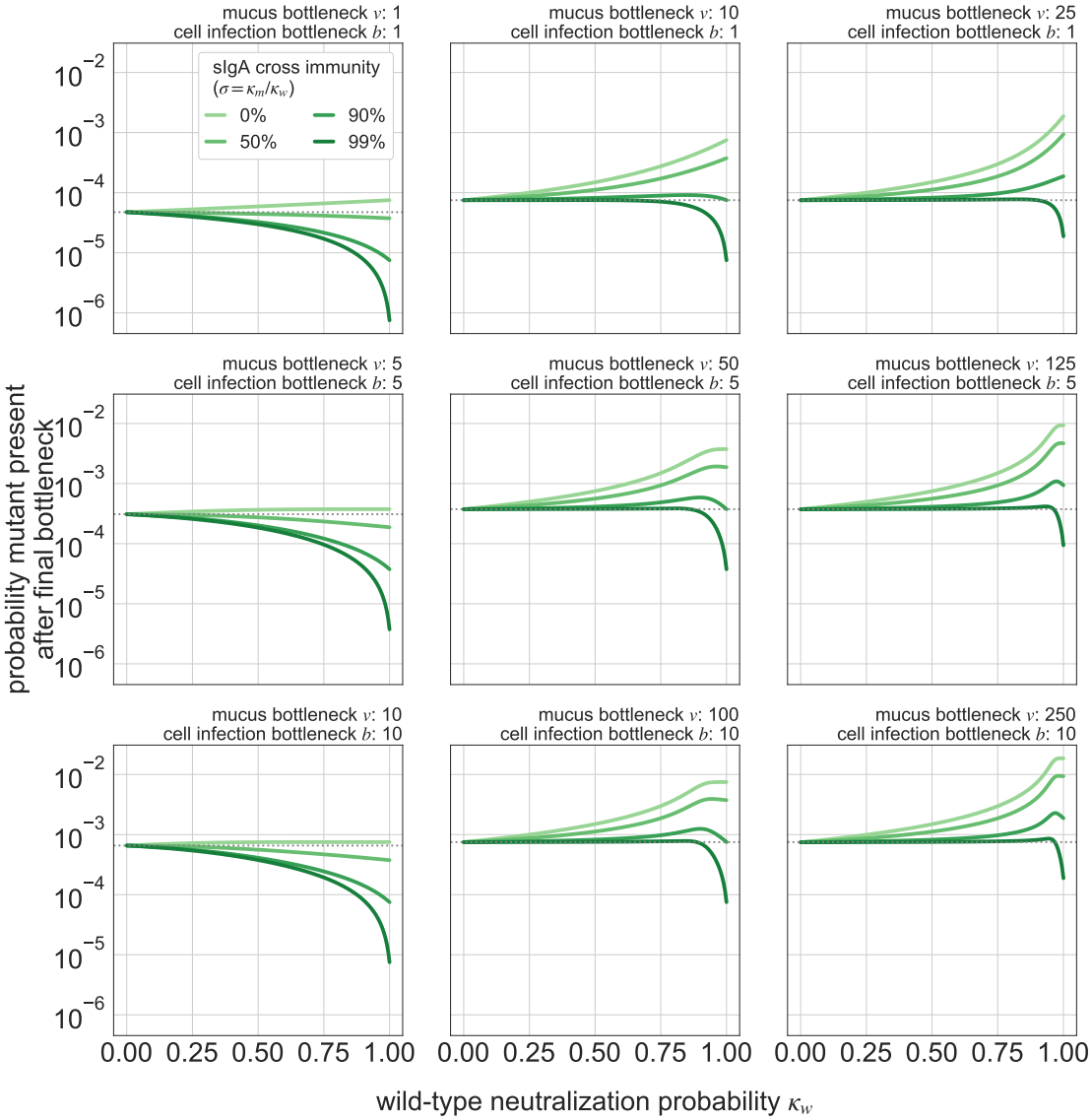

Fig. A1. Probability that a new variant present after cell infection (final) bottleneck as a function of cross immunity and degree of competition discussionfor the final bottleneck. Probability shown as a function of probability of no wild-type infection (z_w), degree of cross immunity between mutant and new variant $\sigma = \kappa_m/\kappa_w$, mucus bottleneck size v, and final bottleneck size b. Gray dotted line indicates probability that a new variant survives the transmission bottleneck in a host who is naive to both wild-type and variants (i.e. drift). $f_{mt} = 7.5 \times 10^{-5}$, a typical value for a naive transmitting host in stochastic simulations

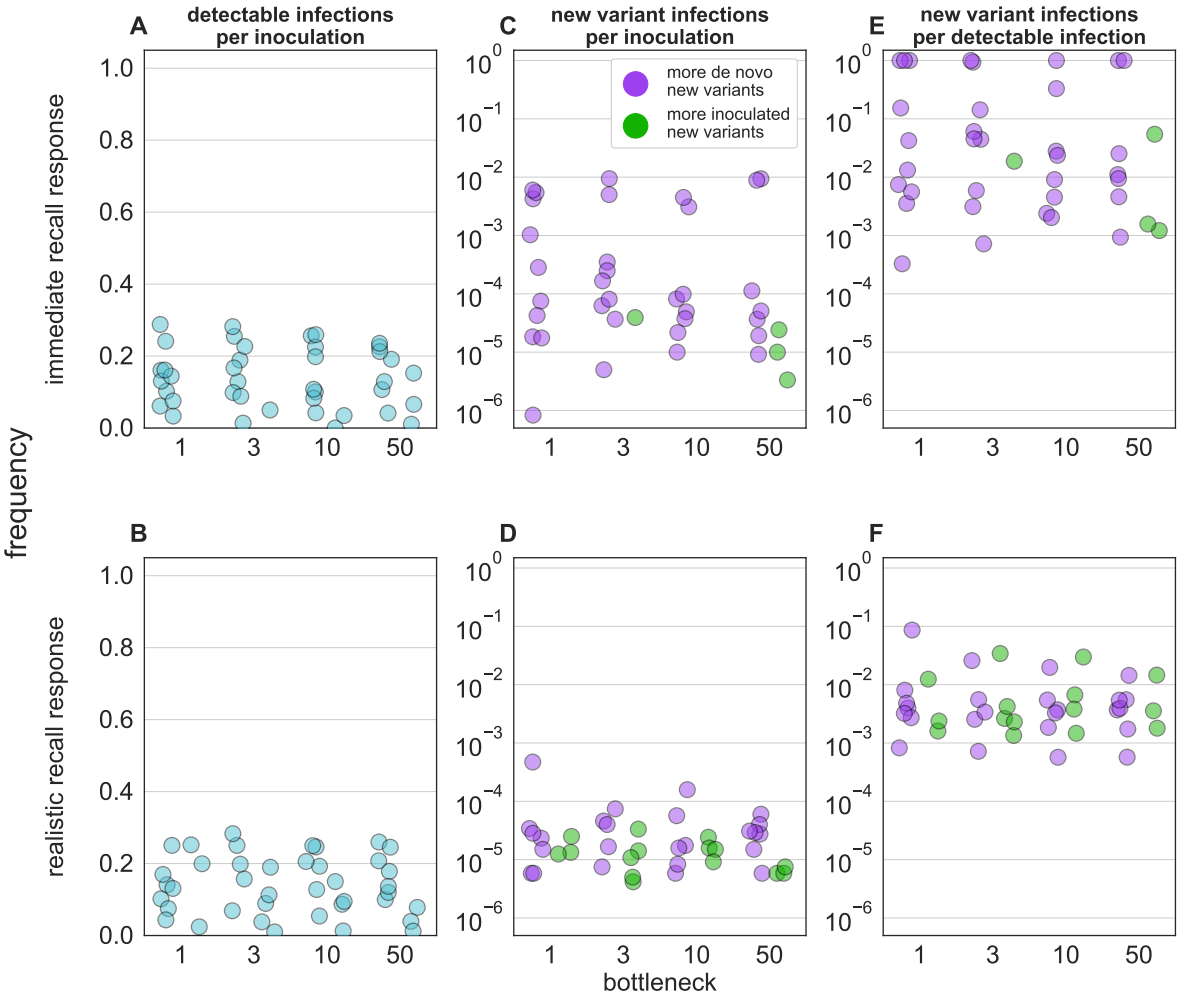

Fig. A2. Sensitivity analysis varying model parameters across biologically-reasonable parameter ranges. (**A, B**) Probability of a detectable infection per inoculation of an experienced host. (**C, D**) Probability of a detectable new variant infections per inoculation of an experienced host. (**E, F**) Fraction of detectable infections of experienced hosts that are new variant infections. Points colored according to whether new variant infections were more frequently caused by *de novo* generated (purple) or inoculated (green) new variant viruses. Each point represents a random parameter set; 10 random parameter sets generated for each bottleneck value shown, and 50 000 inoculations of an experienced host simulated for each parameter set. Two regimes of simulated parameter set shown: (**A, C, E**) an immediate recall response regime, in which t_M varied from 0 to 1, and (**B, D, F**) a realistically timed response regime, in which t_M varied from 2 to 4.5. All other parameters varied across the same ranges in both regimes (see Table 2 for ranges). Parameters Latin Hypercube sampled from within ranges for each regime and bottleneck size.

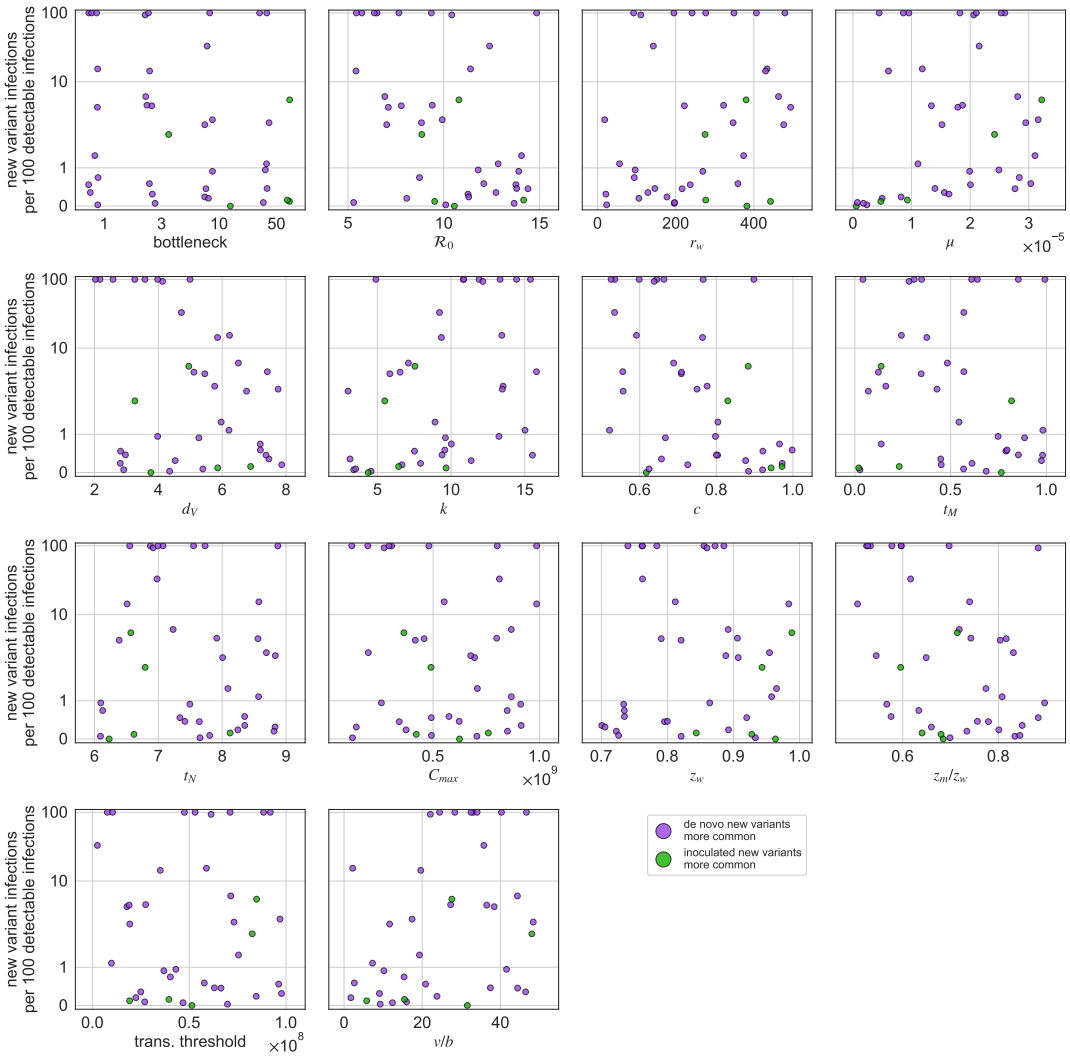

Fig. A3. Sensitivity analysis: parameter values versus rate of new variant infections per 100 detectable infections of an experienced host, given an unrealistically early recall response. Parameters randomly varied across the ranges given in table 2, with t_M varied between 0 and 1. Each point represents a parameter set; the rate of new variant infections per hundred 100 detectable infections is estimated from 50 000 simulated inoculations of an experienced host. A new variant infection is defined as one in which the new variant reached a transmissible frequency of at least 1% at any point in the infection. Points are colored according to whether new variant infections were more frequently caused by *de novo* generated (purple) or inoculated (green) new variant viruses

.

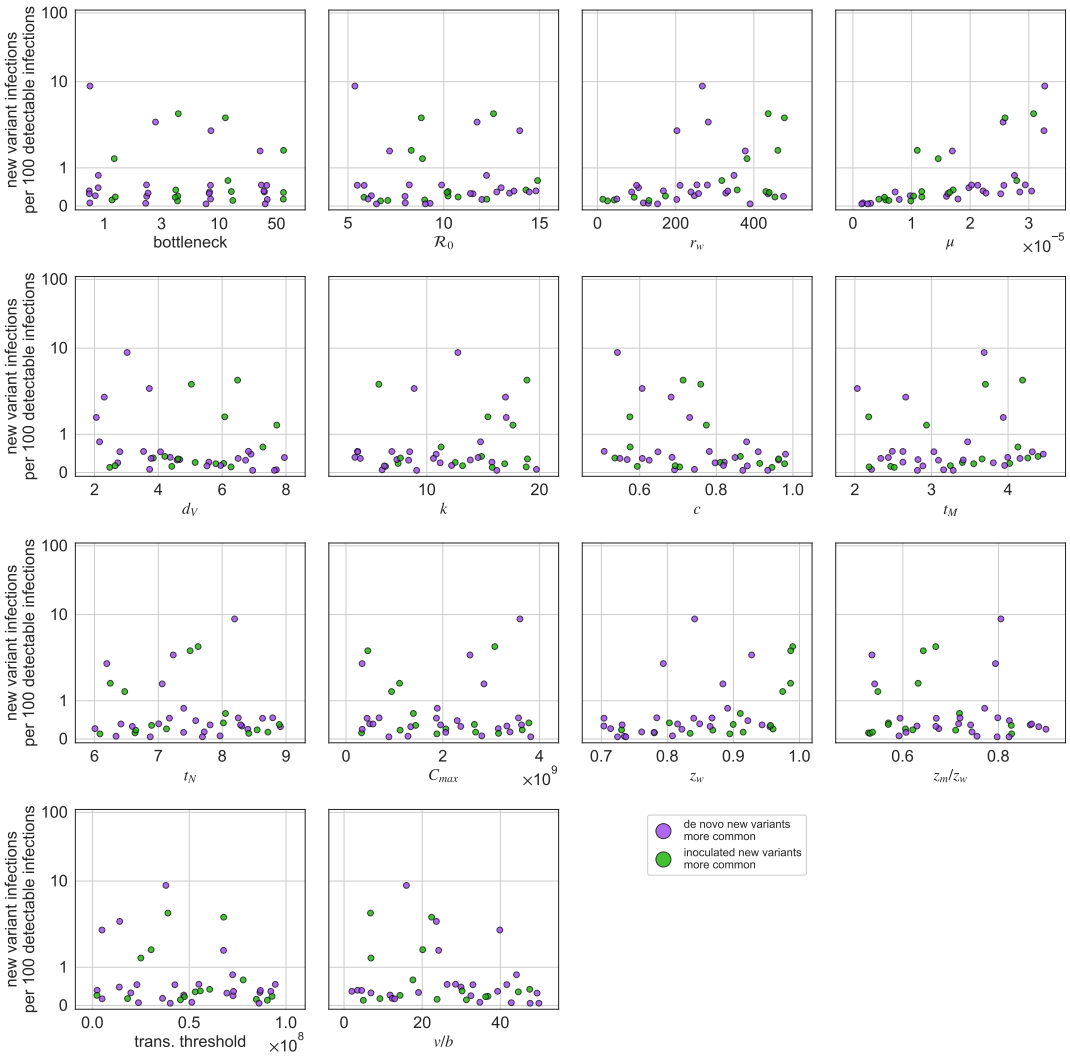

Fig. A4. Sensitivity analysis: parameter values versus rate of new variant infections per 100 detectable infections of an experienced host given a realistic (48 hours or more post-infection) recall response. Parameters randomly varied across the ranges given in table 2, with t_M varied between 2 and 4.5. Each point represents a parameter set; the rate of new variant infections per hundred 100 detectable infections is estimated from 50 000 simulated inoculations of an experienced host. A new variant infection is defined as one in which the new variant reached a transmissible frequency of at least 1% at any point in the infection. Points are colored according to whether new variant infections were more frequently caused by *de novo* generated (purple) or inoculated (green) new variant viruses.

.

6 Polyphyletic emergence of antigenicity altering substitutions

6.1 Background

Amino acid substitutions associated with the emergence of new antigenic variants have reached fixation in parallel in genetically distinct co-circulating lineages in the antigenic evolution of both A/H1N1 and A/H3N2 seasonal influenza viruses. The frequency of polyphyletic emergence of antigenicity altering substitutions across distinct genetic backgrounds is not compatible with current theories posed to explain the disconnect between the rapid and continuous genetic evolution and punctuated antigenic evolution of influenza viruses (see section 7). Many of these models assume that large effect antigenicity-altering substitutions can only emerge in specific genetic contexts (Koelle & Rasmussen, 2015; A. J. Kucharski et al., 2015). Moreover, antigenic polyphyly is suggestive of a rising generation rate of antigenic novelty as a cluster ages, rather than a fixed rate of antigenic emergence. This too is a prediction of the inoculation selection paradigm, in which inoculations of immune hosts may increase the rate of appearance of antigenic novelty.

To show that large effect antigenic changes can occur in multiple backgrounds, we assessed the evolutionary relationships and built phylogenetic trees for known recent polyphyletic antigenicity-altering substitutions that have emerged in A/H1N1 and A/H3N2.

6.2 Phylogenetic Methods

We analyzed polyphyletic antigenic changes using hemagglutinin (HA) gene nucleotide sequences deposited in the GISAID EpiFlu^{TM} database.

We downloaded all seasonal A/H1N1 HA sequences from the period 1999–2008, to center on the antigenic cluster transition from the New Caledonia/1999-like phenotype to the Solomon Islands/2006-like phenotype, excluding pandemic A/H1N1 viruses. We downloaded A/H3N2 virus HA sequences for two periods: 2008 to 2011, to centre on cluster transition from Brisbane/07 to the Perth/2009-like and Victoria/2009-like phenotypic split, and 2012 to 2014, to capture the co-circulation of Clade 3C.2a and 3C.3a (table A1). We discarded all sequences with an incomplete HA1 domain or with more than 1% ambiguous nucleotides.

We aligned sequences using MAFFT v7.397 (Katoh, Misawa, Kuma, & Miyata, 2002) and reconstructed phylogenetic trees using RAxML 8.2.12 under the GTRGAMMA model (Stamatakis, 2014). We performed global optimization of branch length and topology on the RAxML reconstructed tree using Garli 2.01 with model parameters matching the RAxML reconstruction (500,000 generations) (Bazinet, Zwickl, & Cummings, 2014). It was computationally intractable to run Garli on the full phylogeny of A/H3N2 2012–2014 (n = 10107). We visualized phylogenetic trees using Figtree (http://tree.bio.ed.ac.uk/software/figtree) and ggtree (Yu, Smith, Zhu, Guan, & Lam, 2017)

We mapped amino acid substitutions onto branches using custom Python scripts available in the project Github. All numbering complies with H1/H3 numbering scheme (Burke & Smith, 2014).

Table A1: Dataset composition

A/H1N1 1999–2008		A/H3N2 2008–2011		A/H3N2 2012–2014	
Pre-filter	Final dataset	Pre-filter	Final dataset	Pre-filter	Final dataset
4882	3514	7050	5738	11970	10107

6.3 A/H1N1

The HA K140E antigenicity-altering substitution first occurred in 2000 and was detected sporadically prior to its independent fixation in 2006–2007 in three phylogenetically distinct, geographically segregated lineages of A/H1N1 that diverged in 2004 (Fig. A5) (Bedford et al., 2015). The K140E substitution resulted in a cluster transition from the New Caledonia/1999-like antigenic phenotype to the Solomon Islands/2006-like phenotype, with lineage A emerging as the dominant lineage globally before the 2009 H1N1 pandemic (Bedford et al., 2015). Position 140 is located in the Ca2 antigenic site of the HA1 domain immediately adjacent to the receptor binding site, where amino acid composition mediates receptor binding function (Koel et al., 2013).

The three lineages have distinct HA1 mutational trajectories away from their most recent common ancestor, as defined by the set of amino acid substitutions that accumulate along the predominant trunk lineages both prior to and following the fixation of the K140E substitution (table A2, Fig. A5). All three lineages acquired amino acid substitutions at previously characterized antigenic sites, as well as substitutions with suggested functional consequences, including glycosylation gain and loss (Caton, Brownlee, Yewdell, & Gerhard, 1982). The three lineages share the Y94H substitution prior to K140E fixation, with limited overlap of other substitutions: lineage A and B share changes at residue 188, whereas A189T occurs in lineage B and A prior to and post K140E emergence respectively.

Table A2: Substitutions that characterize the co-circulating K140E-defined lineages

Lineage	Geographic composition in first year of co-circulation	Trunk substitutions from MRCA to K140E fixation	Trunk substitutions post-K140E fixation
1	South Asia	Y94H, R188K, E273K	D35N, K145R*, A189T, G185V, N183S, G185S
2	East Asia	Y94H, S36N, A189T, R188M, T193K*	N244S, K82R*, I47K, E68G
3	South-East Asia	Y94H, K73R, V128A*, A128T*	P270S

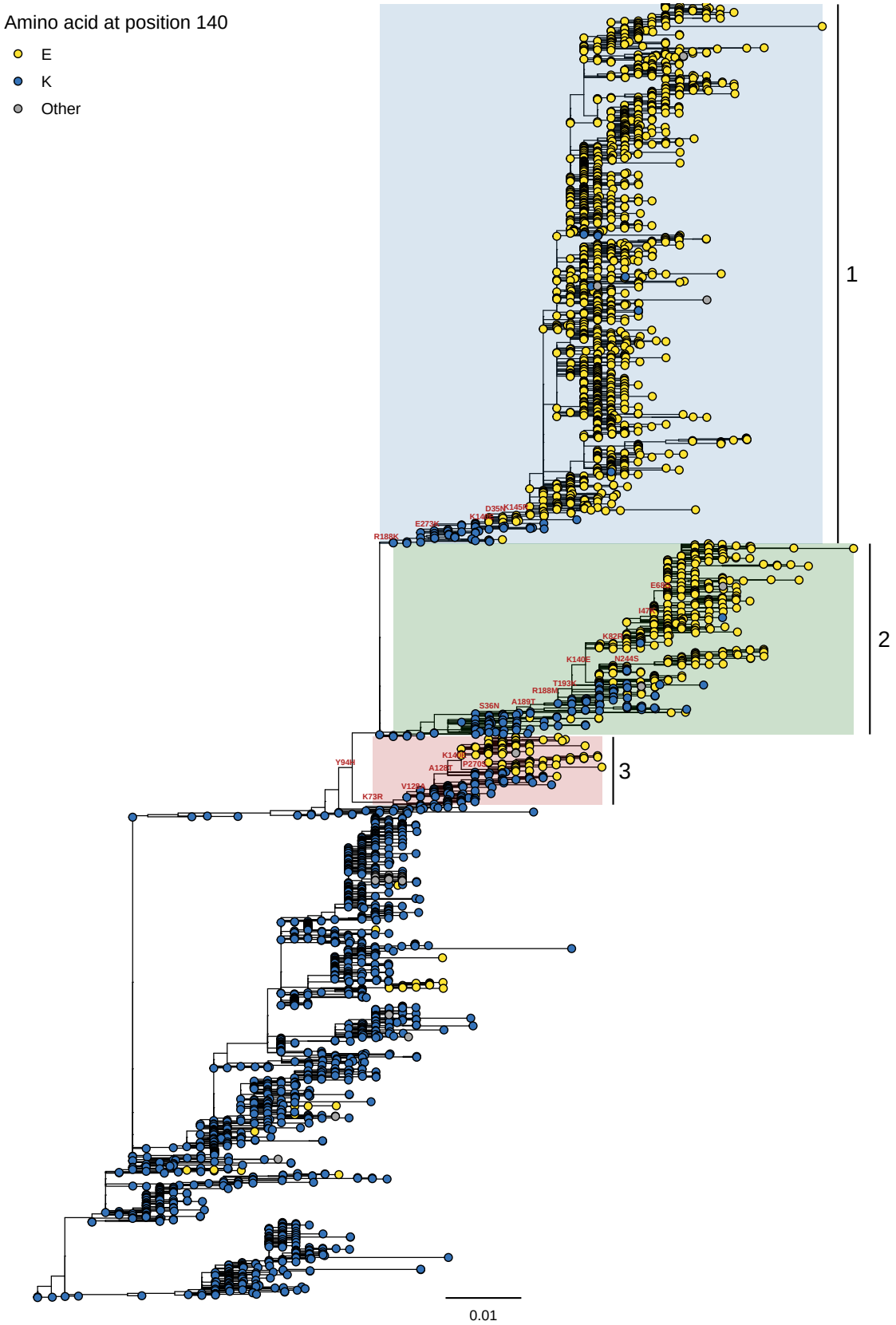

Fig. A5. Phylogeny of A/H1N1 seasonal viruses for the period 1999 to 2008. Branch tip colour indicates the amino acid identity at position 140. Co-circulating lineages defined by the K140E fixation are highlighted. Scale bar indicates the number of nucleotide substitutions per site. Tree rooted to A/New Caledonia/20/1999

6.4 A/H3N2 2008-2011

In the period 2008-2011, the K158N substitution was only detected once in 2009 before fixing in combination with N189K in the same year in two distinct co-circulating A/H3N2 lineages. N189K was not detected before fixing as a K158N/N189K double substitution. The combination of the substitutions resulted in an antigenic phenotype switch from Wisconsin/2005-like to the Perth/2009-like and Victoria/2009-like phenotypes respectively. Residues 158 and 189 are both located in antigenic site B adjacent to the receptor binding site, with substitutions at both residues characterized as cluster-transition substitutions in multiple historic A/H3N2 cluster transitions (Koel et al., 2013). The HA-defined evolutionary trajectories of viruses from the Perth/2009-like lineage and Victoria/2009-like lineages from their most recent common ancestor are characterized by distinct sets of substitutions (table A3, Fig. A6). Both lineages acquired substitutions at previously characterized antigenic sites (Koel et al., 2013), but only share the T212A substitution.

Table A3: Substitutions that characterize the co-circulating genetic / antigenic clades defined by K158N and N189K

Lineage	Trunk substitutions from MRCA to K158N/N189K fixation	Trunk substitutions post- K158N/N189K fixation
1 (Victoria / 2009-like)		T212A, S45N, T48A, K92R, Q57H, A198S, V223I, N312S, N278K,Q33R, N145S, G5E, E62V, D53N, E280A, I230V, Y94H, I192T, S199A
2 (Perth / 2009-like)	E62K	N144K, R261Q, I260M, P162S, E50K, V213A, N133D, T212A, R142G

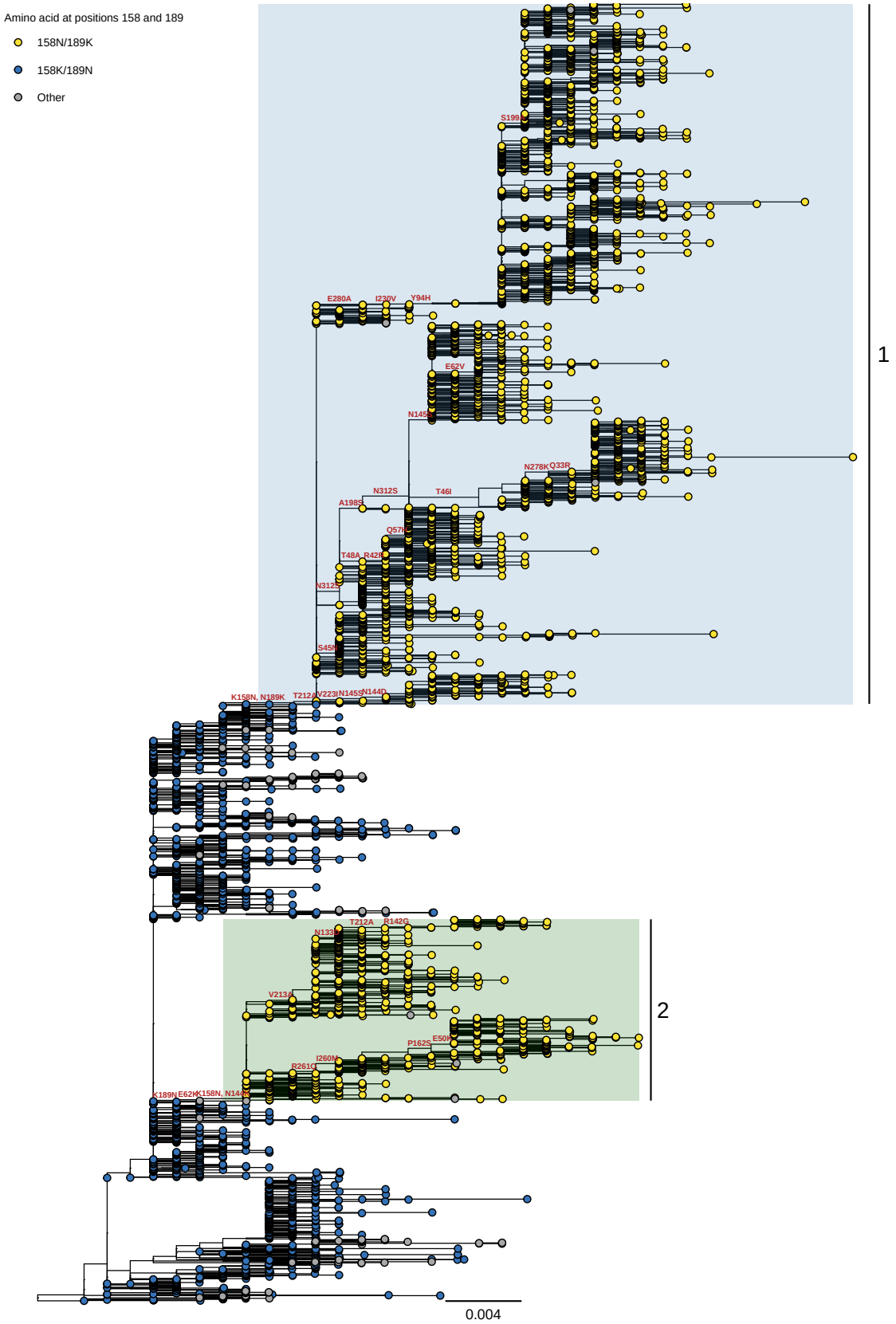

Fig. A6. Phylogeny of A/H3N2 seasonal viruses for the period 2008 to 2011. Branch tip colour indicates the amino acid identity at position 158 and 189. Co-circulating lineages defined by the K158N/N189K fixation are highlighted. Scale bar indicates the number of nucleotide substitutions per site. Tree rooted to A/Brisbane/10/2007.

6.5 A/H3N2 2012–2014

In 2014 two independent substitution at position 159, F159S and F159Y, fixed in distinct A/H3N2 lineages co-circulating globally (Fig. A7). The S159Y substitution was detected sporadically in 2012/2013 before fixing in 2014 to define the A/H3N2 clade 3C.2a, which circulated as the dominant clade globally for the next three years. The F159S substitution was not detected in 2012–2013 before reaching fixation in 2014 to define clade 3C.3a, which continued to circulate globally at low frequencies.

Residue 159 is located in antigenic site B. The S159Y substitution in combination with Y155H and K189R substitutions previously resulted in the transition of the A/H3N2 Bangkok/79-like antigenic phenotype to Sichuan/87-like phenotype (Koel et al., 2013).

The two lineages have independent mutational trajectories for their HA gene away from their most recent common ancestor, excluding both acquiring the N225D substitution prior to F159X-fixation, with changes acquired changes at the major antigenic epitopes (Table A4, Fig. A7) (Koel et al., 2013).

Table A4: Substitutions that characterize the co-circulating genetic / antigenic clades defined by F159Y and F159S

Lineage	Trunk substitutions from MRCA to F159X fixation	Trunk substitutions post-F159X fixation
F159Y (lineage 1, Clade 3C.2a)	L3I, N225D, Q311H, N144S, K160T	R142K, R261L
F159S (lineage 2, Clade 3C.3a)	R142G, T128A, A138S, N225D	

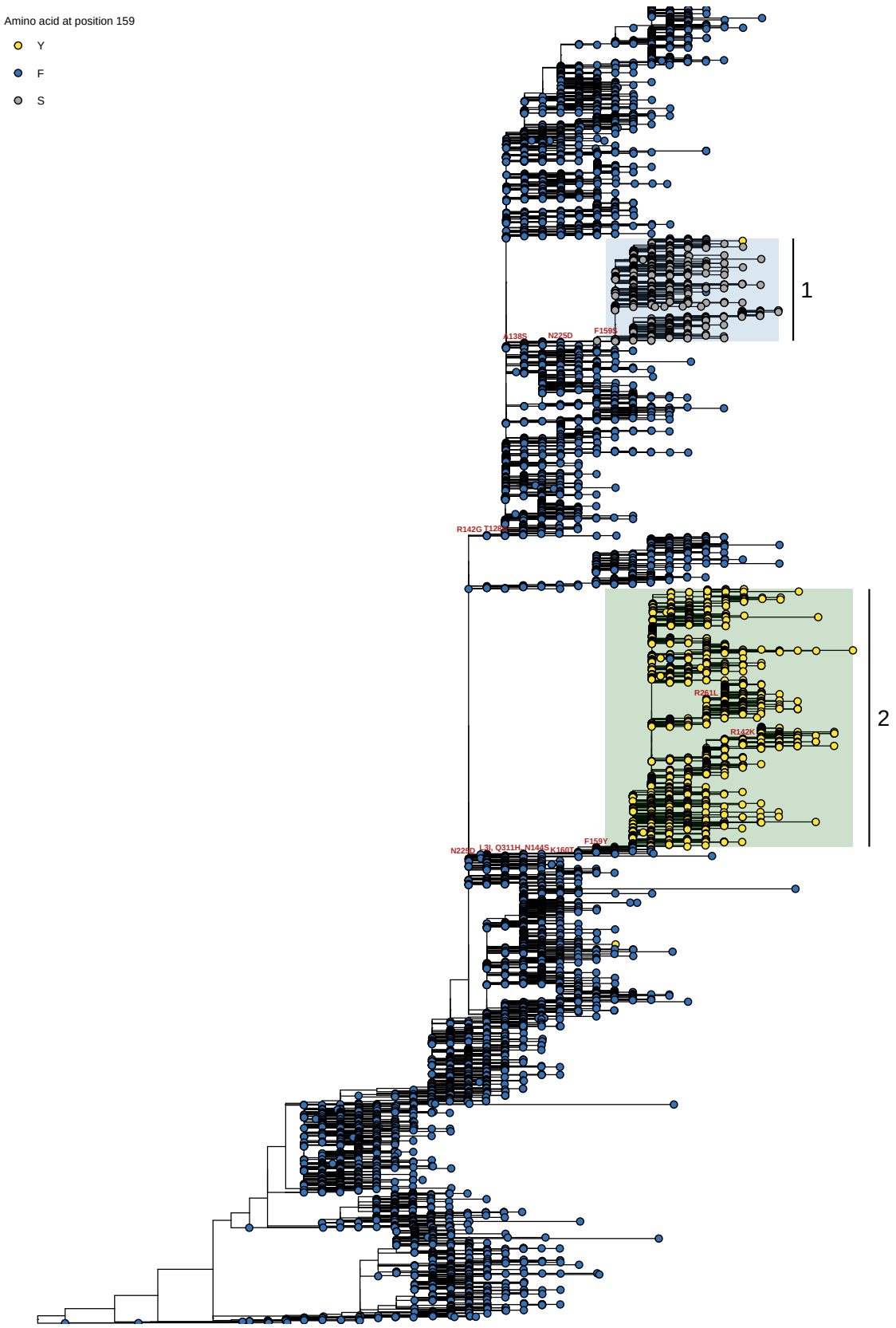

Fig. A7. Phylogeny of A/H3N2 seasonal viruses for the period 2012 to 2014. Branch tip colour indicates the amino acid identity at position 159. Co-circulating lineages defined by the F159X fixation are highlighted. Scale bar indicates the number of nucleotide substitutions per site. Tree is rooted to A/Perth/16/2009.

7 Prior studies and alternative hypotheses

A number of theoretical studies over the last 20 years have addressed the tempo and structure of seasonal influenza virus antigenic evolution. Most have focused on population level dynamics (Ferguson, Galvani, & Bush, 2003; Koelle, Cobey, Grenfell, & Pascual, 2006; Recker, Pybus, Nee, & Gupta, 2007; Gog, 2008; Koelle et al., 2009; Bedford et al., 2012; Wikramaratna, Sandeman, Recker, & Gupta, 2013; Zinder, Bedford, Gupta, & Pascual, 2013; Koelle & Rasmussen, 2015). Two have addressed within-host influenza virus antigenic evolution (Luo et al., 2012; Volkov et al., 2010).

Existing population-level studies treat within-host virus and antibody dynamics implicitly and assume that all transmissions have an equal chance of producing a majority-mutant infection regardless of recipient host immune status. This typically means that models must introduce hypothetical mechanisms to limit population-level antigenic diversity. In the absence of these mechanisms, antigenic and genetic diversity grow at unrealistic rates (Recker et al., 2007; Koelle & Rasmussen, 2015).

The two within-host studies both make two key assumptions: (1) immune selection pressure is strong from the moment of inoculation in experienced hosts and (2) influenza virus transmission bottlenecks are wide (e.g. 10^5 virions (Luo et al., 2012) or sufficient for the three most frequent within-host variants all to be transmitted onward (Volkov et al., 2010)). Antibody-mediated selection pressure is in fact likely to vary substantially over the course of infection, as discussed extensively above, and recent empirical studies suggest that transmission bottlenecks are very small (on the order of a single virion (McCrone et al., 2018)).

Both studies find that antigenic variants are routinely generated *de novo* during an infection and undergo substantial positive selection during that same infection. As discussed above, NGS studies of natural human infections suggest that this is in fact uncommon.

We cannot exclude the possibility that some previously described mechanisms play a role in limiting influenza virus antigenic evolution. But given the evidence that within-host selection on antigenic phenotypes is inefficient (both from our own study and from the studies that provide the biological motivation for our model), it is not clear that there is any need to invoke those mechanisms to explain observed patterns of influenza virus antigenic evolution. In the following section, we go into more depth about how our study contributes to and revises the existing literature on the mechanisms limiting influenza antigenic evolution.

7.1 Models with protection through neutralization during replication

The most crucial assumption in existing within-host models of influenza immune escape (Luo et al., 2012; Volkov et al., 2010) or pathogen immune escape generally (Kennedy & Read, 2017) is that adaptive immunity protects against reinfection by neutralizing pathogens during the timecourse of replication. This is immunologically unrealistic, and our models show that it produces an unrealistically binary outcome: either no reinfection, or detectable reinfection with exclusively mutant viruses. This binary

outcome occurs in the existing models influenza, but it was considered a feature, not a bug, because the frequency of homotypic reinfection was not yet known.

A general model of pathogen immune escape (Kennedy & Read, 2017) studied ideas related to replication selection to argue that prophylactic anti-pathogen interventions (such as pre-exposure vaccination) could be less vulnerable to pathogen evolutionary escape than therapeutic interventions (such as post-symptomatic courses of antivirals). Therapeutic interventions occur after a number of pathogen replication events and therefore select upon on a larger, more diverse array of potential pathogen variants. Prophylactic interventions may limit the number of replications before clearance and thereby limit opportunities for diversification. Like the influenza models, this general model does not address the question of how evolution can be rare in symptomatic or otherwise observable infections, where substantial diversity can be generated.

7.2 The importance of inoculated diversity

Kennedy and Read, 2017 and Luo et al., 2012 study immune escape with $\mathcal{R}^w(0) < 1$ but consider only diversity generated after inoculation. Our study complicates their results: we find that when $\mathcal{R}^w(0) < 1$ the dominant mode of antigenic evolution will be selection on inoculated diversity , not selection on generated diversity. The pace of evolution will depend on how likely an escape mutant is to be transmitted to an experienced host. If bottlenecks in experienced hosts are wide, evolution may be rapid. If these bottlenecks are tight or escape mutants are deleterious within untreated naive hosts (so f_{mt} is low), then $\mathcal{R}^w(0) < 1$ at the start of infection can result in slow evolution, since both replication and inoculation selection will be rare.

In the absence of mucosal neutralization with small f_{mt}, $b \ll \frac{1}{f_{\text{mt}}}$, and small μ, the threshold for where inoculation selection becomes more common than replication selection with $\mathcal{R}^w(0) < 1$ is approximately

$$f_{\text{mt}} b p_{\text{sse}} > \mu \frac{b\mathcal{R}^w(0)}{1 - \mathcal{R}^w(0)} p_{\text{sse}}$$

or simply:

$$f_{\text{mt}} > \mu \frac{\mathcal{R}^w(0)}{1 - \mathcal{R}^w(0)} \tag{A29}$$

the left-hand side comes from equation A19, which gives an probability that a mutant with $\mathcal{R}^m(0) > 1$ is inoculated. The right-hand side comes from equation A18, which gives the probability that an escape mutant is generated in a declining but replicating virus population before that population goes extinct. p_{sse}, which occurs on both sizes and cancels, is the probability that a mutant survives stochastic extinction. We have also ignored the fact the the right-hand side should have a term representing the probability that inoculation selection does not occur, but as we are considering cases when both inoculation selection and replication selection are rare, that term is approximately one.

On average, $f_{\text{mt}} > \mu$ due the asymmetry between forward and back mutation rates when the mutant is rare. It follows that $f_{\text{mt}} > \mu \frac{\mathcal{R}^w(0)}{1-\mathcal{R}^w(0)}$ should hold when (A) the

mutant not is too deleterious in the absence of positive selection (since this reduces f_{mt}) or (B) $\mathcal{R}^w(0)$ is not close to 1 (since then many copies are made on average before the virus goes extinct). Alternatively, if b is sufficiently large – on the order of $\frac{1}{f_{\mathrm{mt}}}$ – selection on inoculated diversity will be the dominant mode of evolution simply because most inocula will include mutants.

Selection on inoculated diversity may be important in many host-pathogen systems, not just in influenza antigenic evolution. Some anti-microbial resistance in bacteria, for instance, is acquired through the uptake of preexisting plasmids, rather than through *de novo* mutation (Perron, Inglis, Pennings, & Cobey, 2015). Whether drug resistance emerges in an individual treated host will depend on whether any of the bacteria inoculated bear the needed plasmid.

7.3 Limits to immune escape through non-strain specific limiting factors

Two studies (Luo et al., 2012; Hartfield & Alizon, 2014) have previously noted that evolutionary emergence of escape mutants or otherwise fitter pathogens can be made more difficult due to ongoing competition from the wild-type for a shared resource, whether susceptible cells within a host, as in Luo et al., 2012 and our model, or susceptible hosts within a population, as in Hartfield and Alizon, 2014.

In our model, non-strain specific limiting factors such as target cell depletion explain why the mutant does not have the opportunity to rise in frequency once the adaptive response – and therefore fitness differences – become substantial. We also invoke non-strain-specific limiting mechanisms to explain why immunocompromised hosts – in whom these mechanisms are weaker – can select for antigenic mutants at the scale of a single infection. Finally, we invoke non-strain-specific limiting factors to explain why infections of naive hosts are typically cleared well before an adaptive immune response can select an escape variant. The third of these three points has been posited previously (Luo et al., 2012), but not the first two.

Hartfield and Alizon, 2014 focus on the probability that a fit mutant strain the emerges at the host population scale goes stochastically extinct before causing a large epidemic, and show that competition for hosts with the wild-type raises this extinction probability. While this may be relevant to influenza at the population level (see section 8.5 below), an analogous within-host argument is unlikely to be a sufficient explanation for the rarity of influenza antigenic mutants within human hosts. New variants are likely to be generated when an influenza virus infection is still well within its exponential growth phase, competition for susceptible cells is relatively unimportant, and probability of stochastic extinction for all incipient lineages is therefore low (due also to influenza's high $\mathcal{R}_0$). The absence of selection, rather than a high rate of stochastic loss of mutants during within-host replication, is the most important component of our explanation for the rarity of observable influenza antigenic evolution within individual human hosts.

Note that Hartfield and Alizon also have a model of within-host immune escape for a general pathogen, but there they focus on estimating the contribution of a partially effective adaptive immune response to the probability that a small escape mutant population goes stochastically extinct (Hartfield & Alizon, 2015), which is not relevant

to situations in which time of mutant first emergence typically precedes time of adaptive immune proliferation (as with influenza viruses).

7.4 Fitness costs for antigenic mutants

Previous population-level studies have argued that non-antigenic fitness costs associated with antigenic substitutions (Gog, 2008; A. Kucharski & Gog, 2011) or deleterious mutational load on the influenza genome (Koelle & Rasmussen, 2015) are necessary to explain the pace of influenza virus antigenic evolution in the human population. These models introduce population-level antigenic novelty at rates 5–10 times higher than predicted by inoculation selection, and at equal rates early and late during the circulation of an antigenic variant.

In the absence of meaningful replication selection, the population level rate of antigenic diversification is the average rate at which new variants survive all transmission bottlenecks to found or co-found infections. In an inoculation selection regime, that rate is unlikely to surpass 2 in 10^4 inoculations. We obtain that estimate assuming no within-host replication cost for antigenic mutants, weak cross immunity between mutant and wild-type viruses, and many experienced hosts who reliably neutralize wild-type virions at the point of transmission. Actual rates of new variant survival are almost certainly lower. First, we have assumed that a new antigenic variant can be produced by a single amino acid substitution (accessible via a single nucleotide substitution), however a recent detailed study of the antigenic evolution of A/H3N2 viruses shows that some new variants require more than one substitution (Koel et al., 2013). Second, some (possibly many) previously infected hosts will not possess well-matched antibodies due to original antigenic sin (Davenport & Hennessy, 1956), antigenic seniority (Lessler et al., 2012), immune backboosting (Fonville et al., 2014), or other sources individual-specific variation in antibody production (Lee et al., 2019). These factors individually, and particularly in combination, which have not been modelled in this study mean that the above 2 in 10^4 transmission estimate is likely to be unrealistically high. By comparison, existing population level models that invoke fitness costs introduce population-level antigenic diversity at much higher rates. One study (Koelle & Rasmussen, 2015) introduces new antigenic variants at a rate of 7.5 per 10^4 transmissions; another (A. Kucharski & Gog, 2011) introduces new population-level mutations at a continuous rate of 6.8×10^{-4} mutations per infected individual per day, which should produce new variant infections by 2 days post infection in at least 1 of every 10^3 infected hosts:

$$1 - \exp\left(-6.8 \times 10^{-4} * 2\right) \approx 0.0013$$

Prior to the accumulation of population immunity, infections dominated by new variants should be rare, and new variants should be nearly neutral relative to the wild-type at the population level. This may be sufficient to explain the absence of diversification early in the circulation of a cluster without invoking non-antigenic fitness costs. That said, additional constraints on the virus, particularly those that reduce the within-host fitness of antigenic variants, should further retard new variant emergence by

reducing variant frequencies in donor hosts and thereby reducing the probability that new variants survive transmission bottlenecks.

In a phylogenetic analysis, we also find multiple instances in which a small subclade with a cluster transition substitution appears and then goes extinct before the emergence of a successful cluster transition clade (section 6). We also find multiple instances of polyphyletic cluster transitions: a cluster transition amino acid substitution arises and proliferate on two or more branches of the virus phylogeny at this same time. Both observations are inconsistent with models that assume antigenic variants must be intrinsically or incidentally unfit prior to the moment that they proliferate at the population level (Gog, 2008; Koelle & Rasmussen, 2015): the cluster transition mutant can reach surveillance-detectable levels even before substantial population immunity has accumulated, and it can fully emerge against multiple genetic backgrounds.

7.5 Previous discussion of selective bottlenecks in the literature

Previous literature on influenza mentions a "selective bottleneck" (Wilker et al., 2013; Moncla et al., 2016; Leonard et al., 2016), but this does not refer to antigenic inoculation selection. Rather, a "selective bottleneck" has been typically used to mean simply a tight neutral bottleneck (that leads to stochastic loss of diversity) or to non-antigenic factors that lead to preferential transmission of certain variants. To our knowledge, ours is the first study to explicitly model the role of selection at the point of transmission versus selection during replication in the promotion of mutants, antigenic or otherwise.

7.6 Comparison with the antimicrobial resistance literature

The antimicrobial resistance literature makes a distinction between "acquired" and "transmitted"(or "primary") drug resistance Bonhoeffer, Lipsitch, and Levin, 1997, but this should not be confused with replication and inoculation selection. Transmitted resistance refers to the acquisition of a resistant infection from a host infected with resistant microbes, without regard for whether those microbes were a minority or majority variant in the transmitting host. Inoculation selection, in contrast, refers to a selective founder effect that *favors* transmitted drug resistance or transmitted antigenic novelty. One strain present in a mixed infection has a higher probability of surviving the transmission bottleneck than its frequency alone would suggest, simply because the recipient host is more susceptible to that strain than to competing inoculated strains.

7.7 Alternative explanations for rare within-host antigenic variants

There are several possible explanations for the observed phenomenon that new antigenic variants within experienced infected hosts could be rare. But only one: small inocula, transmission-blocking mucosal antibodies, but a slow-to-mount recall adaptive immune response – can explain the aforementioned empirical observations simultaneously.

Our proposal is that antibodies are present in the mucosa and effective at blocking transmission, but have only a small effect on viral replication once cells become productively infected. Antigenic selection after successful infection therefore begins with the mounting of a recall response 48–72 hours post infection. In this case, selection pressure can be strong at the point of transmission, but subsequently weak until after 48 hours. Inoculation selection unites strong but not perfect sterilizing homotypic immunity with rare observations of mutants in successfully reinfected experienced hosts.

In this section, we discuss alternative hypotheses and explain why we believe they are less compelling than our proposal.

7.7.1 Protection through neutralization during replication, i.e. an immediate recall response

Adaptive immune pressure could be strong enough that $\mathcal{R}^w(0) < 1$. In that case, a wild-type infection dies out if it does not produce a mutant virion, and it only has, on average, $\frac{b}{1-\mathcal{R}^w(0)} - b$ replication events in order to do so before the infection is cleared (average replication events in b independent subcritical branching processes with branching parameter $\mathcal{R}^w(0)$, see section 3.8). In this case, homotypic reinfection is truly binary: it results in an undetectable infection that is rapidly cleared or it results in a visible infection dominated by an escape mutant. This is how influenza viruses have been hypothesized to behave in previous models of immune escape (Luo et al., 2012), but it is contradicted by recent empirical work (McCrone et al., 2018; Xue et al., 2017) and by challenge studies (Clements et al., 1986), which suggest that detectable reinfection of experienced hosts frequently occurs without observable immune escape.

7.7.2 Heterogeneous neutralization rates during early viral replication

Adaptive immune pressure could be present from the start of replication, but vary substantially among individuals with the same immune history. This heterogeneity could explain why some individuals (k small, $\mathcal{R}^w(0) > 1$) are productively reinfected with wild-type viruses while others (k large, $\mathcal{R}^w(0) < 1$) are protected. In this way we could have protection via neutralization during the timecourse of infection but still have observable reinfection without immune escape.

While individual variation in immunity does exist (Lee et al., 2019), there are two reasons why this hypothesis is implausible:

First, it is unrealistic given our current understanding of the adaptive immune response to influenza, as discussed in section 2, since it requires IgA production before 48 hours post-infection.

Second, it is unlikely that such heterogeneous protection would be sufficiently bimodal as to completely miss the regime of k values in which replication selection is efficient.

Even if this unlikely hypothesis of bimodal early adaptive responses were to be true, there would remain a role for sampling effects at the point of transmission. If individuals either possess sterilizing-strength immunity that acts early in the timecourse of viral replication or possess sufficiently weak immunity that replication selection is

unlikely, antigenic evolution will be dominated by cases in which mutants are inoculated into strongly immune hosts, as in simpler models with $\mathcal{R}^w(0) < 1$. Inoculated mutants remain crucial in this scenario.

7.7.3 A key role for intermediately immune hosts

A model of influenza evolution (Volkov et al., 2010) finds that even a small number of intermediately immune hosts along a transmission chain should reliably promote the evolution of new antigenic variants.

The model predicts this because it features an immediate recall response, which implies efficient replication selection in intermediately immune hosts. Intermediately immune hosts can be productively infected with wild-type ($\mathcal{R}^w(0) > 1$), so they reliably generate antigenic mutants. Those mutants then immediately undergo positive selection and are often transmitted onward. We see the same phenomenon in our own transmission chain model when there is an immediate recall response (see main text Fig. 6).

Intermediately-strong immunity to wild-type viruses is likely to be common in the human population even at the beginning of a cluster's circulation (Fonville et al., 2014), and yet new variants are rarely observed until a new variant has circulated for multiple years (Smith et al., 2004). This suggests that intermediately immune hosts do not generate and select for new antigenic variants as readily as the model in (Volkov et al., 2010) implies.

Our proposed model of immune selection can explain why intermediately immune hosts may not reliably select for new antigenic variants. A realistically timed recall response makes replication selection unlikely. Rates of inoculation selection are limited in all hosts due by low transmitting host mutant frequencies f_{mt}. Intermediately immune hosts who possesses sIgA that is not well-matched to the wild-type may additionally have a relatively low value of κ_w and therefore be little better than a naive host in promoting new variant survival at the point of transmission.

7.7.4 Within-host deleteriousness

Antigenic mutants could be replication-competent, but weakly deleterious in the absence of immune selection and/or compensatory substitutions. Two studies (Gog, 2008; A. J. Kucharski et al., 2015) have invoked this hypothesis to explain population-level antigenic dynamics. If neutralization is sufficiently strong during virus replication, however, replication selection can still promote mutants during infections of experienced hosts, even in the absence of compensatory mutations. Within-host replication costs decrease the value of the fitness difference δ. Recall that:

$$\delta(t) = \big[g_m(t) - g_w(t)\big] - \big[d_m(t) - d_w(t)\big] \tag{A30}$$

Typically $g_m(t) = g_w(t)$ and so $\delta = k(1-c)$. Here, $g_m < g_w$. For instance, we could have $r_m = qr_w$, $q < 1$ and therefore $g_m = qg_w$. In that case:

$$\delta = k(1-c) - g(t)(1-q) \tag{A31}$$

We estimate g to be order 20 early in infection and declining subsequently. k may well be order 10. So it is very plausible that a weakly deleterious mutant ($q = 0.95$, for instance) could still undergo substantial replication selection early in infection if it offered enough immune escape ($c = 0.70$) and antibodies were present (t_M small).

The effect could be particularly extreme in intermediately immune hosts if immunity drops superlinearly with antigenic distance. If the wild-type is neutralized at a rate $kc_w = 4$ but the mutant is barely neutralized at all $c_m \approx 0$, it could easily overcome even substantial within-host deleteriousness.

In the absence of replication selection, even weak within-host deleteriousness should lead mutants to be rapidly purged (purifying selection should be efficient for phenotypes subject to replication selection) (Sigal et al., 2018), reducing f_{mt}. Within-host deleteriousness would therefore make the population-level rate of new variant emergence slower, since p_{surv} and p_{drift} both decrease as f_{mt} decreases (see section 4.4).

A final possibility is strong within-host deleteriousness in the absence of compensatory mutations: q small enough that $\delta < 0$ even when $t > t_M$ (i.e. the wild-type is more fit within-host than the antigenic mutant even in the presence of an adaptive immune response). This scenario is unlikely given the strength of recall responses, but it would make inoculation selection and founder effects even more important for antigenic diversification.

8 Further implications

8.1 Consequences for modeling influenza virus dynamics

Population size, population level emergence ("mutation") rate, and degree of population structure all substantially impact the emergence of new influenza antigenic variants at the population level. It has been hard for population level models to distinguish plausible hypotheses regarding evolutionary constraints on the virus, because achieving simultaneous realism across in all these effects while retaining model tractability has proven extremely difficult.

For epidemiological models of influenza virus evolution overall population size matters: epidemics in larger populations involve more total inoculations, and therefore more opportunities for new variant survival at the point of transmission to occur. Large host populations with high transmission rates, strong population connectivities, and recurrent epidemics should promote antigenic evolution. This helps explain why influenza virus antigenic evolution appears to occur disproportionately in east and southeast Asia (Russell et al., 2008). It also reveals an issue with existing population level models of influenza virus evolution, many of which use host population sizes orders of magnitude smaller than the true global human population (Koelle & Rasmussen, 2015; Bedford et al., 2012). These models likely either overestimate risk of virus extinction or overestimate virus diversification rates.

8.2 Egg and mouse passage experiments

The observation that immune escape can be reliably be selected for in egg (Davis et al., 2018) and mouse (Hensley et al., 2009) passage experiments and yet appears rare in reinfected experienced humans is unsurprising in light of our view that influenza virus evolution is limited more by the failure of selection pressure and antigenic diversity to coincide than by the absence of either.

The egg experiments (Davis et al., 2018) amount to strong replication selection: the viruses were passaged in the presence of sera with highly-specific neutralizing antibodies, with these sera present at all times, including during the exponential growth phase within each egg.

The mouse passage experiments (Hensley et al., 2009) showed that serial passage in immune mice led to the emergence of antigenic escape mutants, but serial passage in naive mice did not. Several details of the experiment suggest that both replication selection and inoculation selection should have been more possible than in typical infected experienced humans. First, the mice were intranasally inoculated with 50 μl of homogenized lung isolate from the previous mouse in the passage chain at two days post-infection. This is likely a substantially more concentrated dose of virions than is inhaled through aerosol or even contact transmission (an inter-host bottleneck much wider than occurs in humans, to use the terminology of main text Fig. 4A). This could produce a very large value of v, the number of virions encountering IgA, and potentially a large value of b, the final (cell infection) bottleneck as well – in the presence of sufficiently many virions, early cell invasions might be sufficiently simultaneous as to produce have observably diverse within-host populations. All of this should tend to facilitate mutant survival and promotion to observable levels, but also to improve chances, relative to humans, that at least some wild-type virus could survive alongside. Second, inoculations were also carried out until a successful inoculation could be achieved. This further improves the chances of observing an escape mutant selected at the point of transmission. Finally, vaccinated mice in the passage chain were inoculated 10–21 days post-vaccination, meaning IgA levels could be higher than the memory baseline. This should at minimum strengthen inoculation selection and perhaps even permit replication selection.

One detail in supplementary table 1 of the mouse passage study (Hensley et al., 2009) is particularly relevant. In the passaging of virus stock #3, two mutants were observed for the first time in the second vaccinated mouse in the chain, but neither at fixation. Both remained present for 5 further passages in experienced mice without either being lost or fixing. This suggests a much wider final bottleneck than occurs in naturally-infected humans (McCrone et al., 2018). It also suggests that replication selection is unlikely to have been at all strong if present at all: over repeated exponential growth phases of two days with wide bottlenecks, even very small fitness differences can be easily amplified, so the more fit escape mutants should have fixed if they were subject to replication selection. Inoculation selection might have fixed them too – one of the two did fix, while the other was purged, in the 8th host. But if cell infection bottlenecks are wide and neutralization probabilities are low for both viruses, as appears to have been the case in these passage experiments, inoculation selection can favor a mutant but allow for a long intermittent period of coexistence.

An example calculation illustrates this: if $v = 1000$, $b = 10$, $f_{\mathrm{mt}} = 0.5$, $\kappa_m/\kappa_w > 0.9$, and $\kappa_w < 0.8$ the mutant has an inoculation-selective advantage, but the expected mutant frequency at after the next transmission event approximately 0.58 or less. Letting $\bar{w} = E(x_w)$ and $\bar{m} = E(x_m)$:

$$\begin{aligned} \bar{w} > v(1 - f_{\mathrm{mt}})(1 - \kappa_w) &= (1000)(0.5)(0.20) = 100 \\ \bar{m} > v(f_{\mathrm{mt}})(1 - \kappa_m) &= (1000)(0.5)(0.28) = 140 \end{aligned} \tag{A32}$$

And since $\bar{w}, \bar{m} \gg b$, the hypergeometric sampling is approximately binomial, and therefore the expected frequency of mutant is just $\frac{\bar{m}}{\bar{m}+\bar{w}} \approx 0.58$

While it is difficult to compare fitness differences during replication to fitness differences in mucosal neutralization, a very small fitness difference of $\delta = 0.5$ should raise the fitter type from frequency 0.5 to frequency 0.73 over the course of two days.

8.3 Magnitude of antigenic change and population level patterns

When antigenic effect size of mutations approaches zero, the effects of stochastic loss and mistimed selection pressure dominate, and inoculation and replication selection become sufficiently weak that true drift dominates as a force for introducing new antigenic variants. In such a regime, we expect the influenza viruses to evolve gradually, fail to cause large epidemics, and possibly diversify, not unlike influenza B viruses (Bedford et al., 2015). In particular, slow spread enables a kind of immunological niche partitioning: if population immune histories are not spatially uniform because epidemiological spread is slow relative to antigenic diversification, multiple variants that are each locally favored in distinct areas could co-circulate and form separate lineages, as has happened with B/Victoria and B/Yamagata.

When antigenic jump size approaches the maximum size possible, such that all population immunity disappears each time there is an antigenic cluster transition (Smith et al., 2004), we expect influenza viruses to follow a strongly clock-like pattern with high-amplitude oscillations in case numbers. They would cause massive punctuated epidemics during jump years and then in the next year either select for a new variant or go extinct. There would be huge booms followed by one or more years of bust. In between, at intermediate degrees of escape, a punctuated but somewhat less clocklike pattern – such as the pattern observed in nature for A/H3N2 viruses (Smith et al., 2004) – becomes possible.

8.4 Preview substitutions and mutation limitation

"Preview" substitutions and polyphyletic ultimate emergences also imply that the influenza virus is not typically mutation-limited at the population level – a substantial-effect escape mutant is usually accessible in sequence-space – but that the virus may nonetheless be highly constrained in its evolutionary trajectory. The virus repeatedly finds the same substitution as a solution to its antigenic evolutionary problem. This could occur either because only one escape mutant is available or

because one of the available escape mutants provides substantially more immune escape (on average) than the others.

8.5 Selection on bottlenecked diversity at higher scales

Without an explanation for why within-host dynamics do not more frequently promote antigenic mutants, it is difficult to explain the slow pace and noisy trajectory of influenza evolution. But such a within-host explanation, though likely necessary, may not be sufficient. It is conceivable that in a sufficiently large and well-connected global host population, population-level antigenic selection favoring mutants with higher $\mathfrak{R}_e$ would lead even small effect antigenic mutants rapidly to emerge and fix.

One important mechanism by which evolution might be also slowed at higher scales is analogous to the within-host dynamic of founder effects and inoculation selection: mutant lineages may be frequently lost (though perhaps selectively favoured) at the bottleneck that occurs between distinct influenza epidemics.

Prior modeling work has found that population-level host competition between pathogen strains reduces the probability that a fit mutant strain causes a large epidemic in the population in which it first emerges (Hartfield & Alizon, 2014). This is likely to be relevant in influenza epidemics, since the virus is thought to provoke short-term strain-transcending immunity (Ferguson et al., 2003).

We propose a previously unexplored consequence of this argument: successful establishment of a mutant lineage at the population level requires that the mutant lineage be exported to a new host subpopulation where susceptible hosts are common. This is rare but potentially selective sampling event.

When a mutant lineage emerges at the population level, it is likely to be surrounded by many propagating wild-type lineages due to the generator-selector dynamic discussed in the main text (see main text Fig. 6F,G). Moreover, most mutant lineage generation events will occur as an epidemic is peaking, since that is when the most inoculations occur. The consequence is that most generated population-level mutant lineages will encounter severe competition for susceptible hosts (especially if we consider realistic, spatial host contact networks rather than well-mixed epidemic models). So a generated mutant lineage is unlikely to account for many cases – or even necessarily more than one case – in the epidemic in which it emerges.

Many local influenza epidemics are likely to be evolutionary dead ends with no cases exported that establish chains of transmission in other locations. Because only a minority of the human population is likely to travel to or from the site of any particular epidemic, the majority of virus diversity generated within each epidemic is likely to be lost in between-epidemic bottlenecks. Conditional on being exported, mutant lineages could have competitive advantages over wild-type lineages because they spread should spread more rapidly and go stochastically extinct less easily due to their higher $\mathfrak{R}_e$. It follows that there is analogous dynamic to inoculation selection at the population level: mutant lineages are rarely exported from one sub-population (host, epidemic) to another, but conditional on being exported, they have an advantage in any potential competition with exported wild-type lineages.

The rate of proliferation of mutants at the population level, then, may be limited by the rarity of early generation of mutant lineages during an epidemic (analogous to the rarity of very early within-host *de novo* generation of mutants) and by the rarity of successful mutant lineage exportation when generation is not early (analogous to the rarity of mutant virions surviving the transmission bottleneck between hosts).

9 Mathematical derivations in full

9.1 Full derivation of the within-host replicator equation

The derivation in this section establishes equation 24:

$$\frac{\mathrm{d}f_m}{\mathrm{d}t} = f_m(1-f_m)\Big(\big[g_m(t)-g_w(t)\big]-\big[d_m(t)-d_w(t)\big]\Big)$$

Derivation. We note that:

$$f_m(t) := \frac{V_m(t)}{V_{\mathrm{tot}}(t)}$$

where $V_{\mathrm{tot}}(t) = V_w(t) + V_m(t)$. Let $\dot{V}_i$ denote $\frac{\mathrm{d}V_i}{\mathrm{d}t}$. Note that $\dot{V}_i = V_i\alpha_i(t)$ where $\alpha_i(t) = g_i(t) - d_i(t)$, and that $\frac{V_w(t)}{V_{\mathrm{tot}}(t)} = 1 - f_m(t)$. By the quotient rule:

$$\frac{\mathrm{d}f_m}{\mathrm{d}t} = \frac{V_{\mathrm{tot}}\dot{V}_m - V_m(\dot{V}_m + \dot{V}_w)}{V_{\mathrm{tot}}^2}$$

$$= \frac{V_{\mathrm{tot}}(\alpha_m V_m) - V_m(\alpha_m V_m + \alpha_w V_w)}{V_{\mathrm{tot}}^2}$$

Dividing through by V_{tot}^2 yields:

$$\alpha_m f_m - f_m(\alpha_m f + \alpha_w(1-f_m))$$

$$= \alpha_m f_m - \alpha_m f_m^2 - \alpha_w f_m(1-f_m)$$

$$= \alpha_m f_m(1-f_m) - \alpha_w f_m(1-f_m)$$

$$= f_m(1-f_m)(\alpha_w - \alpha_m)$$

$$= f_m(1-f_m)\Big(\big[g_m(t)-g_w(t)\big]-\big[d_m(t)-d_w(t)\big]\Big)$$

■

9.2 Replicator equation with symmetric mutation

With symmetric mutation at a rate μ, the replicator equation remains calculable.

Derivation. Given symmetric mutation, $\dot{V}_i = V_i\alpha_i(t) + \mu g_j(t)V_j$ where $\alpha_i(t) = (1-\mu)g_i(t) - d_i(t)$

Substituting in to the previous derivation yields:

$$\begin{aligned}\frac{\mathrm{d}f_m}{\mathrm{d}t} &= \frac{V_{\text{tot}}(\alpha_m V_m + \mu g_w(t)V_w) - V_m(\alpha_m V_m + \mu g_w(t)V_w + \alpha_w V_w + \mu g_m(t)V_m)}{V_{\text{tot}}^2} \\ &= \alpha_m f_m + \mu g_w(t)(1-f_m) - f_m\Big(\alpha_m f_m + \mu g_w(t)(1-f_m) + \alpha_w(1-f_m) + \mu g_m(t)f_m\Big)\end{aligned}$$

$$\begin{aligned}&= \alpha_m f_m + \mu g_w(t)(1-f_m) - \alpha_m f_m^2 - \mu g_w(t)f_m(1-f_m) - \alpha_w f_m(1-f_m) - \mu g_m(t)f_m^2 \\ &= \alpha_m f_m(1-f_m) - \alpha_w f_m(1-f_m) + \mu\left(g_w(t)(1-f_m) - g_w(t)f_m(1-f_m) - g_m(t)f_m^2\right) \\ &= f_m(1-f_m)(\alpha_m - \alpha_w) + \mu\Big(g_w(t) - 2g_w(t)f_m + g_w(t)f_m^2 - g_m(t)f_m^2\Big)\end{aligned}$$

Note that if $g_w(t) = g_m(t) = g(t)$, this simplifies to:

$$\frac{\mathrm{d}f_m}{\mathrm{d}t} = f_m(1-f_m)\big[d_m(t) - d_w(t)\big] + \mu g(t)(1-2f_m)$$

■

9.3 Replicator equation with one-way mutation

Derivation. To find the case with one-way mutation, we simply let all $\mu g_m(t)V_m$ terms from the symmetric mutation replicator equation be zero. This yields:

$$\frac{\mathrm{d}f_m}{\mathrm{d}t} = f_m(1-f_m)(\alpha_m - \alpha_w) + \mu g_w(t)\Big(1 - 2f_m + f_m^2\Big) \tag{A33}$$

■

9.4 Derivation of $t^*(x,t)$

This establishes the expression for the time t^* by which a mutant must emerge to reach at least frequency x by time t given in the Methods:

$$t^*(x,t) = \frac{\ln\left(x + \left[e^{\delta(t-t_M)}(1-x)\right]\right) - \ln(b) - \ln(x)}{g_0 - d_V}$$

Derivation. Notice that the frequency of the mutant depends on the quantity

$$\psi(t) = \exp\big(\delta(t - \max\{t_M, t_e\})\big)$$

Neglecting ongoing forward mutation the mutant must emerge at some frequency f_e in order to reach frequency x by time t:

$$\frac{\psi(t)}{\psi(t) + f_e^{-1} - 1} > x$$

Solving for f_e^{-1} yields:

$$f_e^{-1} < \left(\psi(t)\frac{1-x}{x}\right) + 1 \tag{A34}$$

If $t_e < t_M$, $f_e^{-1} \approx be^{(g_0 - d_V)t_e}$, the approximate number of wild-type virions at time t_e

$$be^{(g_0-d_V)t_e} \leq \left(\psi(t)\frac{1-x}{x}\right) + 1 = \left(e^{\delta(t-t_M)}\frac{1-x}{x}\right) + 1$$

Taking the natural log of both sides and subtracting off $\ln b$ from both sides:

$$(g_0 - d_V)t_e \leq \ln\left(\left(e^{\delta(t-t_M)}\frac{1-x}{x}\right) + 1\right) - \ln b$$

$$t_e \leq \frac{\ln\left(\left(e^{\delta(t-t_M)}\frac{1-x}{x}\right) + 1\right) - \ln b}{g_0 - d_V}$$

This establishes a value for t^* when $t_e < t_M$:

$$t^*(x,t) = \frac{\ln\left(\left(e^{\delta(t-t_M)}\frac{1-x}{x}\right) + 1\right) - \ln b}{g_0 - d_V} \tag{A35}$$

If $t > t_e > t_M$, the calculation is slightly more involved, as there are then t_e terms on both sides.

$$t_e < \frac{\ln\left(\left(e^{\delta(t-t_e)}\frac{1-x}{x}\right) + 1\right) - \ln b}{g_0 - d_V}$$

It is easy to see that a calculation based on positive selection occurring over the time interval $\tau = t - t_M$ will overestimate the probability of replication selection; it gives the virus longer than it strictly possesses to undergo positive selection, and thus estimates that the virus can emerge later, at some t^* greater than the true, earlier needed

emergence time. This effect is slightly counteracted by the fact that f_M is increased, since the wild-type grows more slowly once adaptive immunity is present:

$$f_M = \frac{1}{b \exp\left[(g_0 - d_V)t_M + (g_0 - d_V - k)(t_e - t_M)\right]} = Be^{g_1 t_e} \tag{A36}$$

where $B = be^{(g_0 - d_V)t_M - (g_0 - d_V - k)t_M} = be^{kt_M}$ and $g_1 = g_0 - d_V - k$

One way to deal with this is simply to make the approximation:

$$f_m(t) = \frac{e^{\delta\tau}}{e^{\delta\tau} + f_M^{-1}}$$

which underestimates $f_m(t)$, but not substantially so for smaller values of δ. In any case, we would like to be conservative about the probability of replication selection at small δ and early t_M to avoid biasing ourselves in favor of our hypothesis (namely, that replication selection is unrealistically common if t_M is early, even if δ is small).

Letting $f_m(t) = x$, we wish to solve:

$$x \geq \frac{e^{\delta(t - t_e)}}{e^{\delta(t - t_e)} + Be^{g_1 t_e}}$$

$$x \geq \frac{e^{\delta(t - t_e)}}{e^{\delta(t - t_e)} + Be^{g_1 t_e}}$$

We find:

$$t_e < \frac{\ln\left(\frac{1}{xB} - \frac{1}{B}\right) + \delta t}{g_1 + \delta}$$

$$t_e < \frac{\ln\left(\frac{1}{b}\right) + \ln\left(\frac{1-x}{x}\right) + \delta t - kt_M}{g_1 + \delta}$$

So when $t_e > t_M$,

$$t^*(x, t) \approx \frac{\ln\left(\frac{1}{b}\right) + \ln\left(\frac{1-x}{x}\right) + \delta t - kt_M}{g_0 - d_V - k + \delta} \tag{A37}$$

Note that this approximation is a lower bound on the true t^*; it may be that the virus can actually emerge later and still be replication selected to the desired frequency x.

■

9.5 Derivation of the closed form for p_{cib}

The derivation in this section establishes equation 16:

$$p_{\text{cib}}(\kappa_w, f_{\text{mt}}, wb) = E(p_{\text{cib}}(x_w, 1, b)) = (1 - e^{-\bar{w}})\frac{b}{\bar{w}} + e^{-\bar{w}} \sum_{j=0}^{b-1} \frac{\bar{w}^j}{j!}\Big(1 - \frac{b}{j+1}\Big)$$

where $\bar{w} = v(1 - f_{\text{mt}})(1 - \kappa_w)$ is the mean number of wild-type virions present after IgA neutralization.

Derivation.

$$p_{\text{cib}}(x_w, 1, b) = \frac{b}{x_w + 1}$$

$$\begin{aligned} E(p_{\text{cib}}(x_w, 1, b)) &= b \sum_{k=0}^{\infty} \frac{\bar{w}^k}{k!} e^{-\bar{w}} \frac{1}{k+1} \\ &= \frac{b}{\bar{w}} \sum_{k=0}^{\infty} \frac{\bar{w}^{k+1}}{(k+1)!} e^{-\bar{w}} \\ &= \frac{b}{\bar{w}} \sum_{j=1}^{\infty} \frac{\bar{w}^j}{j!} e^{-\bar{w}} \end{aligned}$$

We know that:

$$e^{-\lambda} + \sum_{j=1}^{\infty} \frac{\lambda^j}{j!} e^{-\lambda} = 1$$

since the Poisson is a proper probability distribution and therefore:

$$\sum_{j=1}^{\infty} \frac{\lambda^j}{j!} e^{-\lambda} = 1 - e^{-\lambda}$$

So substituting in:

$$\frac{b}{\bar{w}} \sum_{j=1}^{\infty} \frac{\bar{w}^j}{(j)!} e^{-\bar{w}} = \frac{b}{\bar{w}}(1 - e^{-\bar{w}})$$

This is exact when $b = 1$, but in other cases $p_{\text{cib}}(x_w, 1, b)$ is more properly given by $\max\{\frac{b}{x_w+1}, 1\}$, since whenever we have $x_w + 1 < b$, a new variant survives with certainty. So for each such $x_w < b - 1$ we need to add on correction term equal to $1 - \frac{b}{x_w+1}$, weighted by the probability of that x_w takes on that value: $e^{-\bar{w}} \frac{\bar{w}^{x_w}}{x_w!}$.

Summing from $x_w = 0$ to $x_w = b - 1$ and factoring out $e^{-\bar{w}}$ gives us the complete correction term:

$$e^{-\bar{w}} \sum_{j=0}^{b-1} \frac{\bar{w}^j}{j!}\Big(1 - \frac{b}{j+1}\Big)$$

Adding that to the expression derived above completes the derivation.

■

9.6 $p_{\text{cib}} = 1$ only if there is no competition

$p_{\text{cib}} < 1$ if $\kappa_w < 1$ and $f_{\text{mt}} < 1$, and $p_{\text{cib}} = 1$ if $\kappa_w = 1$ or $f_{\text{mt}} = 1$.

Derivation. This is most easily seen by rewriting p_{cib} as an infinite sum:

$$p_{\text{cib}}(\kappa_w, v, b) = e^{-\bar{w}} \Big[\sum_{j=0}^{b-1} \frac{\bar{w}^j}{j!} 1 + \sum_{j=b}^{\infty} \frac{\bar{w}^j}{j!} \frac{b}{j+1} \Big] \tag{A38}$$

If $\bar{w} = v(1 - f_{\text{mt}})(1 - \kappa_w) = 0$, we have $p_{\text{cib}} = 1$, as expected. Since $v > 0$, this occurs either when there is no wild-type ($f_{\text{mt}} = 1$) or when the wild-type is neutralized with probability 1 ($\kappa_w = 1$). Otherwise, $\bar{w} > 0$ and we therefore have:

$$p_{\text{cib}} = e^{-\bar{w}} \Big[\sum_{j=0}^{b-1} \frac{\bar{w}^j}{j!} 1 + \sum_{j=b}^{\infty} \frac{\bar{w}^j}{j!} \frac{b}{j+1} \Big] < e^{-\bar{w}} \Big[\sum_{j=0}^{b-1} \frac{\bar{w}^j}{j!} 1 + \sum_{j=b}^{\infty} \frac{\bar{w}^j}{j!} 1 \Big] = 1 \tag{A39}$$

The last step uses the fact that the Poisson distribution is a proper probability distribution, and therefore sums to 1. ■

9.7 p_{cib} is decreasing in $\bar{w}$

p_{cib} is decreasing in $\bar{w}$: the more competing wild-type virions, the less likely the new variant is to pass through the cell infection bottleneck.

Derivation. For $b = 1$,

$$\frac{\mathrm{d}p_{\text{cib}}}{\mathrm{d}\bar{w}} = \frac{e^{-\bar{w}} \left(\bar{w} - e^{\bar{w}} + 1\right)}{\bar{w}^2}$$

This is negative for $\bar{w} > 0$, as $e^x > x + 1$ for $x > 0$.

That p_{cib} is decreasing in $\bar{w}$ for $b > 1$ can be seen by writing:

$$\begin{aligned} p_{\text{cib}} &= e^{-\bar{w}} S(\bar{w}) \\ S(\bar{w}) &:= \sum_{j=0}^{b-1} \frac{\bar{w}^j}{j!} + \sum_{j=b}^{\infty} \frac{\bar{w}^j}{j!} \frac{b}{j+1} \end{aligned} \tag{A40}$$

This can be rewritten in two useful ways:

$$S(\bar{w}) = 1 + \sum_{j=1}^{b-1} \frac{\bar{w}^j}{j!} + \sum_{j=b}^{\infty} \frac{\bar{w}^j}{j!} \frac{b}{j+1} \tag{A41}$$

$$S(\bar{w}) = \sum_{j=0}^{b-2} \frac{\bar{w}^j}{j!} + \sum_{j=b-1}^{\infty} \frac{\bar{w}^j}{j!} \frac{b}{j+1} \tag{A42}$$

This uses the fact that $\frac{b}{j+1} = 1$ when $j = b - 1$.

We begin by showing that $S'(\bar{w}) < S(\bar{w})$. We differentiate A41 with respect to $\bar{w}$:

$$\begin{aligned} S'(\bar{w}) &= 0 + \sum_{j=1}^{b-1} \frac{\bar{w}^{j-1}}{(j-1)!} + \sum_{j=b}^{\infty} \frac{\bar{w}^{j-1}}{(j-1)!} \frac{b}{j+1} \\ &= \sum_{j=0}^{b-2} \frac{\bar{w}^j}{j!} + \sum_{j=b-1}^{\infty} \frac{\bar{w}^j}{j!} \frac{b}{j+2} \end{aligned} \tag{A43}$$

The first $b - 1$ terms in $S'(\bar{w})$ are equal to the corresponding terms in equation A42 for $S(\bar{w})$. Each subsequent term is smaller in $S'(\bar{w})$ than in $S(\bar{w})$, since $\frac{b}{j+2} < \frac{b}{j+1}$ for $b, j > 0$. So we have established that $S'(\bar{w}) < S(\bar{w})$ for $b > 1$.

Now we find $\frac{\mathrm{d}p_{\mathrm{cib}}}{\mathrm{d}\bar{w}}$:

$$\frac{\mathrm{d}p_{\mathrm{cib}}}{\mathrm{d}\bar{w}} = -e^{-\bar{w}} S(\bar{w}) + e^{-\bar{w}} S'(\bar{w}) \quad = e^{-\bar{w}} \Big[S'(\bar{w}) - S(\bar{w}) \Big] < 0 \tag{A44}$$

since $e^{-\bar{w}} > 0$ and $S'(\bar{w}) - S(\bar{w}) < 0$.

It follows that p_{cib} is decreasing in $\bar{w}$. ■

9.8 p_{cib} is increasing in b

Derivation. This follows from the infinite sum expression for p_{cib} (equation A38). We will show that $p_{\mathrm{cib}}(b+1) > p_{\mathrm{cib}}(b)$ for integers $b \geq 1$ by showing that $p_{\mathrm{cib}}(b+1) - p_{\mathrm{cib}}(b) > 0$

$$\begin{aligned} p_{\mathrm{cib}}(\kappa_w, v, b) &= e^{-\bar{w}} \Big[\sum_{j=0}^{b-1} \frac{\bar{w}^j}{j!} 1 + \sum_{j=b}^{\infty} \frac{\bar{w}^j}{j!} \frac{b}{j+1} \Big] \\ p_{\mathrm{cib}}(\kappa_w, v, b+1) &= e^{-\bar{w}} \Big[\sum_{j=0}^{b} \frac{\bar{w}^j}{j!} 1 + \sum_{j=b+1}^{\infty} \frac{\bar{w}^j}{j!} \frac{b+1}{j+1} \Big] \\ &= e^{-\bar{w}} \Big[\sum_{j=0}^{b-1} \frac{\bar{w}^j}{j!} 1 + \sum_{j=b}^{\infty} \frac{\bar{w}^j}{j!} \frac{b+1}{j+1} \Big] \end{aligned} \tag{A45}$$

This uses the fact that $\frac{b+1}{j+1} = 1$ when $j = b$.

For any $0 \leq \kappa_w \leq 1$, any $v \geq 1$, and $b \geq 1$, consider $p_{\text{cib}}(b+1) - p_{\text{cib}}(b)$:

$$\begin{aligned} p_{\text{cib}}(b+1) - p_{\text{cib}}(b+1) &= e^{-\bar{w}} \Big[\sum_{j=b}^{\infty} \frac{\bar{w}^j}{j!} \frac{(b+1)-b}{j+1} \Big] \\ &= e^{-\bar{w}} \Big[\sum_{j=b}^{\infty} \frac{\bar{w}^j}{j!} \frac{1}{j+1} \Big] \\ &> 0 \end{aligned} \tag{A46}$$

since this is a sum of positive terms, multiplied by a positive number.

■

9.9 $p_{\text{surv}}/p_{\text{drift}}$ is decreasing in b

Derivation. We follow an approach similar to 9.8, showing that $\frac{p_{\text{surv}}(b+1)}{p_{\text{drift}}(b+1)} - \frac{p_{\text{surv}}(b)}{p_{\text{drift}}(b)} < 0$ for integer $b \geq 1$.

$$\begin{aligned} \frac{p_{\text{surv}}(b)}{p_{\text{drift}}(b)} &\approx \frac{v}{b}(1-\kappa_m) p_{\text{cib}} \\ &= \frac{v}{b}(1-\kappa_m) e^{-\bar{w}} \Big[\sum_{j=0}^{b-1} \frac{\bar{w}^j}{j!} 1 + \sum_{j=b}^{\infty} \frac{\bar{w}^j}{j!} \frac{b}{j+1} \Big] \\ &= v(1-\kappa_m) e^{-\bar{w}} \Big[\sum_{j=0}^{b-1} \frac{\bar{w}^j}{j!} \frac{1}{b} + \sum_{j=b}^{\infty} \frac{\bar{w}^j}{j!} \frac{1}{j+1} \Big] \end{aligned}$$

Similarly:

$$\begin{aligned} \frac{p_{\text{surv}}(b+1)}{p_{\text{drift}}(b+1)} &\approx \frac{v}{b+1}(1-\kappa_m) e^{-\bar{w}} \Big[\sum_{j=0}^{b} \frac{\bar{w}^j}{j!} 1 + \sum_{j=b+1}^{\infty} \frac{\bar{w}^j}{j!} \frac{b+1}{j+1} \Big] \\ &= \frac{v}{b+1}(1-\kappa_m) e^{-\bar{w}} \Big[\sum_{j=0}^{b-1} \frac{\bar{w}^j}{j!} 1 + \sum_{j=b}^{\infty} \frac{\bar{w}^j}{j!} \frac{b+1}{j+1} \Big] \\ &= v(1-\kappa_m) e^{-\bar{w}} \sum_{j=0}^{b-1} \frac{\bar{w}^j}{j!} \frac{1}{b+1} + \sum_{j=b}^{\infty} \frac{\bar{w}^j}{j!} \frac{1}{j+1} \end{aligned}$$

We have again used the fact that $\frac{b+1}{j+1} = 1$ when $j = b$.

Taking the difference of the approximate ratios:

$$\frac{p_{\text{surv}}(b+1)}{p_{\text{drift}}(b+1)} - \frac{p_{\text{surv}}(b)}{p_{\text{drift}}(b)} \approx v(1-\kappa_m) e^{-\bar{w}} \sum_{j=0}^{b-1} \frac{\bar{w}^j}{j!} \left(\frac{1}{b+1} - \frac{1}{b} \right) < 0$$

That the expression is negative follows from the fact that all terms in the sum are negative, since $\frac{1}{b+1} < \frac{1}{b}$ for $b \geq 1$ while $\frac{\bar{w}^j}{j!}$ is always positive. The terms multiplying the sum are all positive.

It follows that $p_{\text{surv}}/p_{\text{drift}}$ is decreasing in b ■

9.10 In the absence of selection, the probability of surviving the bottleneck is approximately linear for large v and small $f_{\mathbf{mt}}$

Derivation. If $\kappa_w = \kappa_m = 0$, we have:

$$p_{\text{inoc}} = (1 - e^{-vf_{\text{mt}}})$$
$$\bar{w} = v(1 - f_{\text{mt}}) \approx v$$

$$e^{-\bar{w}} \approx 0$$
$$p_{\text{cib}} \approx \frac{b}{v}$$

$$p_{\text{surv}} \approx (1 - e^{-vf_{\text{mt}}})(\frac{b}{v})$$

And since $-vf_{\text{mt}}$ is small, we can use the linear approximation to the exponential:

$$p_{\text{surv}} \approx vf_{\text{mt}}\frac{b}{v} = bf_{\text{mt}}$$

■